DETERMINATION OF RESILIENT PROPERTIES OF UNBOUND MATERIALS WITH REPEATED LOAD TRIAXIAL AND DIAMETRAL TEST SYSTEMS

By

Shih-Ying Hsu and Ted S. Vinson

HP & R Study: 082-5154

Technical Report Documentation Page

1. Report No.	2. Government Accession No.	3. Recipient's Catalog No.
FHWA-OR-81-5		

4. Title and Subtitle	5. Report Date
Determination of Resilient Properties of Unbound Materials with Repeated Load Triaxial and Diametral Test Systems	December 1981
	6. Performing Organization Code
7. Author(s) Hsu, Shih-Ying and Ted S. Vinson	8. Performing Organization Report No. TE 81-6
9. Performing Organization Name and Address Oregon State University Department of Civil Engineering Corvallis, OR 97331-2302	10. Work Unit No. (TRAIS)
	11. Contract or Grant No. HPR-082-5154
	13. Type of Report and Period Covered Final
12. Sponsoring Agency Name and Address Oregon DOT, Materials & Research Section, Salem, OR and U.S. DOT, Federal Highway Administration Office of R. & D., Washington, D.C. 20590	14. Sponsoring Agency Code

15. Supplementary Notes

16. Abstract

Repeated load diametral test systems are experiencing increased use to determine resilient properties of asphalt concrete and admixture stabilized materials; they have not been used extensively to determine the resilient properties of unbound materials. This is due in part to the fact that comparative studies between the properties obtained with the diametral test system and the repeated load triaxial test system have not been made. In response to the need to establish a correlative data base between resilient properties determined with diametral and repeated load triaxial test systems, a laboratory test program was conducted. Specifically, resilient properties of two-base course and two subgrade materials were determined using both repeated load triaxial and diametral test systems. The resilient properties of duplicate specimens (with respect to water content, dry density, method of compaction) were compared over the range of material conditions considered. The resilient properties determined with either the repeated load diametral or triaxial test systems were approximately equivalent. The differences between resilient moduli for comparable states of stress were ± 80%. Correlations between resilient moduli can only be made for a specific material at a given water content, dry density, and method of compaction. It is not possible with the data set developed in the study to establish general correlation factors between resilient properties determined with diametral or triaxial test systems with those of the conventional R-value test. The differences between resilient moduli determined with either the diametral or triaxial test system led to negligible differences in the design thickness of materials in representative pavement structures.

17. Key Words	18. Distribution Statement
Soils; Resilient moduli; Repeated Load Triaxial testing; Diametral testing	No Restrictions

19. Security Classif. (of this report)	20. Security Classif. (of this page)	21. No. of Pages	22. Price
Unclassified	Unclassified		

DETERMINATION OF RESILIENT PROPERTIES OF UNBOUND MATERIALS WITH REPEATED LOAD TRIAXIAL AND DIAMETRAL TEST SYSTEMS

BY

SHIH-YING HSU AND TED S. VINSON

FINAL REPORT TO:

OREGON DEPARTMENT OF TRANSPORTATION
OREGON HIWAY DIVISION
SALEM, OR

AND

U.S. DEPARTMENT OF TRANSPORTATION
FEDERAL HIGHWAY ADMINISTRATION
SALEM, OR

TRANSPORTATION RESEARCH REPORT 81-6

TRANSPORTATION RESEARCH INSTITUTE
OREGON STATE UNIVERSITY
CORVALLIS, OR

DECEMBER 1981

ACKNOWLEDGEMENTS

This report is the second and final report concerned with the evaluation of unbound (subgrade and base) materials. Both reports present the results of extensive testing to better understand the behavior of these materials under repeated loading. Assistance provided by Gordon Beecroft and Clarence Gregg, both of Oregon Department of Transportation and by R. G. Hicks of the O.S.U. Transportation Research Institute in the collection of data and review of the report is acknowledged.

The project was funded by the U.S. Department of Transportation, Federal Highway Administration and the Oregon Department of Transportation.

DISCLAIMER

TABLE OF CONTENTS

TABLE OF CONTENTS

TABLE OF CONTENTS

LIST OF FIGURES

LIST OF TABLES

CHAPTER 1

INTRODUCTION

1.1 Problem Statement

Many highways in eastern Oregon are built with cinder or overlie volcanic materials. These highways, when designed using empirical procedures based upon Hveem Stabilometer resistance values, often do not perform as expected. In order to more accurately predict pavement life, an analytical approach based upon multilayer elastic theory (MET) and suitable failure criteria for pavement structures could be employed.

The analytical approach based upon MET and suitable failure criteria requires a knowledge of the mechanical properties of each component of the pavement structure under repeated loading test conditions. For untreated base materials and subgrade soils, repeated load triaxial test methods have been extensively employed in the laboratory to obtain mechanical properties under repeated loading conditions, i.e., resilient properties. In recent years, the diametral test method has been used to investigate resilient properties for asphalt concrete mixtures, concrete cement mixtures and open graded asphalt emulsion mixtures (Adedimila (1975), Evans (1980), Pong (1981), Clemmons (1979), Hull (1980)). The diametral test method has not been extensively used to evaluate resilient properties for untreated base materials and subgrade soils.

1.2 Purpose

The purpose of this study is to: (1) investigate the resilient properties of unbound volcanic base materials and subgrade soils using both repeated load triaxial and diametral test systems; (2) compare the resilient

properties of laboratory prepared, unbound base materials and cohesionless subgrade soils determined with diametral and triaxial test systems; and (3) compare the thickness design of flexible pavements determined with an empirical procedure employing Hveem Stabilometer resistance values to the thickness design based upon an analytical procedure employing MET and resilient moduli.

1.3 Scope

A general literature review of (1) the evaluation of the resilient properties determined with repeated load triaxial and diametral test methods, and (2) the thickness design of flexible pavements based on empirical procedures and MET is presented in Chapter 2. The experiment design, including (1) the overall test program, (2) the test procedure to determine Hveem Stabilometer resistance value, (3) the test equipment and procedure associated with repeated load triaxial resilient modulus test, and (4) the test equipment and procedure associated with the repeated load diametral resilient modulus test are presented in Chapter 3. The test results for each test program are summarized in Chapter 4. The application of the test results to flexible highway pavement thickness design is presented in Chapter 5. Chapter 6 presents the conclusions and recommendations for further study.

CHAPTER 2

LITERATURE REVIEW

Over the years, numerous studies have been conducted to improve pavement design procedures. Advances have been made in laboratory and field test techniques, and analytical design procedures. Deacon (1970) listed the material response variables that might be included in evaluation for pavement design. The major variables, given in Table 2.1, include loading, type of material, and environment. Table 2.2, following the work developed by Deacon (1970), shows the wide range of laboratory test configurations which might be used to evaluate pavement materials as well as untreated base and subgrade materials. Kennedy, et al (1978) compared some common laboratory test methods which might be employed to obtain fundamental material properties (Table 2.3). At present (1981), the repeated load triaxial test method is the most common laboratory technique to evaluate the resilient properties of unbound materials. The repeated load diametral test method is experiencing increased use to determine resilient modulus and fatigue life of asphalt concrete mixtures and stabilized materials. A general literature review of the evaluation of resilient properties determined from repeated load triaxial and diametral test methods and the thickness design of flexible pavements determined with empirical procedures based upon Hveem Stabilometer resistance values and with analytical procedures based upon MET are presented in this Chapter.

2.1 Repeated Load Triaxial Resilient Modulus Test

There are many types of the repeated load triaxial test systems. Although a triaxial test system may vary from unit to unit, the basic system should include at least the following features: (1) triaxial cell, (2) load-

TABLE 2.1 VARIABLES AFFECTING MATERIAL RESPONSE

(after Deacon, 1970)

I. LOADING VARIABLES
- A. Stress history (nature of prior loading)
  - 1. Non-repetitive loading (such as preconsolidation)
  - 2. Repetitive loading
    - a. Nature
      - (1) Simple
      - (2) Compound
    - b. Number of repetitive applications
- B. Initial stress state (magnitude and direction of normal and shear stresses)
- C. Incremental loading
  - 1. Mode of loading
    - a. Controlled stress (or load)
    - b. Controlles strain (or deformation)
    - c. Intermediate modes
  - 2. Intensity (magnitude and direction of incremental normal and shear stresses)
  - 3. Stress path (relation among stresses - both normal and shear - as test progresses)
  - 4. Time path
    - a. Static
      - (1) Constant rate of stress (or load)
      - (2) Constant rate of strain (or deformation)
      - (3) Creep
      - (4) Relaxation
    - b. Dynamic
      - (1) Impact
      - (2) Resonance
      - (3) Other
        - (a) Sinusoidal (rate of loading is variable)
        - (b) Pulsating (duration, frequency, and shape of load curve are variables)
  - 5. Type of behavior observed
    - a. Strength (limiting stresses and strains)
    - b. Deformability
  - 6. Homogeneity of stresses
  - 7. Drainage (drained or undrained)

II. MIXTURE VARIABLES
- A. Mineral particles
  - 1. Maximum and minimum size
  - 2. Gradation
  - 3. Shape
  - 4. Surface texture
  - 5. Angularity
  - 6. Mineralogy
  - 7. Adsorbed ions
  - 8. Quantity
- B. Binder
  - 1. Type
  - 2. Hardness
  - 3. Quantity
- C. Water
  - 1. Quantity
- D. Voids
  - 1. Quantity
  - 2. Size
  - 3. Shape
- E. Construction Process
  - 1. Density
  - 2. Structure
  - 3. Degree of anisotrophy
  - 4. Temperature
- F. Homogeneity

III. ENVIRONMENTAL VARIABLES
- A. Temperature
- B. Moisture
- C. Alteration of Material Properties
  - 1. Thixotropy
  - 2. Aging
  - 3. Curing
  - 4. Densification

TABLE 2.2 LABORATORY TEST CONFIGURATIONS (after Deacon, 1970)

I. Tension A. Uniaxial tension B. Indirect tension 1. Splitting tension 2. Cohesiometer	II. Compression A. Unconfined, uniaxial compression B. Triaxial compression 1. Open system a) Isotropic Compression b) Conventional triaxial compression (1) Normal (2) Vacuum (3) High pressure c) Box with cubical specimen 2. Closed system a) Oedometer b) Cell c) Hveem stabilometer	III. Flexure A. Rotation 1. Rotating 2. Non-rotating B. Loading 1. Cantilever 2. Simple a) Point supports b) Uniform supports
IV. Direct shear A. Direct shear (rigid split box) B. Double direct shear C. Uniform direct shear (rigid caps with confined rubber membrane and split rings for lateral restraint) D. Uniform strain direct-shear (hinged box) E. Punching shear	V. Torsion A. Pure torsion B. Triaxial torsion C. Specimen shape 1. Solid cylinder 2. Thick-walled, hollow cylinder	VI. Indirect A. Penetration B. Squeeze tests C. Marshall stability D. Angle of repose E. Others

TABLE 2.3 COMPARISON OF COMMON TEST METHODS TO OBTAIN FUNDAMENTAL MATERIAL PROPERTIES (After Kennedy et al, 1978)

	Basic Test	Variations of Basic Test	Fundamental Properties Usually Determined By Test	Relationships Test Commonly Used For	Structural Subsystem Applicability			Criteria		Remarks
					Fatigue	Permanent Deformation	Low Temperature Cracking	Ease of Testing & Economy	Reproducibility	
Tests for Elastic Properties	Indirect Tensile Test	Static	Stiffness Modulus S	Fatigue Permanent Deformation	Yes	Yes	Yes	Excellent	Good	Easy acquisition of specimens (i.e. from Marshall test or field cores)
		Dynamic Repeated	Resilient Modulus E_H							
	Triaxial	Complex Modulus Test[1]	Complex Modulus E		No	Yes	No	Good	Good	Output of test used for layer analyses rather than for fatigue permanent deformation or cracking relationships
		Resilient Modulus Test[2]	Resilient Modulus M_H					Fair	Good	
	Beam Bending		Stiffness Modulus S	Fatigue	Yes	No	No	Fair	Fair	
	Direct Tension	Triaxial[3]		Permanent Deformation	Yes	Yes	No	Poor	Good	Specimen preparation usually requires sawing
		Beam Test[4]	Stiffness Modulus S	Strain vs. Temperature	Yes	No	Yes	Good	Poor	
Tests for Viscoelastic or Time Dependent Properties	Triaxial	Static Creep[5]	Creep Compliance	Permanent Deformation	No	Yes	No	Good	Good	
		Dynamic Repeated	Gnu and Alpha[6]					Fair	Fair	
	Indirect Tensile Test[7]	Static Creep[5]	Creep Compliance	Permanent Deformation	Yes	Yes	No	Excellent	Good	Limited experience in applying this test to viscoelastic analysis
		Dynamic Repeated	GNU and Alpha[6]							

1 For bituminous materials, unconfined test
2 For unbound base materials and subgrade soils, triaxial compression
3 For bituminous materials triaxial tension
4 For bituminous materials beam tension
5 For bituminous materials unconfined test axial tension or compression
6 Parameters used in VESYS IIM which characterize slope and intercept of permanent deformation vs N relationship
7 For bituminous materials

ing system, (3) timing device, and (4) suitable readout equipment for the type of loading and deformation monitoring devices which are to be incorporated. A simple version of the load configuration and the sequence of loading for a repeated load triaxial test system is shown in Fig. 2.1. The results from the repeated load triaxial test are expressed in terms of resilient modulus, M_R, defined as:

$$M_R = \frac{\sigma_d}{\varepsilon_a} \qquad (2.1)$$

in which, σ_d = cyclic axial deviator stress

ε_a = recoverable axial strain

2.1.1 Theoretical Stress-Time Relationships in Layered Systems

Barksdale (1971) examined the compressive stress pulse times in flexible pavements for use in the repeated load triaxial test. He concluded:(1) the vertical compressive stress pulse times using either a nonlinear (stress dependent) or linear elastic model are not significantly different; (2) triangular or sinusoidal stress pulses could be used in a repeated load triaxial test; (3) the stress pulse times increased significantly with depth beneath the pavement surface; (4) the compressive pulse time varies almost inversely with vehicle speed up to at least a speed of 45 mph; and (5) the pavement geometry and layer properties do not have a significant influence on the stress pulse times.

Monismith, et al (1973) also investigated stress states and stress-time relationships for use in the triaxial test. They found: (1) vertical and horizontal compressive stresses obtained from the multilayered configuration compare closely with those obtained using two-layer analysis; (2) the duration of loading for vertical stress depends only on depth and is independent

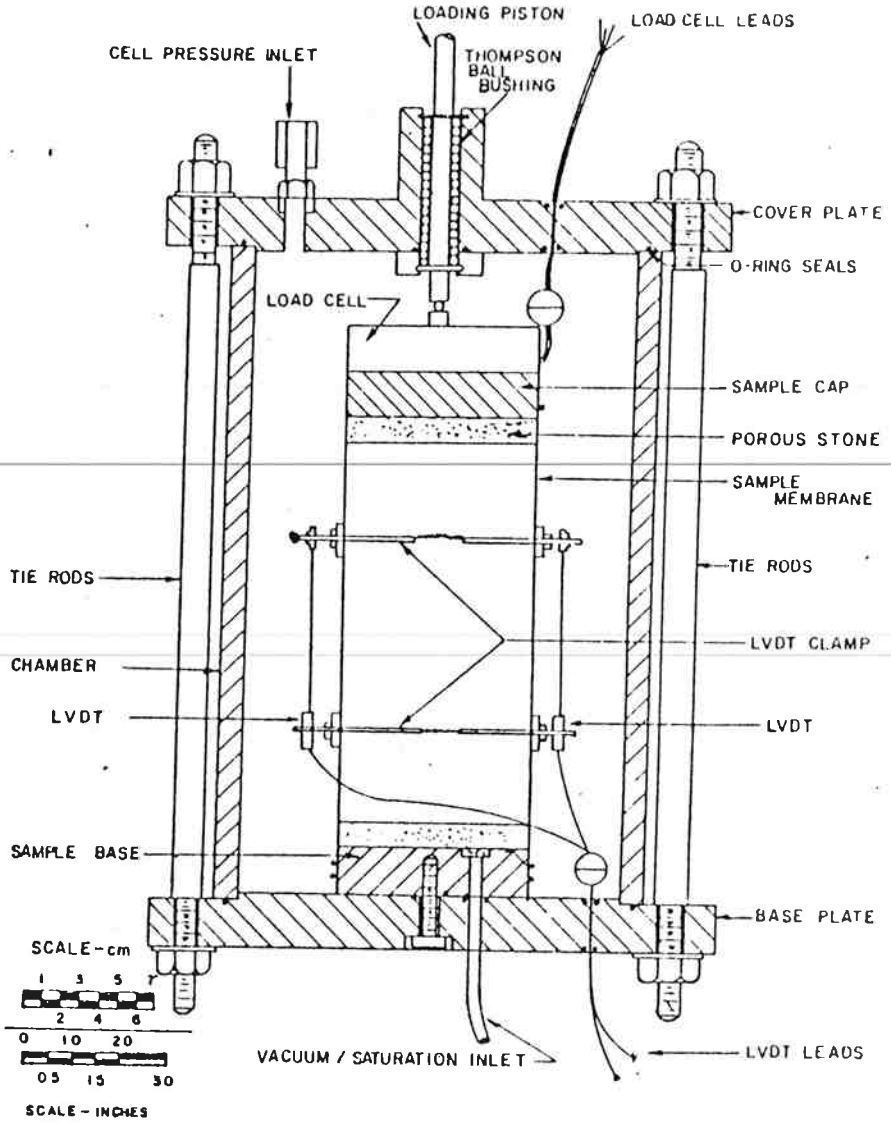

FIG. 2.1 REPEATED LOAD TRIAXIAL TEST SYSTEM (after Asphalt Institute, 1973)

of structural characteristics of the pavement materials (structural effect); (3) the duration of loading for horizontal stresses depends on both depth and the structural effect; (4) a square form of load-time relationships should be employed for vertical stresses near the top of the surface layer and triangular shape of load-time relationships should be employed for other conditions; and (5) the temperature effects on the stress-time relationships are small while the effects on the stress magnitude are significant.

2.1.2 Resilient Properties of Base and Cohesionless Subgrade Materials

Numerous studies have been conducted to evaluate resilient properties of base and cohesionless subgrade materials using the repeated load triaxial test method. The stress-dependent characteristics of unbound aggregates are generally expressed as follows:

$$M_R = k_1 \theta^{k_2} \tag{2.2}$$

or

$$M_R = k_1' \sigma_c^{k_2'} \tag{2.3}$$

in which θ = sum of principal stresses

σ_c = confining pressure

k_1, k_2, k_1', k_2' = regression constants

Hicks and Monismith (1971) examined factors influencing the resilient properties of granular materials. They concluded (1) resilient modulus increased considerably with increasing confining pressure but only slightly with increasing deviator stress; (2) Poisson's ratio increased with decreasing confining pressure and with increasing deviator stress; (3) at a given stress level, the modulus increased with increasing density, increasing particle

angularity or surface roughness, decreasing fine content and decreasing degree of saturation; and (4) at a given stress level, Poisson's ratio was influenced slightly by density and decreased as fine content and the degree of saturation increased.

Clemmons (1979) evaluated the resilient properties of coastal Oregon marginal aggregates. The effects of stress levels for the four aggregates tested have the same trends as those found by Hicks and Monismith. No conclusions were obtained concerning the effects of water contents and dry densities on the resilient properties.

Hull, et al (1980) investigated the resilient properties of two eastern Oregon volcanic aggregates. The effects of stress level agreed with those previous studies. The regression constant k_1 decreased with increasing water content and the constant k_2 increased slightly with increasing water constant. It appears that the variations in regression constants k_1 and k_2 with water contents and dry densities should be examined on a individual basis.

Hull, et al (1980) also examined the resilient properties of two cohesionless subgrade soils obtained from eastern Oregon. In general, the effects of confining pressure are much more pronounced than the effects of the deviator axial stress on the resilient modulus. The resilient modulus increased with increasing dry density and with decreasing water content.

2.2 Repeated Load Diametral Test

To date, repeated load diametral test systems have not been used extensively to determine the resilient properties of unbound materials.

2.2.1 Theoretical Considerations

2.2.1.1 Stress State

A stress state for a disc or cylinder subjected to a diametral compressive line load was obtained by Frocht (1948). Frocht's solution assuming a linear elastic material may be expressed as follows:

Stresses along the horizontal diameter

$$\sigma_x = \frac{2P}{\pi td}\left(\frac{d^2 - 4x^2}{d^2 + 4x^2}\right)^2 \qquad (2.4)$$

$$\sigma_y = \frac{-2P}{\pi td}\left(\frac{4d^2}{d^2 + 4x^2} - 1\right) \qquad (2.5)$$

$$\tau_{xy} = 0$$

Stress along the vertical diameter

$$\sigma_x = \frac{2P}{\pi td} \qquad (2.6)$$

$$\sigma_y = \frac{-2P}{\pi t}\left(\frac{2}{d-2y} + \frac{2}{d+2y} - \frac{1}{d}\right) \qquad (2.7)$$

$$\tau_{xy} = 0$$

in which, t = thickness of specimen

d = diameter of specimen

x = horizontal distance from the center of specimen

y = vertical distance from the center of specimen

P = compressive line load

(Note: tensile stresses are positive and compressive stresses are negative, any consistent set of units may be used in Equations 2.4 to 2.7). Figure 2.2 and 2.3 illustrate the manner in which these stresses vary across the diameter of a test specimen.

In a diametral test, the specimen is subjected to a strip load instead of a line load. A refinement to account for this was made by Hondros (1959). Hondros' solutions may be expressed as follows:

Stress along the horizontal diameter

tangential stress: (2.8)

$$\sigma_{\theta x} = \frac{-2P}{\pi at}\left\{\frac{(1-r^2/R^2)\sin 2\alpha}{1+2r^2\cos 2\alpha/R^2+r^4/R^4}+\tan^{-1}\left(\frac{1-r^2/R^2}{1+r^2/R^2}\right)\tan\alpha\right\}$$

radial stress: (2.9)

$$\sigma_{rx} = \frac{2P}{\pi at}\left\{\frac{(1-r^2/R^2)\sin 2\alpha}{1+2r^2\cos 2\alpha/R^2+r^4/R^4}-\tan^{-1}\left(\frac{1-r^2/R^2}{1+r^2/R^2}\right)\tan\alpha\right\}$$

shear stress:

$$\tau_{r\theta} = 0$$

Stress along the vertical diameter

tangential stress: (2.10)

$$\sigma_{\theta y} = \frac{2P}{\pi at}\left\{\frac{(1-r^2/R^2)\sin 2\alpha}{1-2r^2\cos 2\alpha/R^2+r^4/R^4}-\tan^{-1}\left(\frac{1+r^2/R^2}{1-r^2/R^2}\right)\tan\alpha\right\}$$

radial stress: (2.11)

$$\sigma_{ry} = \frac{-2P}{\pi at}\left\{\frac{(1-r^2/R^2)\sin 2\alpha}{1-2r^2\cos 2\alpha/R^2+r^4/R^4}+\tan^{-1}\left(\frac{1+r^2/R^2}{1-r^2/R^2}\right)\tan\alpha\right\}$$

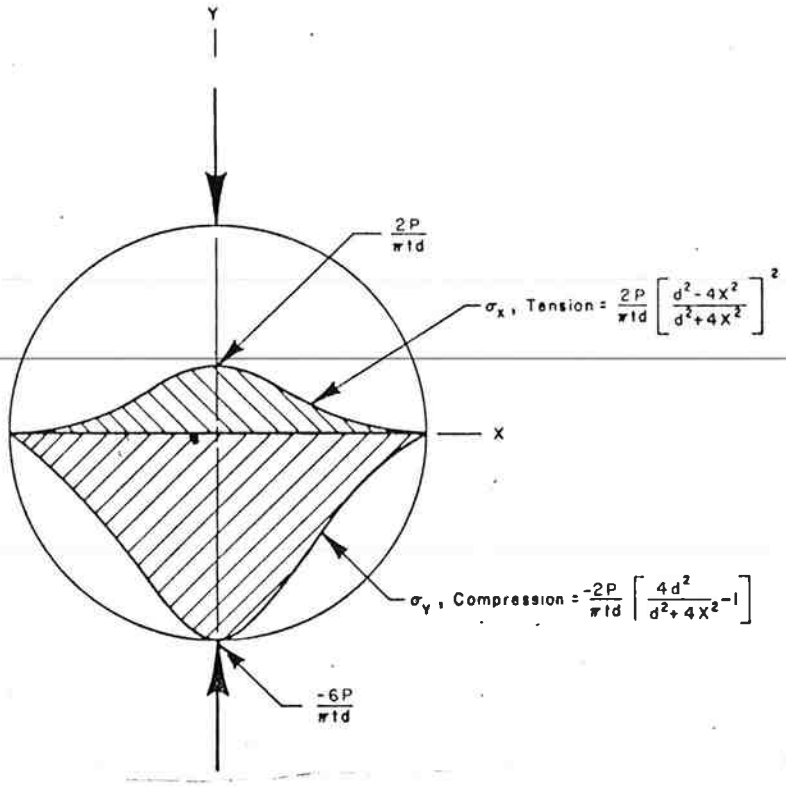

FIG. 2.2 STRESS DISTRIBUTION ON HORIZONTAL DIAMETER - LINE LOAD (after Kennedy and Hudson, 1968)

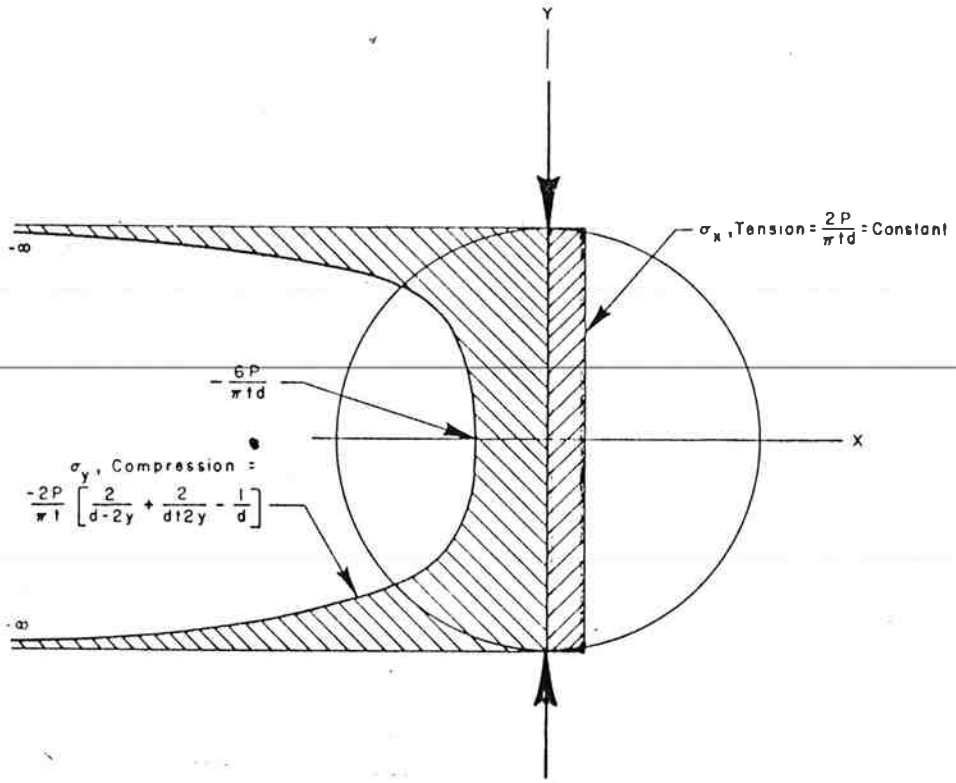

FIG. 2.3 STRESS DISTRIBUTION ON VERTICAL DIAMETER - LINE LOAD (after Kennedy and Hudson, 1968)

shear stress:

$$\tau_{r\theta} = 0$$

in which, a = projected width of the loaded section of the rim

t = thickness of specimen

r = radial distance from the center of specimen

R = radius of specimen

2α = angle at the origin subtended by the loaded section of the rim

P = diametral compressive load

(Note: tensile stresses are positive and compressive stresses are negative, any consistent set of units may be used in Equations 2.8 to 2.11). The notations for polar stress components in a circular element compressed by two diametrically opposed short loading strips is shown in Figure 2.4. Figures 2.5 and 2.6 show the manner in which stresses vary across the diameter. The major difference between the line load and strip load case is the stress along the vertical diameter.

Figure 2.7 indicates that compressive stresses along the vertical diameter are reduced near the loading area for the strip load case. In addition, the tensile stresses are changed to compressive stresses at approximately $\frac{5d}{12}$ from the center for the strip load case. Hondros (1959) also pointed out that the stress states for the case of a strip load are valid for conditions of both plane stress (discs) and plane strain (cylinders).

Wallace and Monismith (1980) examined the stress regimes of stress dependent materials using a linear finite element program (SAP 4) and an iterative technique. Figure 2.8 and 2.9 show the comparisons of the stress variation along the vertical and horizontal diameter for a linear elastic and

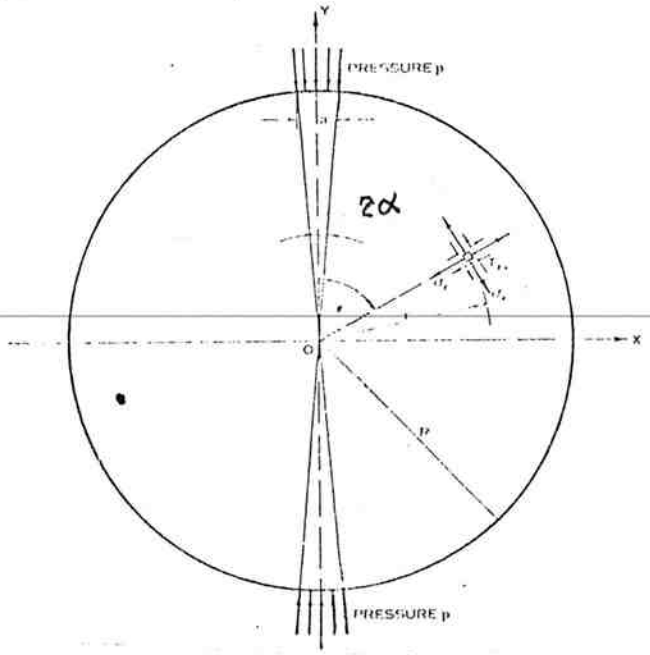

FIG. 2.4 NOTATION FOR POLAR STRESS COMPONENTS IN A CIRCULAR ELEMENT COMPRESSED BY DIAMETRICALLY SHORT STRIP LOADING (after Hondros, 1956)

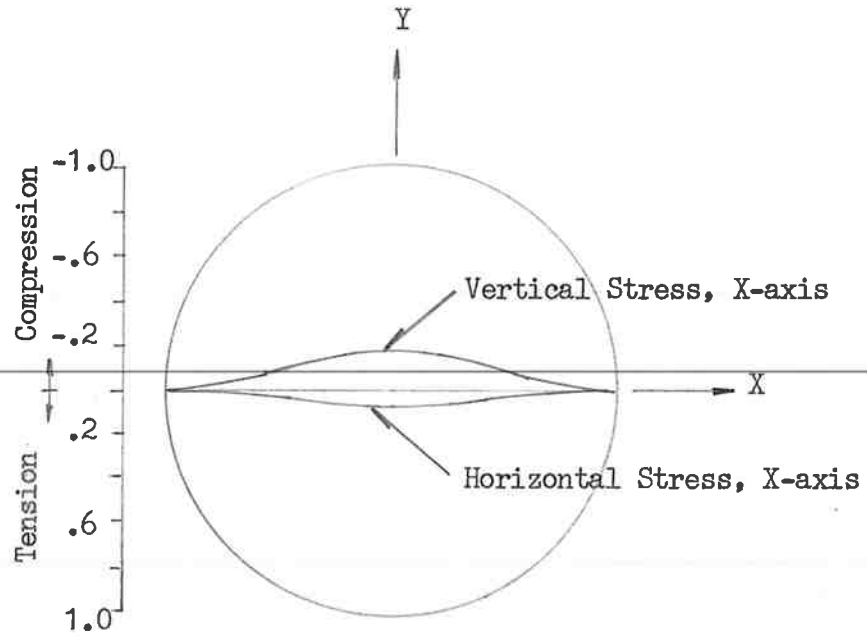

FIG. 2.5 STRESS DISTRIBUTION ON HORIZONTAL DIAMETER - STRIP LOAD

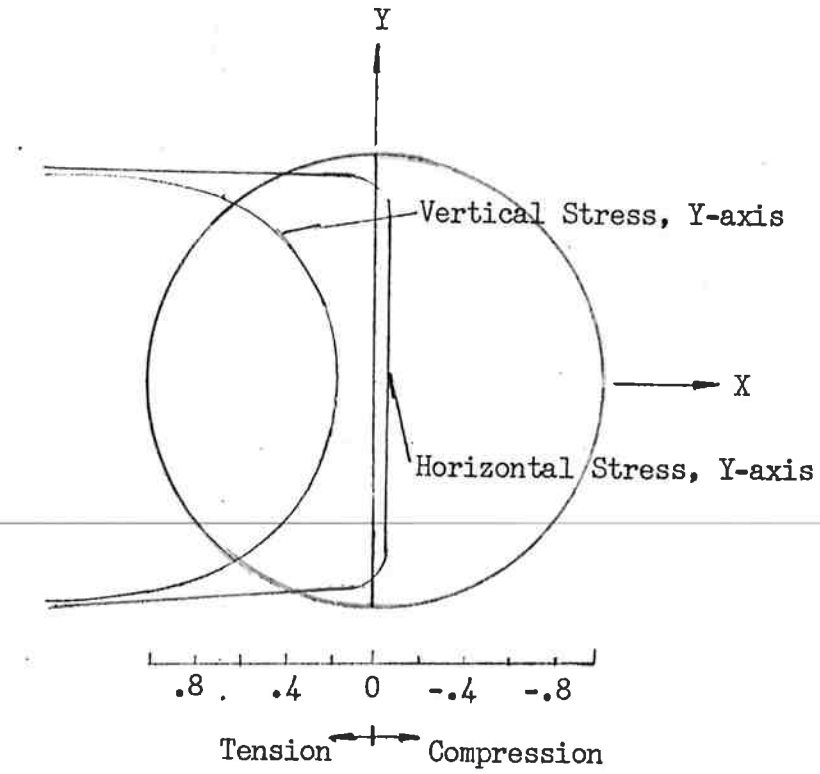

Fig. 2.6 Stress Distribution on Vertical Diameter
Strip Load

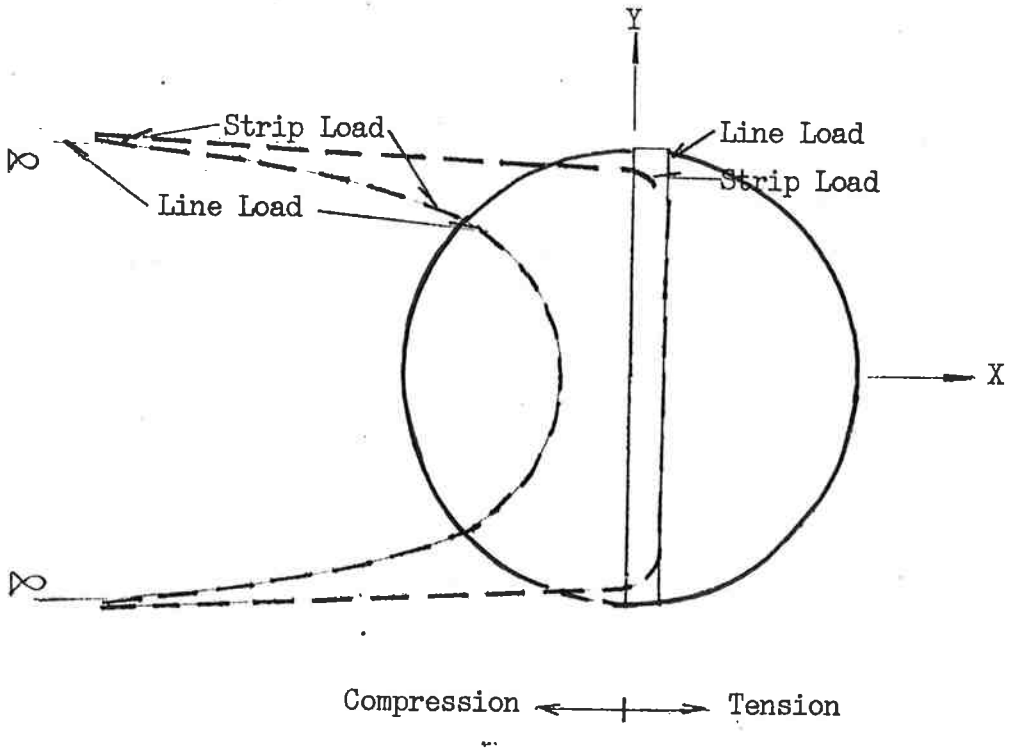

Fig. 2.7 Comparison of Stress Distribution on Vertical Diameter for Line Load and Strip Load

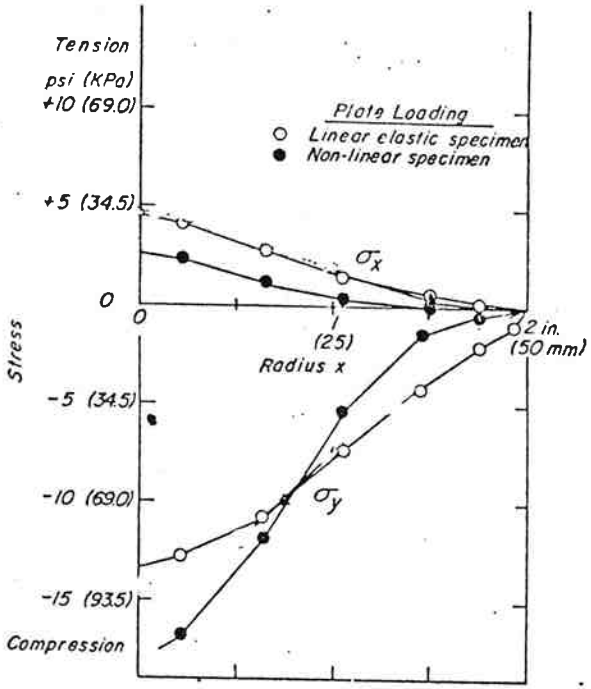

FIG. 2.8 COMPARISON OF STRESS DISTRIBUTION BETWEEN STRESS-DEPENDENT AND LINEAR ELASTIC MATERIAL - ALONG HORIZONTAL DIAMETER (after Wallace and Monismith, 1980)

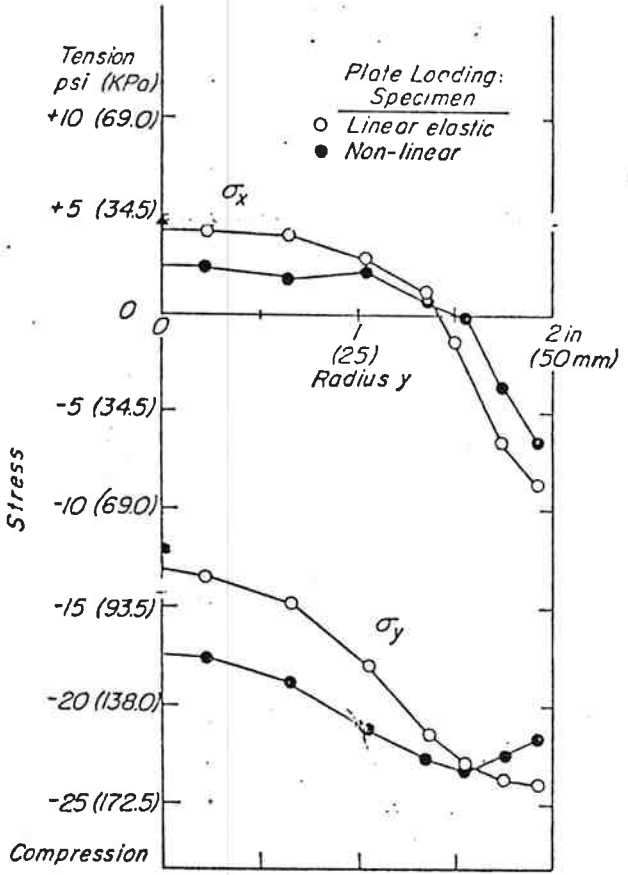

FIG. 2.9 COMPARISON OF STRESS DISTRIBUTION BETWEEN STRESS-DEPENDENT AND LINEAR ELASTIC MATERIAL - ALONG VERTICAL DIAMETER (after Wallace and Monismith, 1980)

a stress dependent specimen (100 mm (4 in.) in diameter, 63 mm (2.5 in.) in height) subjected to a strip load 330 N (75 lb.), and a strip width of 18.8 mm (0.75 in.).

It is interesting to note that along the horizontal diameter (1) the tensile stresses along the inner half diameter for a linear specimen are approximately twice those for a stress dependent specimen; (2) the compressive stresses for a linear elastic specimen along the outer half diameter are greater than those for a stress dependent specimen; and (3) the compressive stresses for a linear elastic specimen along the inner half diameter are smaller than those for a stress dependent specimen. Therefore, some deviations of diametral resilient modulus for unbound materials computed based on linear elasticity may be excepted when compared with triaxial resilient modulus for this reason alone.

2.2.1.2 Strain, Deformation, Poisson's Ratio and Young's Modulus

A thin disc subjected to a diametral load can be treated as a two dimensional plane stress problem. The stress-strain relationships for plane stress problems can be simplified, since $\alpha = 0$ and, for principal planes, $\tau_{xy} = 0$. Hence,

$$\varepsilon_x = \frac{1}{E} (\sigma_x - \mu\sigma_y) \qquad (2.12)$$

$$\varepsilon_y = \frac{1}{E} (\sigma_y - \mu\sigma_x) \qquad (2.13)$$

Solving for E, and

$$E = \frac{\sigma_x - \mu\sigma_y}{\varepsilon_x} \qquad (2.14)$$

or

$$E = \frac{\sigma_y - \mu\sigma_x}{\varepsilon_y} \tag{2.15}$$

and

$$\sigma_x = \frac{\sigma_y - E\,\varepsilon_y}{\mu} \tag{2.16}$$

or

$$\sigma_y = \frac{\sigma_x - E\,\varepsilon_x}{\mu} \tag{2.17}$$

To solve for Poisson's ratio one can equate 2.14 and 2.15 as follows:

$$\frac{\sigma_x - \mu\,\sigma_y}{\varepsilon_x} = \frac{\sigma_y - \mu\,\sigma_x}{\varepsilon_y}$$

rearranging terms,

$$\frac{\sigma_x}{\varepsilon_x} - \frac{\sigma_y}{\varepsilon_y} = \left(\frac{\sigma_y}{\varepsilon_x} - \frac{\sigma_x}{\varepsilon_y}\right)\mu$$

therefore,

$$\mu = \frac{\sigma_x\,\varepsilon_y - \sigma_y\,\varepsilon_x}{\sigma_y\,\varepsilon_y - \sigma_x\,\varepsilon_x} \tag{2.18}$$

Equating 2.16 and 2.17, one obtains alternate expressions for Young's modulus as follows:

substituting 2.17 into 2.16

$$\sigma_x = \frac{(\sigma_x - E \varepsilon_x)/ \; - E \varepsilon_y}{\mu}$$

rearranging terms,

$$\sigma_x (\mu^2 - 1) = - E (\varepsilon_x + \mu \varepsilon_y)$$

and

$$E = \frac{\sigma_x (1 - \mu^2)}{\varepsilon_x + \mu \varepsilon_y} \qquad (2.19)$$

Substituting 2.16 into 2.17, one obtains

$$E = \frac{\sigma_y (1 - \mu^2)}{\varepsilon_y + \mu \varepsilon_x} \qquad (2.20)$$

One may also obtain from Equations 2.4 to 2.7 that, at the center of the specimen,

$$\sigma_y = - 3 \sigma_x \qquad (2.21)$$

Substituting Equation 2.21 into Equation 2.18 one obtains

$$\mu = - \frac{3 \varepsilon_x + \varepsilon_y}{3 \varepsilon_y + \varepsilon_x} \qquad (2.22)$$

Equation 2.22 represents an expression for Poisson's ratio in terms of the strain at the center of the test specimen. Young's modulus in terms of the

center strain and diametral load may be obtained by combining Equations 2.4 or 2.5 and 2.20 as follows:

$$E = \frac{2P}{\pi dt} \quad \frac{(1 - \mu^2)}{(\varepsilon_x + \mu \varepsilon_y)} \tag{2.23}$$

or

$$E = \frac{-6P}{\pi dt} \quad \frac{(1 - \mu^2)}{(\varepsilon_y + \mu \varepsilon_x)} \tag{2.24}$$

A thick cylinder subjected to a diametral load can be treated as a two dimensional plane strain problem. The stress-strain relationship can be simplified, since $\varepsilon_z = 0$ and for the principal planes $\tau_{xy} = 0$. Hence,

$$\varepsilon_x = \frac{1 + \mu}{E} \quad ((1 - \mu) \sigma_x - \mu \sigma_y) \tag{2.25}$$

or

$$\varepsilon = \frac{1 + \mu}{E} \quad ((1 - \mu) \sigma_y - \mu \sigma_x) \tag{2.26}$$

Solving for E, σ_x and σ_y, one obtains,

$$E = \frac{1 + \mu}{\varepsilon_x} \quad ((1 - \mu) \sigma_x - \mu \sigma_y) \tag{2.27}$$

or

$$E = \frac{1 + \mu}{\varepsilon_y} \quad ((1 - \mu) \sigma_y - \mu \sigma_x) \tag{2.28}$$

and

$$\sigma_x = \frac{(1+\mu)\mu\,\sigma_y + E\,\varepsilon_x}{1-\mu^2} \tag{2.29}$$

$$\sigma_y = \frac{(1+\mu)\mu\,\sigma_x + E\,\varepsilon_y}{1-\mu^2} \tag{2.30}$$

To solve for Poisson's ratio, one can equate 2.27 and 2.28 to obtain:

$$\mu = \frac{\sigma_x\,\varepsilon_y - \sigma_y\,\varepsilon_x}{(\sigma_x + \sigma_y)(\varepsilon_y - \varepsilon_x)} \tag{2.31}$$

Equating 2.29 and 2.30, one obtains alternate expressions for Young's modulus as follows:

substituting 2.30 into 2.29

$$E = \frac{\sigma_x\,(1+\mu)(1-2\mu)}{\mu\,\varepsilon_y + (1-\mu)\,\varepsilon_x} \tag{2.32}$$

or substituting 2.29 into 2.30

$$E = \frac{\sigma_y\,(1+\mu)(1-\mu)}{\mu\,\varepsilon_x + (1-\mu)\,\varepsilon_y} \tag{2.33}$$

It has been shown that the stress at the center of the specimen,

$$\sigma_y = -3\,\sigma_x \tag{2.21}$$

then substituting 2.21 into 2.31,

$$\mu = \frac{-(\varepsilon_y + 3\,\varepsilon_x)}{2(\varepsilon_y - \varepsilon_x)} \tag{2.34}$$

This represents an alternate expression for Poisson's ratio in terms of the strain at the center of the test specimen. Young's modulus in terms of the center strain and diametral load may be obtained by combining equation 2.4 or 2.5 and 2.32 or 2.33 as follows:

$$E = -\frac{2P}{\pi dt} \quad \frac{(1+\mu)(1-2\mu)}{\mu\,\varepsilon_y + (1-\mu)\,\varepsilon_x} \tag{2.35}$$

or

$$E = \frac{-6P}{\pi dt} \quad \frac{(1+\mu)(1-2\mu)}{\mu\,\varepsilon_x + (1-\mu)\,\varepsilon_y} \tag{2.36}$$

If the strains are measured during the test, Poisson's ratio and Young's modulus can be calculated from Equations 2.22, 2.23 and 2.24 for a disc or Equations 2.34, 2.35 and 2.36 for a cylinder.

The comparisons of the theoretical strain distribution along the diameter for the case of plane stress and plane strain have been given by Hondros (1959) and the solution is illustrated in Figure 2.10. Apparently, the differences of the strains for the case of plane stress and plane strain are not critical.

If the deformations are measured, the equations which permit the calculation of Poisson's ratio and Young's modulus for the case of plane stress may be derived as follows:

horizontal deformation

$$\Delta H = \int \varepsilon_x \, dx \tag{2.37}$$

vertical deformation

$$\Delta V = \int \varepsilon_y \, dy \tag{2.38}$$

recall Equation 2.12

$$\varepsilon_x = \frac{\sigma_x - \mu\,\sigma_y}{E}$$

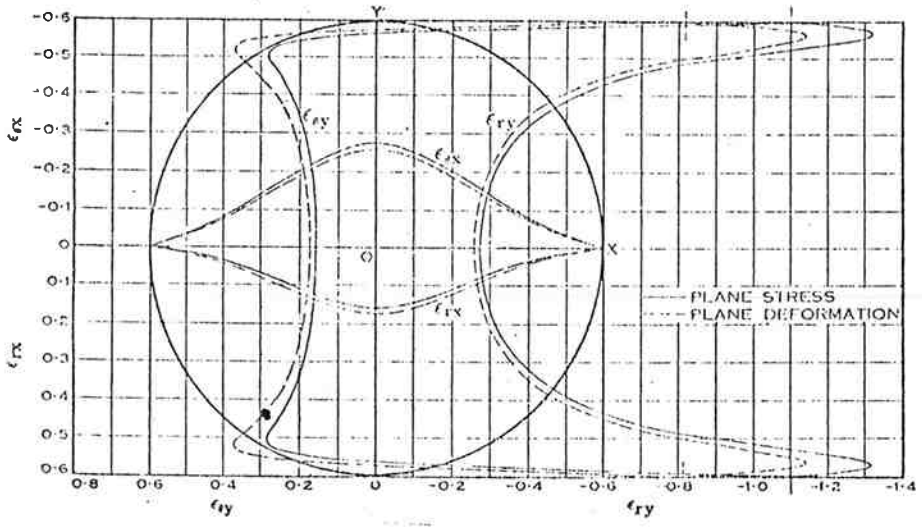

FIG 2.10 COMPARISON OF THEORETICAL STRAIN DISTRIBUTION ALONG VERTICAL AND HORIZONTAL DIAMETER BETWEEN PLANE STRESS AND PLANE STRAIN PROBLEM (after Hondros, 1956)

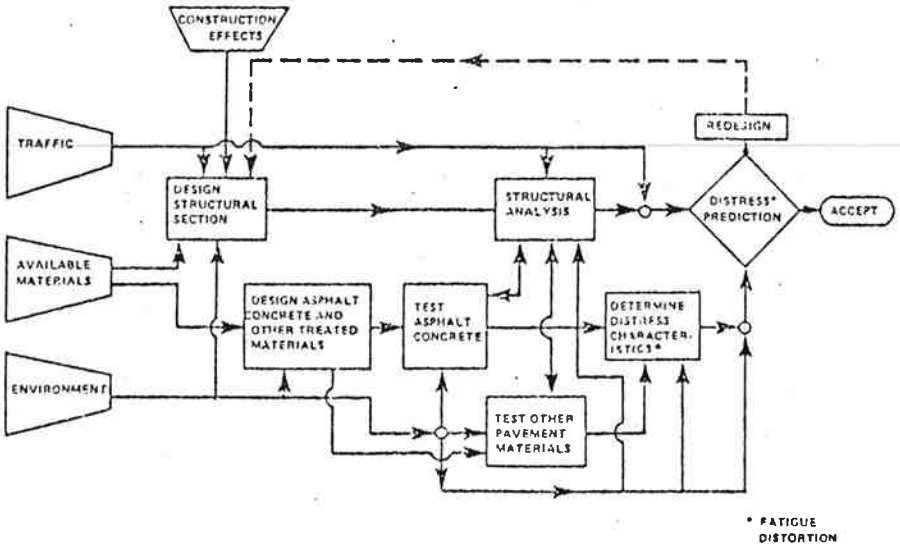

FIG. 2.11 FRAMEWORK OF ANALYTICAL BASED DESIGN PROCEDURE FOR ASPHALT SURFACED PAVEMENTS (after Monismith, 1981)

substituting 2.12 into 2.37, one obtains,

$$\Delta H = \frac{1}{E} \left(\int \sigma_x dx - \mu \int \sigma_y dx \right)$$

and

$$E = \frac{1}{\Delta H} \left(\int \sigma_x dx - \mu \int \sigma_y dx \right) \qquad (2.39)$$

similarly, one can obtain,

$$E = \frac{1}{\Delta V} \left(\int \sigma_y dy - \mu \int \sigma_x dy \right) \qquad (2.40)$$

Poisson's ratio may be derived as follows:

equating 2.39 and 2.40,

$$\frac{1}{\Delta H} \left(\int \sigma_x dx - \mu \int \sigma_y dx \right) = \frac{1}{\Delta V} \left(\int \sigma_y dy - \mu \int \sigma_x dy \right)$$

rearranging terms,

$$\frac{1}{\Delta H} \int \sigma_x dx - \frac{1}{\Delta V} \int \sigma_y dy = \mu \left(\frac{1}{\Delta H} \int \sigma_y dx - \frac{1}{\Delta V} \int \sigma_x dy \right)$$

therefore,

$$\mu = \frac{(1/\Delta H) \int \sigma_x dx - (1/\Delta V) \int \sigma_y dy}{(1/\Delta H) \int \sigma_y dx - (1/\Delta V) \int \sigma_x dy}$$

the numerator and denominator are multiplied by V to obtain,

$$\mu = \frac{(\Delta V/\Delta H) \int \sigma_x dx - \int \sigma_y dy}{(\Delta V/\Delta H) \int \sigma_y dx - \int \sigma_x dy} \qquad (2.41)$$

Kennedy, et al (1970, 1972, 1975) carried out integrations of Equations 2.8 to 2.11 using a computer program, MODLAS. Integration of Equations 2.8 to 2.11 provide the formulas which permit the computation of Poisson's ratio and modulus. For a 100 mm (4 in.) diameter specimen and 12.5 mm (0.5 in.) wide loading strip, the formulas are given as follows:

instantaneous resilient Poisson's ratio

$$\mu = \frac{DR\ (0.0673) + (-0.8954)}{DR\ (-0.2494) + (-0.0156)} \qquad (2.42)$$

instantaneous resilient modulus

$$M_R = \frac{P\ (\ 0.2692 + \mu\ (0.99)\ )}{\Delta Ht} \qquad (2.43)$$

in which, DR = deformation ratio,

P = diametral load

H = horizontal deformation

V = vertical deformation

t = thickness of specimen (length of loading strip)

(Note: any consistent set of units may be used in Equations 2.42 and 2.43).

Equations 2.42 and 2.43 may be modified for a plane strain problem based on the following assumptions:

(1) the specimen is linear elastic, homogeneous and isotropic material;

(2) the stress solutions for a specimen subjected to diametral load are valid for both plane stress and plane strain problems;

(3) the strain solutions for a specimen subjected to diametral load are valid for both plane stress and plane strain problems;

Based on the assumptions above, Poisson's ratio, μ^*, for the plane strain problem can be obtained by transforming Poisson's ratio (μ) computed from equation 2.42 as follows:

$$\mu^* = \frac{\mu}{1 + \mu} \qquad (2.42.a)$$

The modulus can be obtained using Poisson's ratio as follows:

$$M_R = \frac{P}{\Delta H t} \left((1 + \mu^*)(1 - \mu^*) 0.2692 + (1 + \mu^*)(\mu^*) 0.9974 \right) \qquad (2.43b)$$

2.2.2 Applications to Bound Materials

In recent years, repeated load diametral test systems have experienced increasing use to determine the resilient properties of asphalt concrete and admixture stabilized materials. Values of resilient modulus are usually calculated based upon Equation 2.43, and an assumed value for Poisson's ratio. This is owing to the fact that variations of Poisson's ratio over a theoretical range of 0.2 to 0.5 only affect resilient modulus by about ± 25%.

Experimental values of Poisson's ratio have not been quoted very often for the repeated load diametral test. Adedimila and Kennedy (1975) investigated the fatigue and resilient characteristics of asphalt concrete using the repeated load diametral test. Values of Poisson's ratio ranging from negative to greater than 0.5 were reported in their studies. The deviations from the theoretical values of Poisson's ratio are associated with violation of the assumptions that Equation (2.44) is based upon.

$$\Delta V = V_o \cdot (2\mu - 1) \geq 0 \qquad (2.44)$$

in which, V_o = initial volume

V = final volume

ε = axial strain

u = Poisson's ratio

These assumptions include (1) materials are homogeneous, isotropic and linear elastic, and (2) volume change in tension is positive (expansion) while volume change in compression is negative (contraction). Adedimila and Kennedy concluded that (1) when there is an internal or external crack, it is possible to obtain a Poisson's ratio greater than 0.5, and (2) Poisson's ratio increases with increasing stress applications up to the time associated with 70 to 80 percent of the fracture life.

Schmidt (1972) compared the resilient moduli of asphalt concrete specimens determined with direct tension, direct compression and diametral test methods. The direct tension resilient moduli, direct compression resilient moduli and diametral resilient moduli based upon an assumed Poisson's ratio of 0.2, 0.35 and 0.5 agreed quite well over the range of comparable stress states.

Pong (1981) compared the resilient characteristics of asphalt concrete determined with repeated load triaxial and diametral test methods. Little

variation of the values of the Poisson's ratio were observed in the triaxial test. An average value of Poisson's ratio of 0.35 was selected to calculate the diametral resilient modulus. Based upon linear elasticity, Pong concluded (1) the relationships of the diametral resilient modulus versus compressive stress at the center of the specimen and triaxial resilient modulus versus deviator stress were in good agreement over the stress range of 275 kPa to 620 kPa (40 psi to 90 psi) and, (2) the relationships of the diametral tensile strain (center of the specimen) versus average compressive stress along the horizontal diameter and triaxial compressive axial strain versus deviator stress are identical, the diametral resilient moduli are about 25% higher than the triaxial resilient moduli over the stress range of 100 kPa to 620 kPa (15 psi to 90 psi).

To date, repeated load diametral test systems have not been used to determine the resilient properties of unbound materials. This is owing primarily to the fact that comparable studies between the resilient properties determined with the repeated load diametral and other test methods such as triaxial test have not been made.

From the preceding materials, several considerations associated with the evaluation of the resilient properties of unbound materials employing repeated load diametral test system may be noted and summarized as follows:

(1) To simplify the problem associated with the evaluation of the resilient properties employing repeated load diametral test systems, plane stress solutions based upon linear elasticity were used. Specifically, Equations 2.42 and 2.43 were employed to compute the resilient modulus and Poisson's ratio. This does not mean to imply that non-linearity, and heterogeneous characteristics of unbound

materials do not exist or are not important. In fact, in many cases it is probable that these characteristics dominate the response of the test material.

(2) Poisson's ratio should be determined during the test and be employed to detect the deviation of a test material from an idealized linear elastic, homogeneous and isotropic material.

(3) The stress states are not well-defined in the repeated load diametral test for unbound materials. The computations employed in the study were based on linear elasticity and do not take nonlinear characteristics of test material into account. Accordingly, the comparisons of the resilient modulus test results determined with diametral test and triaxial test methods may be examined in terms of the deviator compressive stress at the center of the specimen for the diametral test and deviator compressive stress for the triaxial test.

2.3 Thickness Design for Flexible Pavements Based on Multilayer Elastic Theory (MET)

The major development in the thickness design of flexible pavements over the past 25 years has been the analytical design approach based on MET. The success of the analytical design approach depends largely on a thorough understanding of the mechanical characteristics of each component layer of the pavement structure and the development of suitable failure criteria. A general literature review of thickness design for flexible pavements is presented in this section.

2.3.1 Design Model and Stress Analysis

Many researchers and engineers have attempted to provide a comprehensive and realistic pavement model which results in a design procedure that is both economical and physically sound. Most of early development of work for flexible pavement structures is based on the assumptions that the materials comprising the structure are linear elastic, homogeneous and isotropic, in spite of the contradiction between these assumptions and actual behavior. The stress analysis for these simplified pavement models were solved by tabular, graphical solutions, or computer programs. Solutions in the form of computer programs are very useful and capable of great versatility. Hicks, et al (1978) considered five computer programs (CHEV5L, CHEV5L w/iteration (PSAD), PSAD2A, ELSYM5 and SHELL BISAR) and evaluated their limitations as well as their applications to analytical pavement design.

2.3.2 Design Criteria

The design approach based on MET limits distress caused by fatigue cracking at the bottom of asphalt concrete layer and rutting (permanent deformation) at the surface of the pavement. Investigations of the fatigue phenomena in asphalt concrete pavements have shown that maximum tensile strain is a good indicator of fatigue phenomena both in the laboratory and in the field pavement. The fatigue characteristics of asphalt concrete are generally expressed as follows:

$$N_f = C \frac{1}{\varepsilon_t} \qquad (2.45)$$

in which, N_f = number of strain cycles to failure

ε_t = maximum tensile strain

C, m = constants which depend on the mix characteristics

The relationship between the maximum allowable tensile strain for asphalt mixes as a function of number of load repetitions to failure developed by

Santucci (1977) was selected in the study. Investigations of the permanent deformation phenomena of pavements have shown that the vertical compressive strain at the top of a subgrade soil layer may be adopted as a design criteria. The relationship between allowable vertical compressive subgrade strain as a function of the number of 80 kN (18 kip) equivalent axle load applications developed by Monismith and Mclean (1971) was selected in the study.

2.3.3 Design Systems

The elements of an analytical pavement thickness design system include: (1) selecting a design model, (2) estimating traffic growth in terms of a legal axle load, (3) evaluating the material variables, (4) examining the environment factors, (5) analyzing pavement structure and, (6) selecting a suitable failure criteria.

Employing such a system is essentially a trial and error approach. A flow chart suggested by Monismith (1981) is shown in Figure 2.11. Having determined the traffic volume, pavement materials and an assumed pavement section, a test program considering the environment factors and loading conditions are conducted to determine the mechanical properties and distress characteristics. The results from the laboratory test are employed as input values for the pavement structure analysis. The results from the structural analysis are compared to the results from the laboratory distress characteristics or failure criteria. The thickness of the layers are adjusted until the failure criteria is satisfied.

2.4 Empirical Thickness Design of Flexible Pavements Based on Hveem Stabilometer "R" Value

The empirical design method based on Hveem stabilometer resistance value has been used by the Oregon Department of Transportation since 1951. This

method is essentially the same procedure as used by the California Department of Transportation with modifications for Oregon's soil conditions, traffic and environment. Aggregate base materials and subgrade soils are tested for exudation pressure, expansion pressure and Hveem stabilometer "R" value. For those materials containing less than 90% passing the 6 mm (No. 4) sieve, a 2070 kPa (300 psi) exudation pressure design "R" value used for the thickness design of pavements. For other materials, a design "R" value is selected at the "wet side" water content corresponding to 95% maximum dry density (T-99). The exudation pressure in this instance may vary from 340 kPa to 1030 kPa (50 to 150 psi).

Having determined the design "R" value and traffic volume, the required total structural thickness in terms of the equivalent crushed base aggregate thickness is obtained from:

$$CBE = 0.03546 \; (\; TC \;) \; (\; 100 - R \;) \qquad (2.46)$$

in which, CBE = an equivalent thickness for various materials complying with the Standard Specifications and Special Provisions required by ODOT

TC = Traffic coefficient

"R" = Hveem stabilometer resistance value

The actual thickness of each layer to use in the design is determined by the use of appropriate substitution ratios to transform the CBE to the materials employed in the construction phase (see Table 5.2).

A provision which requires minimum thickness for various traffic volumes based on the construction, maintenance and under-design considerations is employed by the Oregon Department of Transportation and is referred to in the ODOT flexible pavement design procedure (see Figure 5.1).

CHAPTER 3

EXPERIMENT DESIGN

3.1 Test Program

The test program undertaken in the study for untreated volcanic cinder base materials and cohesionless subgrade soils is shown in Figure 3.1. The program consists of five major phases as follows:

(1) determination of material index properties,

(2) test specimen preparation,

(3) Hveem stabilometer resistance value tests,

(4) repeated load diametral resilient modulus test,

(5) repeated load triaxial resilient modulus test.

The Hveem stabilometer resistance value test consists of two subphases. The flow chart for each subphase is shown in Figure 3.2 and 3.3. The terms "Wet specimen" and "Dry specimen" are defined according to the exudation pressure test results. Specifically, those specimens which have exudation pressures less than 5500 kPa (800psi) are defined as "Wet specimen", and those specimens which have exudation pressures higher than 5500 kPa (800 psi) are defined as "Dry specimen".

Normally, the "Dry specimen" is excluded from the Standard Hveem stabilometer resistance value test; however, in an attempt to correlate "R" value to resilient modulus over a wide range of water contents and dry densities the "Dry specimen" is included in the "R" value tests.

To evaluate the sensitivity of "R" value to dry density, the "R" value tests for the "Dry specimen" were conducted employing two different procedures. One group of specimens were subjected to 5500 kPa (800 psi) axial pressure whereas for the other group of specimens, the exudation pressure

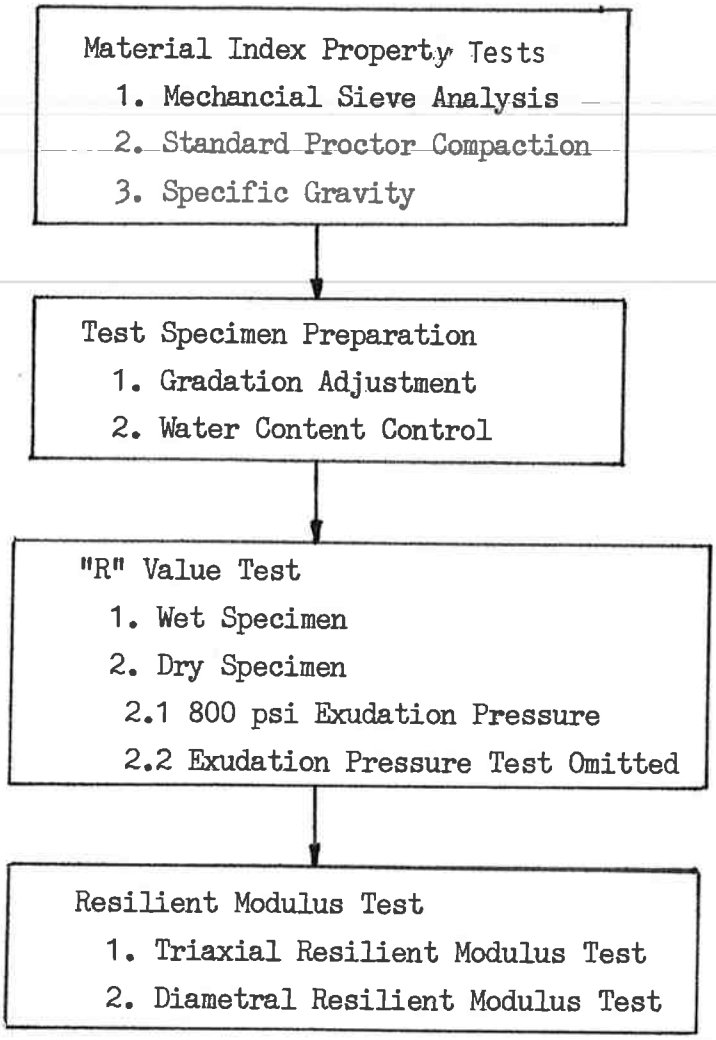

FIG 3.1 FLOW CHART OF TEST PROGRAM

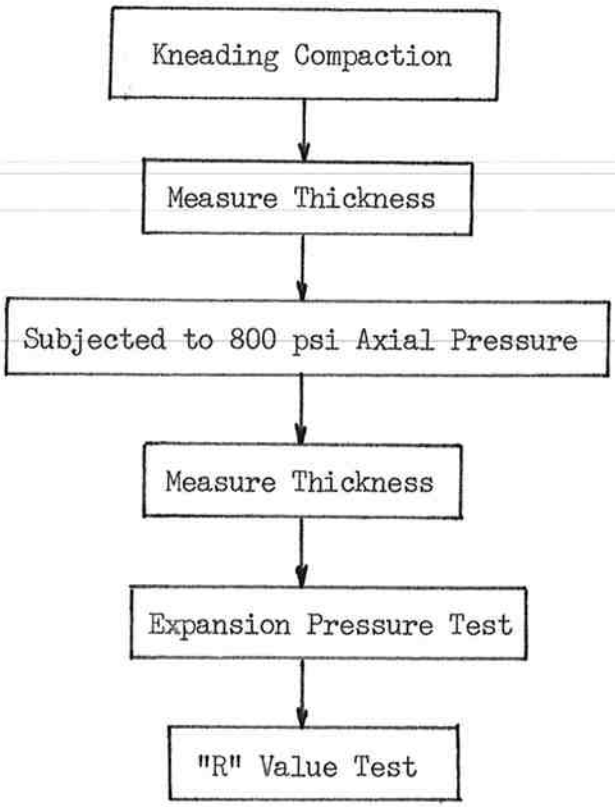

FIG. 3.2 "R" VALUE TEST FOR "DRY SPECIMEN" - SUBJECTED TO 800 PSI AXIAL PRESSURE

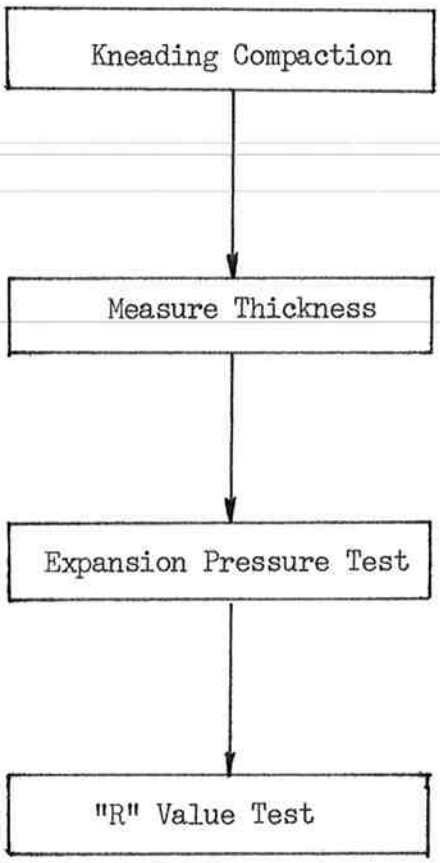

FIG 3.3 "R" VALUE TEST FOR "DRY SPECIMEN" -
EXUDATION PRESSURE TEST OMITTED

phase was omitted. Therefore, dry densities (and "R" values) for these two groups of test specimens were substantially different. All wet tests were conducted in accordance with standard ODOT procedures (ODOT test method No. 105). In addition to the test results developed in this project for the base and subgrade materials considered, index and "R" value tests were previously conducted at the ODOT test laboratories. The results from the ODOT test program are given in Appendix C.

3.2 Material Index Properties

The volcanic cinder base materials and subgrade soils tested in this project were obtained from two locations in Deschutes County, Oregon, as shown in Figure 3.4. Two cinder base materials were tested in the study, specifically, a well-graded gray cinder aggregate and a rather poorly-graded red cinder aggregate both classified as A-1-a (AASHTO). Two subgrade soils were also tested. They were classified as A-2-4 (AASHTO). The grain size distribution for each material is shown in Figure 3.5 to 3.8.

The specific gravities ranged from 1.89 to 2.69 for the materials considered as indicated in Table 3.1. It is interesting to note that a low value of specific gravity for gray cinder aggregate was obtained. This is owing to the fact that the cinder aggregate is very porous, therefore, a longer soaking period may be required to obtain a bulk specific gravity (saturated surface dry basis). The specific gravity test results from ODOT ranged from 2.60 to 2.75.

The results of the Standard Proctor Compaction test for two subgrade soils are shown in Figure 3.9 and 3.10. The maximum dry density and optimum water content for the McKenzie subgrade soil are about 1750 kg/m^3 (109 pcf) and 15.5%, respectively, and the test results from ODOT are about 1570 kg/m^3 (98 pcf) and 17.5%, respectively. The maximum dry density and optimum water

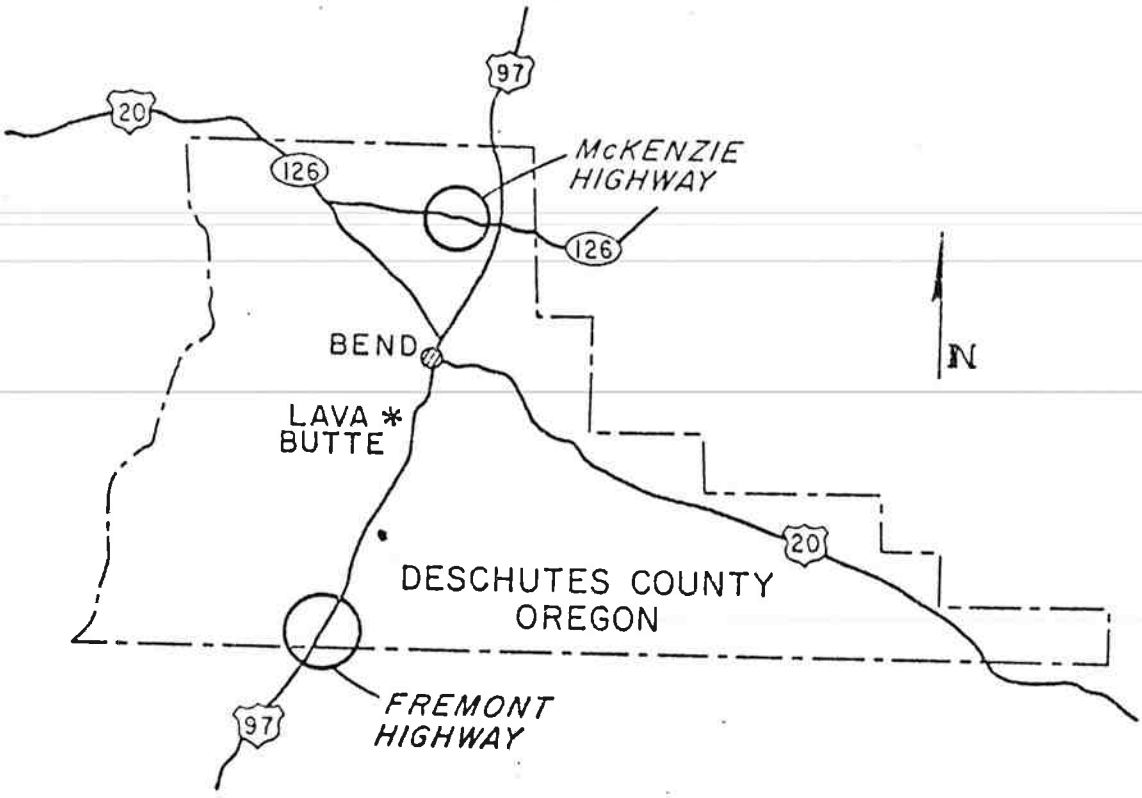

Note: Study Locations are circled

FIG. 3.4 LOCATION MAP - FREMONT AND MCKENZIE HIGHWAY STUDY LOCATIONS (after Hull et al, 1980)

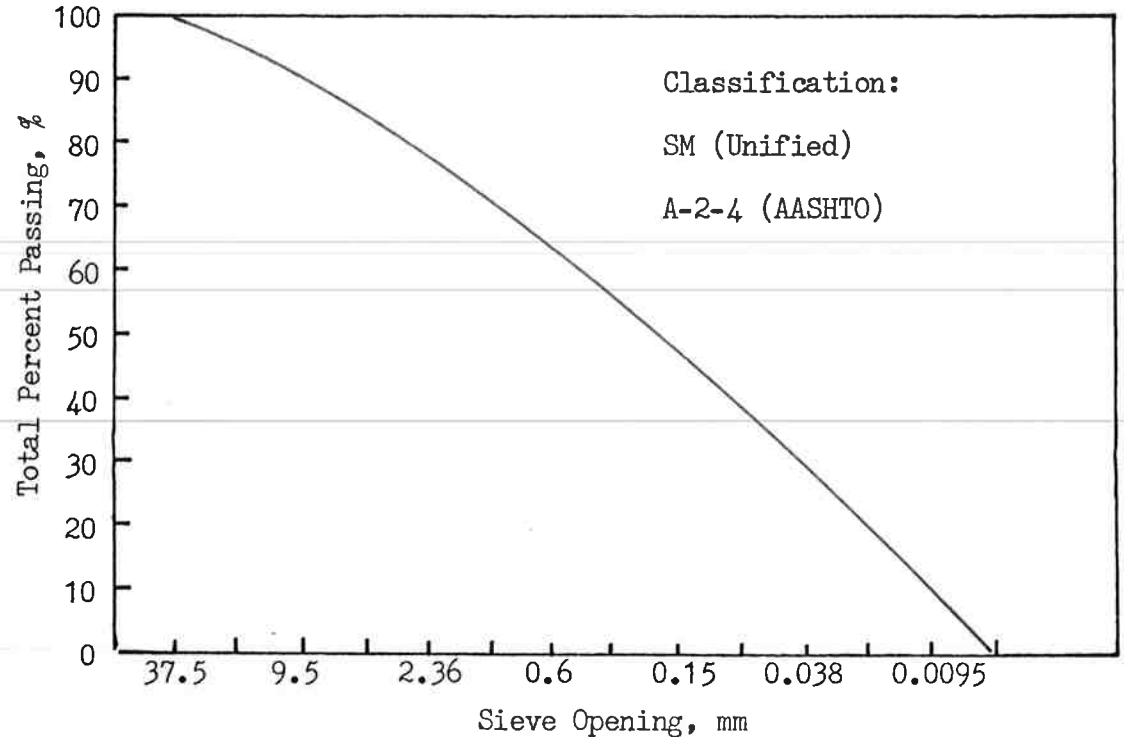

FIG. 3.5 GRADATION ANALYSIS - MCKENZIE SUBGRADE SOIL

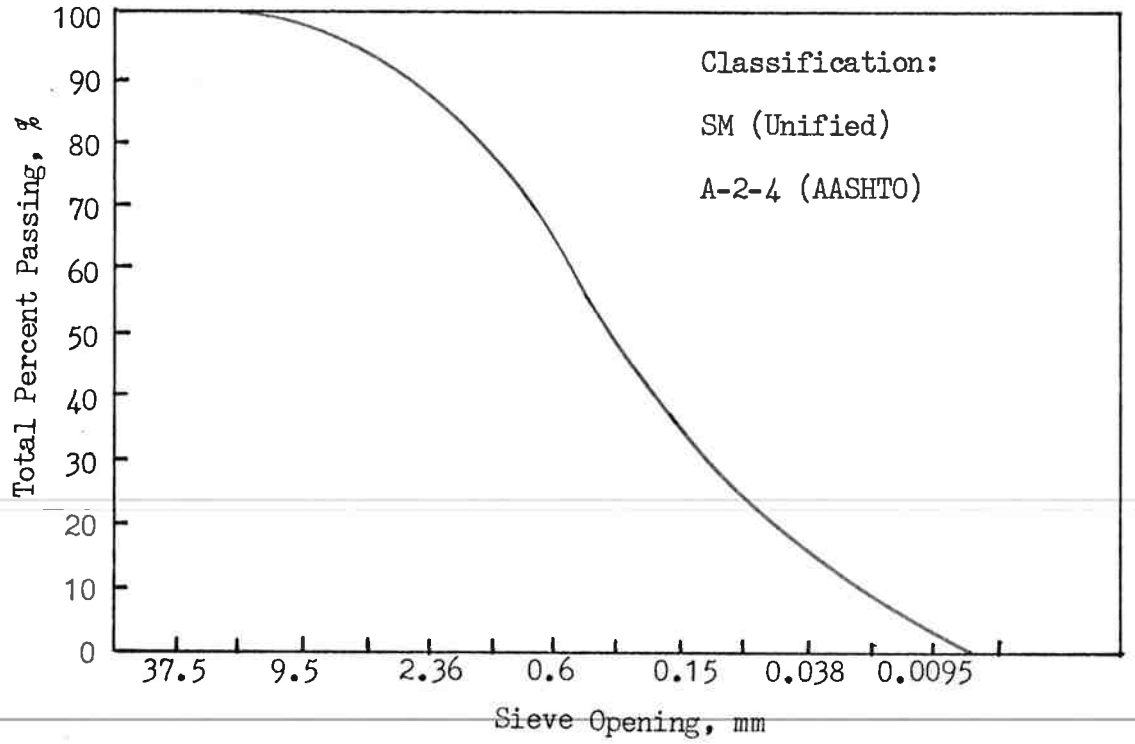

FIG. 3.6 GRADATION ANALYSIS - FREMONT SUBGRADE SOIL

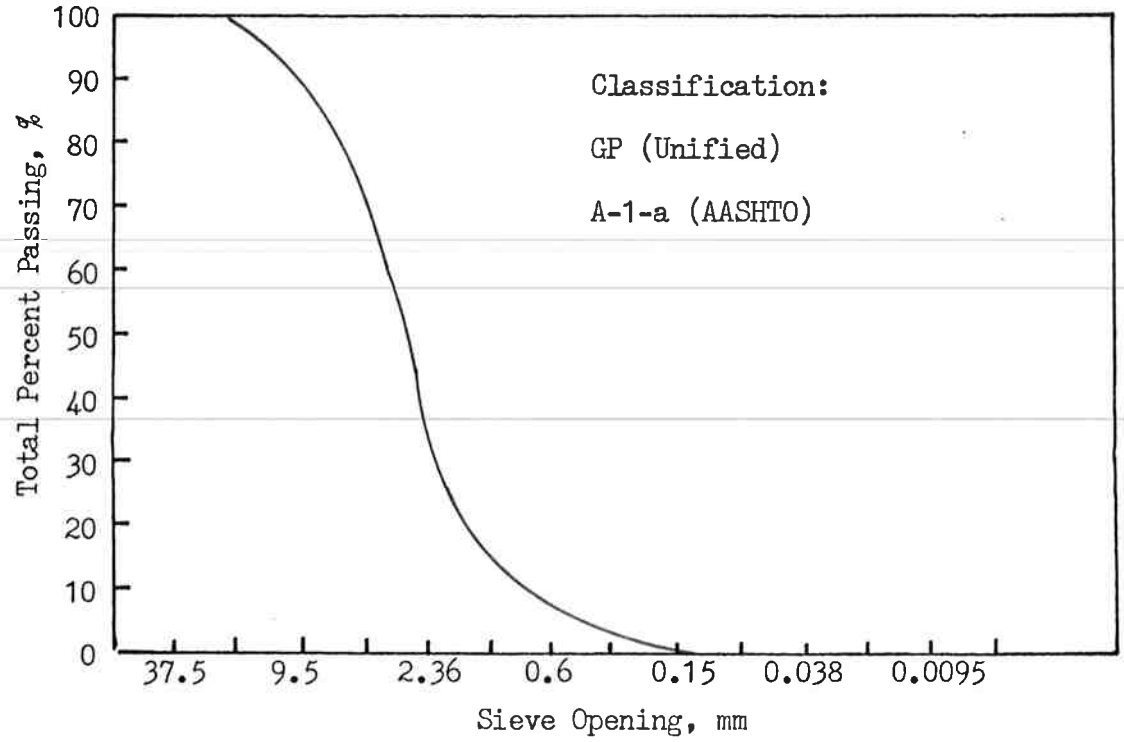

FIG. 3.7 GRADATION ANALYSIS - GRAY CINDER BASE

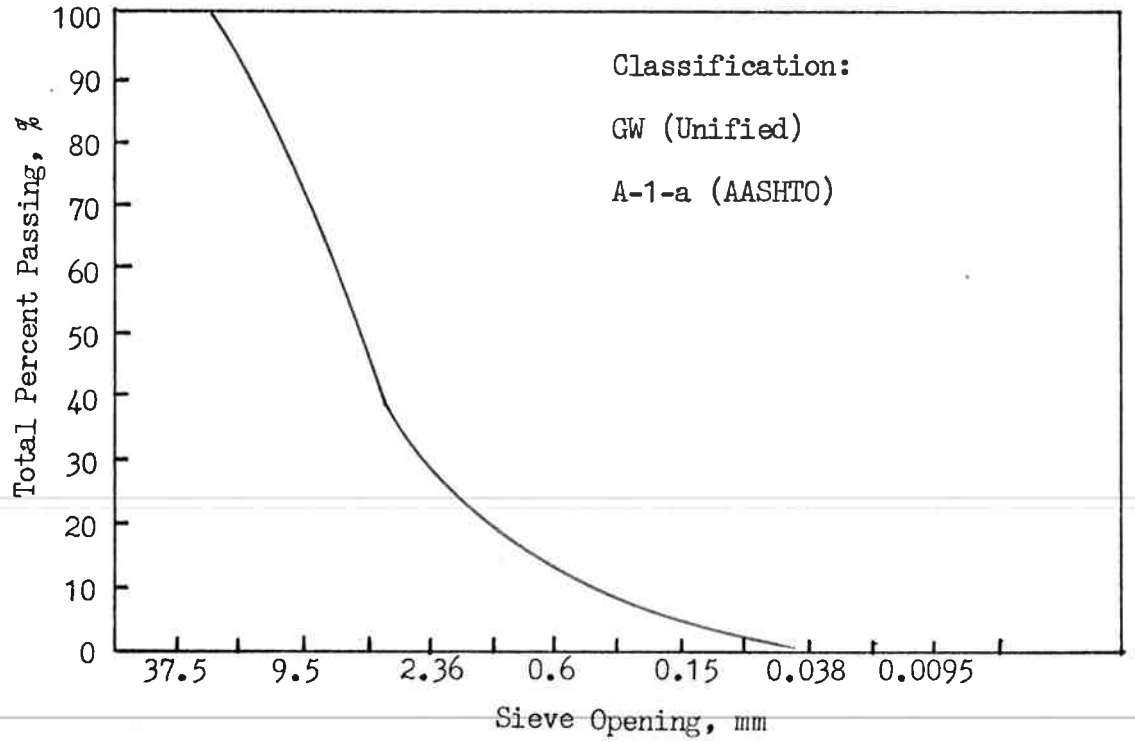

FIG. 3.8 GRADATION ANALYSIS - RED CINDER BASE

Table 3.1 SPECIFIC GRAVITY OF TEST MATERIALS

	Fremont Subgrade	McKenzie Subgrade	Gray Cinder	Red Cinder
Specific Gravity	2.53	2.55	1.89	2.69

Note: Only materials passing 6 mm No. 4 sieve was used in the specific gravity test.

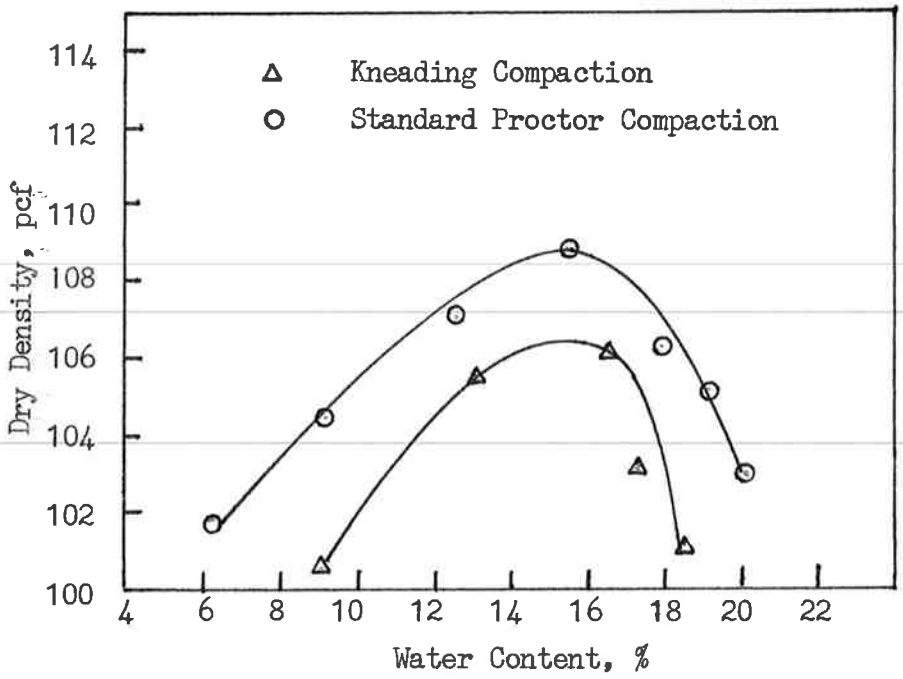

FIG. 3.9 MOISTURE-DENSITY RELATIONSHIP - MCKENZIE SUBGRADE SOIL

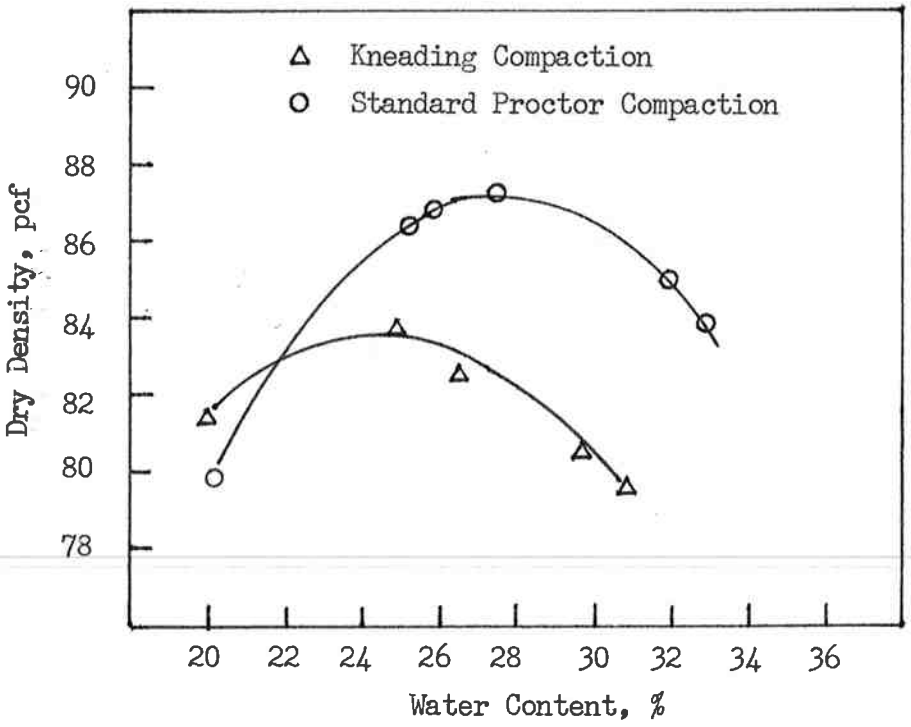

FIG. 3.10 MOISTURE-DENSITY RELATIONSHIP - FREMONT SUBGRADE SOIL

content for the Fremont subgrade soil are about 1400 kg/m^3 (87.5 pcf) and 28%, respectively, and the test results from ODOT are about 1300 kg/m^3 (81 pcf) and 26%, respectively.

3.3 Specimen Preparation

3.3.1 Gradation Adjustment

The gradations of the materials as received are given in Table 3.2. Before a material can be tested the gradation must be adjusted (ODOT Test Method 108-74). Only the materials passing the 19 mm (3/4 in.) sieve are used in the "R" value tests, as well as the resilient modulus tests. The adjusted specimen gradations for each material are given in Table 3.3.

3.3.2 Water Content and Dry Density

Specimens for the "R" value test were prepared at water contents above and below the optimum water content determined from the Standard Proctor Compaction test. The specimens were compacted with a kneading compactor. Specimens for the modulus tests were prepared at water contents and dry densities determined from the "R" value test and were compacted with a 24.5 N (5.5 lb) compaction hammer.

In all tests, the water contents were controlled by drying the batched sample in an oven at 100°C for 6 to 12 hours. One half to two-thirds of the required water was added and the samples were placed in a covered container with an identification ticket and stored in a humidity room for another 6 to 12 hours. Before compaction, the amount of water necessary to reach the desired water content was added and mixed thoroughly.

The detailed test procedure for the sample batching and specimen preparation for the "R" value test is given in ODOT Test Method 108-74.

Table 3.2 GRAIN SIZE ANALYSIS AS RECEIVED

	McKenzie Subgrade	Fremont Subgrade	Gray Cinder	Red Cinder
Sieve Size	% Passing	% Passing	% Passing	% Passing
25 mm (1 in.)	97.9	100	100	100
19 mm (3/4 in.)	97.0	100	99.0	99.2
12.5 mm (1/2 in.)	93.3	100	96.3	83.6
9.5 mm (3/8 in.)	89.3	99.5	88.2	64.3
6.3 mm (1/4 in.)	87.2	98.1	80.1	50.3
4.75 mm (No. 4)	85.1	96.9	69.1	45.5
2.36 mm (No. 8)	80.2	91.4	34.9	25.2
.425 mm (No. 40)	59.1	50.3	2.4	9.9
.250 mm (No. 60)	47.4	31.6	0.9	7.6
.075 mm (No. 200)	34.7	17.0	0.1	2.9

Table 3.3 GRAIN SIZE ADJUSTED FOR "R" VALUE AND RESILIENT MODULUS TEST

	McKenzie Subgrade	Fremont Subgrade	Gray Cinder	Red Cinder
Sieve Size	% Retained	% Retained	% Retained	% Retained
12.5 mm (1/2 in.)	3.8	0	2.7	15.7
9.5 mm (3/8 in.)	4.2	0.5	8.1	19.5
6.3 mm (1/4 in.)	2.1	1.4	8.1	8.0
4.75 mm (No. 4)	2.2	1.2	11.1	10.9
Passing 4.75 mm (No. 4)	87.7	96.9	70.0	45.9

3.4 Test Equipment and Procedures

This section briefly describes the test equipment and procedures for the repeated load triaxial and diametral modulus tests and the Hveem stabilometer "R" value test.

3.4.1 Repeated Load Triaxial Resilient Modulus Test

The repeated load triaxial test system employed in the study is shown in Figure 3.11. The electro-pneumatic repeated load test system is capable of testing with a load pulse over a range of frequencies from 0.5 to 7.0 Hz and a duration range from 0.02 to 1.0 sec. A repeated load duration of 0.1 sec and load frequency of 0.5 Hz was chosen in the study.

The test specimens, 100 mm (4 in.) in diameter by 250 mm (10 in.) in height, were enclosed in rubber membranes. The repeated load was measured with a 4450 N (1000 lb) load cell. The vertical deformations were measured with two Linear Variable Differential Transformers (LVDT's). The voltage output from the load cell and LVDT's were input to a two channel strip chart recorder. The specimens were preconditioned with 1200 load repetitions of a deviator axial stress of 69 kpa (10 psi) and a confining pressure of 28 kpa (4 psi) before resilient modulus tests were conducted. Four confining pressures (14 kpa (2 psi), 28 kPa (4 psi), 42 kpa (6 psi) and 55 kPa (8 psi)) and three deviator stress levels (29 kPa (4.2 psi), 41 kpa (6.0 psi) and 58 kPa (8.4 psi)) were used for the subgrade soils in the study. Seven confining pressures (14 kPa (2 psi), 28 kPa (4 psi), 35 kPa (5 psi), 42 kPa (6 psi), 55 kPa (8 psi), 69 kPa (10 psi), 138 kPa (20 psi)) and six axial deviator stress levels (29 kPa (4.2 psi), 41 kPa (6.0 psi), 58 kPa (8.4 psi), 104 kPa (15.1 psi), 209 kPa (30.3 psi), and 407 kPa (59 psi)) were used in the study for the cinder aggregates. The test procedures employed are essentially the same as used in previous studies (Filz (1978), Clemmons (1979)).

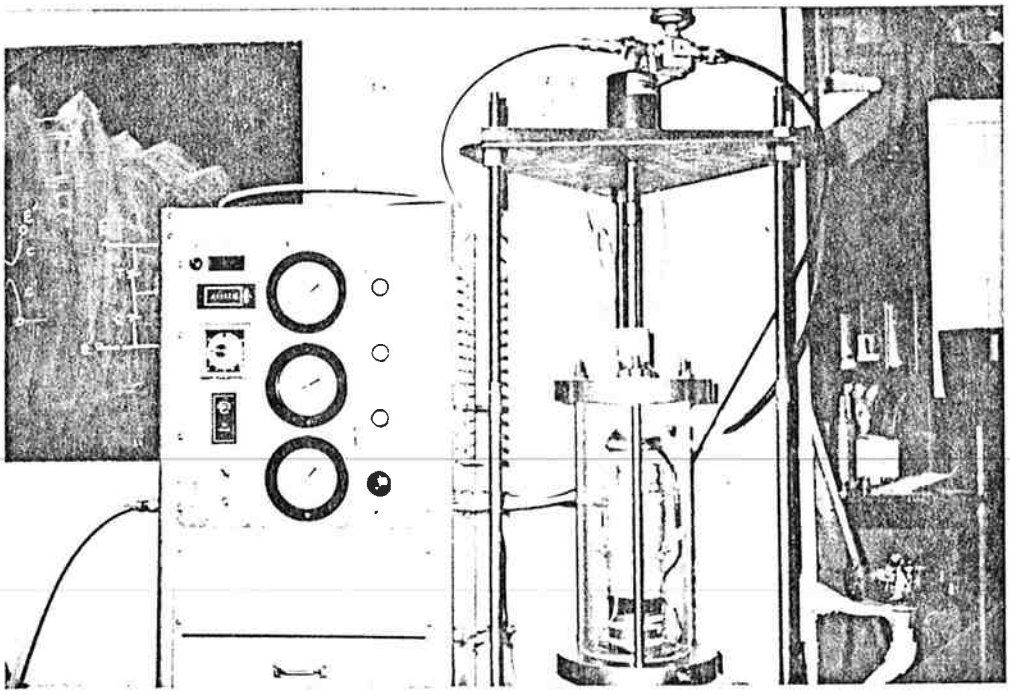

(a) Overall System

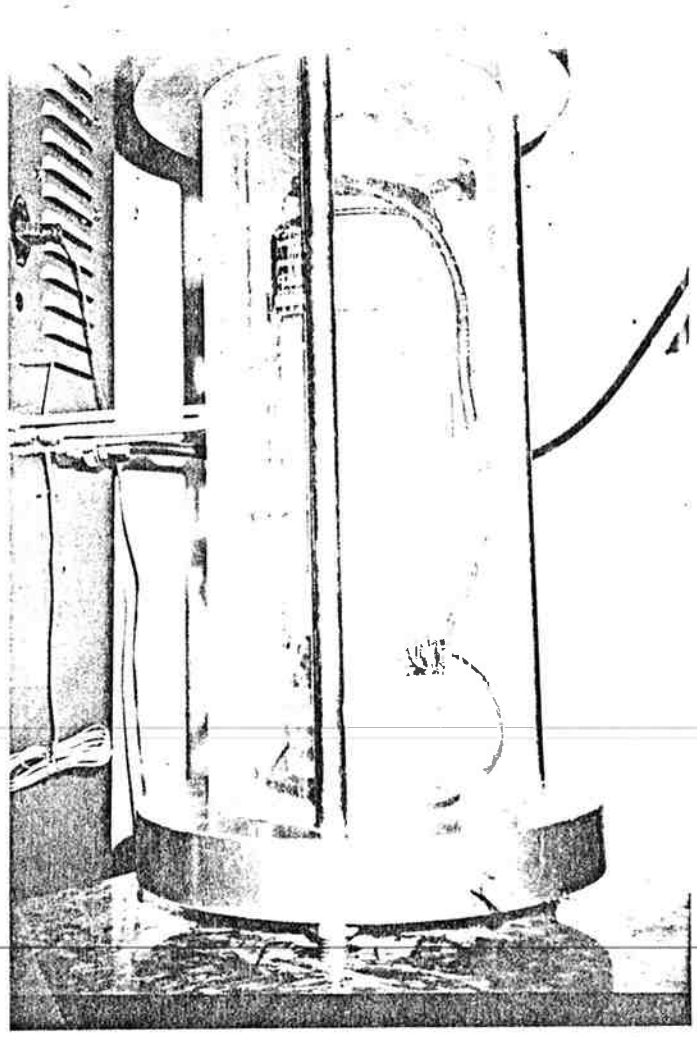

(b) Close-up of Triaxial Cell

FIGURE 3.11 REPEATED LOAD TRIAXIAL CELL

3.4.2 Repeated Load Diametral Resilient Modulus Test

The repeated load diametral test system used in the study is essentially the same as the system employed by Evans (1980) with some modifications to measure the vertical deformation (see Figure 3.12). The electro-pneumatic repeated load test system is capable of testing with a load pulse over a range of frequencies from 0.5 to 7 Hz and a duration from 0.02 to 1.0 sec. A cyclic load duration of 0.1 sec and a load frequency of 0.5 Hz were used in the study.

The test specimens were compacted with a 24.5 N (5.5 lb) compaction hammer. The compacted specimens were transferred to a split mold (as shown in Figure 3.13). The specimen was enclosed between two aluminum plates, two teflon sheets and a rubber membrane (as shown in Figure 3.14). A vacuum was applied to confine the specimen. The specimens were preconditioned with 1200 load repetitions of a 116 N (26.2 lb) deviator diametral load and confining pressure of 28 kPa (4 psi).

The repeated load was measured with a 4450 N (1000 lb) load cell. The horizontal deformations were measured with two ± 0.25mm (± 0.01 in.) Statham UC-3 transducers. The vertical deformations were measured with a ± 6.35 mm (0.25 in.) Schaevitz GCA-121-250 gage head LVDT. The voltage output from the load cell, transducer and LVDT were input to a Hewlett-Packard two channel strip chart recorder. A close-up of the test system is shown in Figure 3.15.

All materials were tested with three confining pressures (28, 41 55 kPa (4, 6, 8 psi)) and five diametral load levels (12, 16, 31, 47, 59 kPa (26, 35, 69, 104, 130 lb)).

The use of aluminum plates and teflon sheets in the repeated load diametral load test system violates the assumption that Equations 2.42 and 2.43 are based upon. These equations are valid only for two dimensional problems

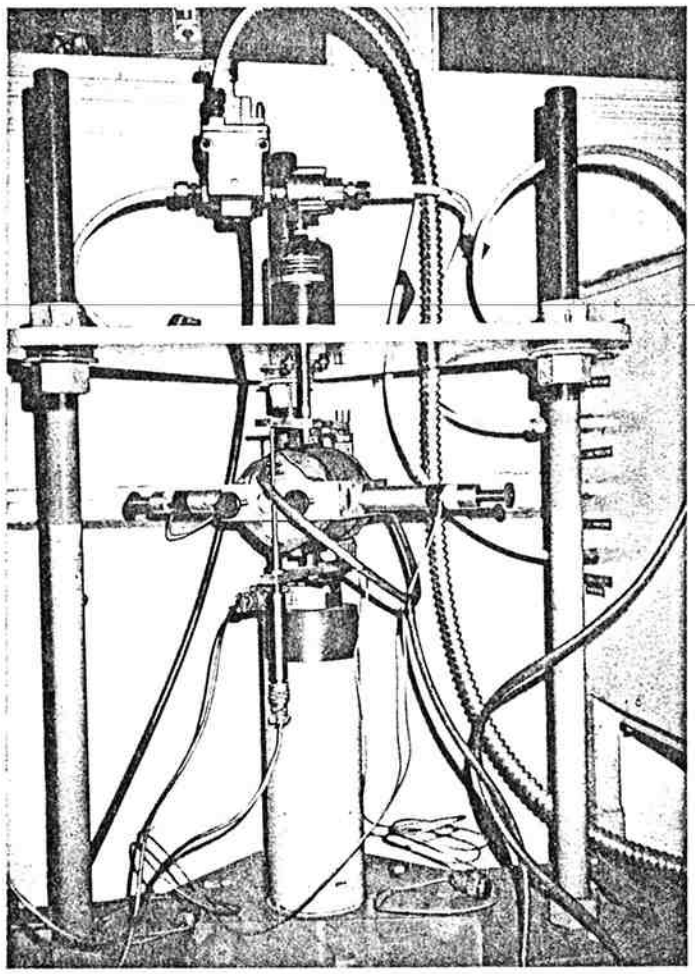

Fig. 3.12 Repeated Load Diametral Test System

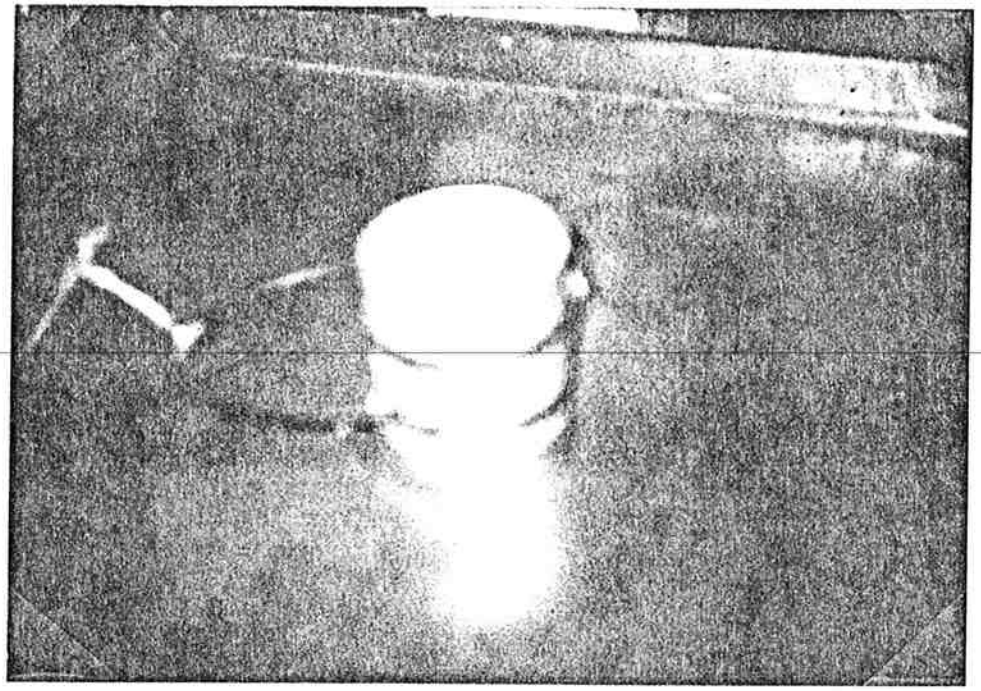

Fig. 3.13 Split Mold Used in Diametral Resilient Modulus Test

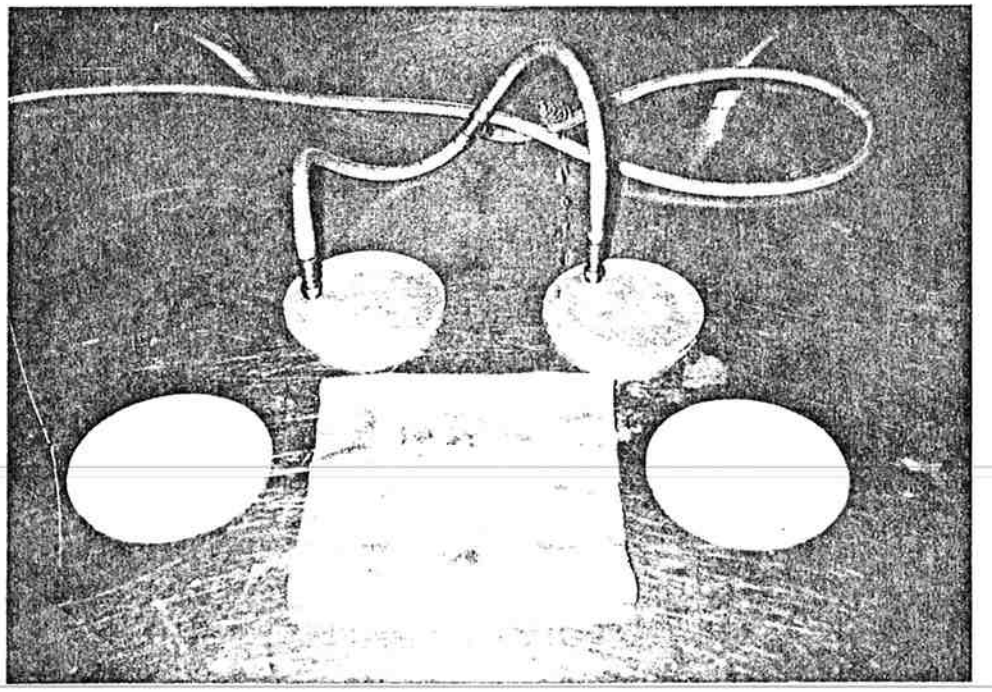

Fig. 3.14 Membrane, Aluminum Plates and Teflon Sheets Used in Diametral Resilient Modulus Test

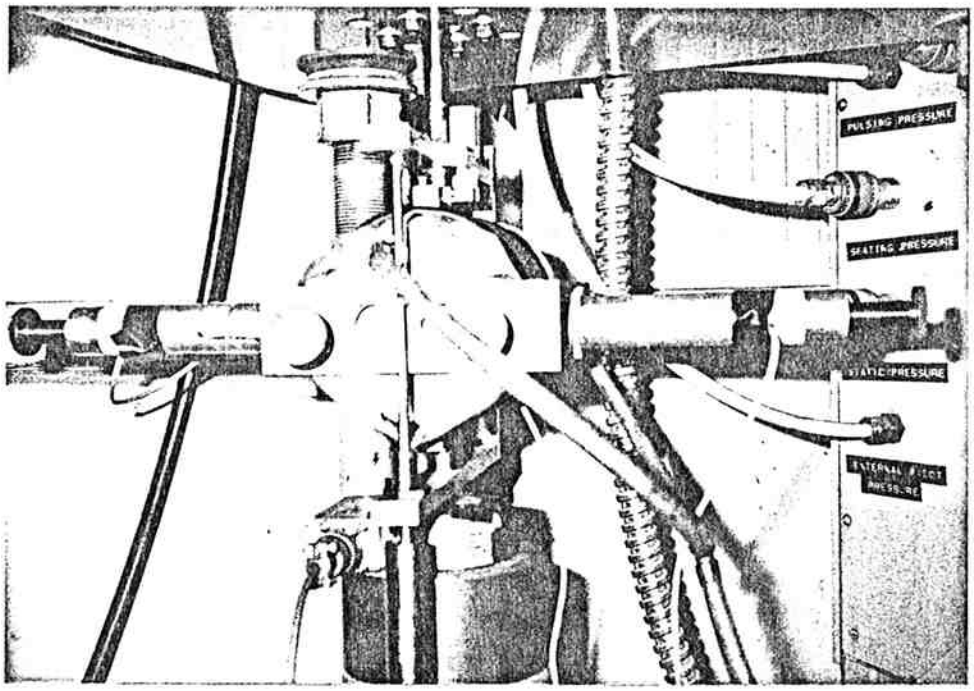

a) Front View

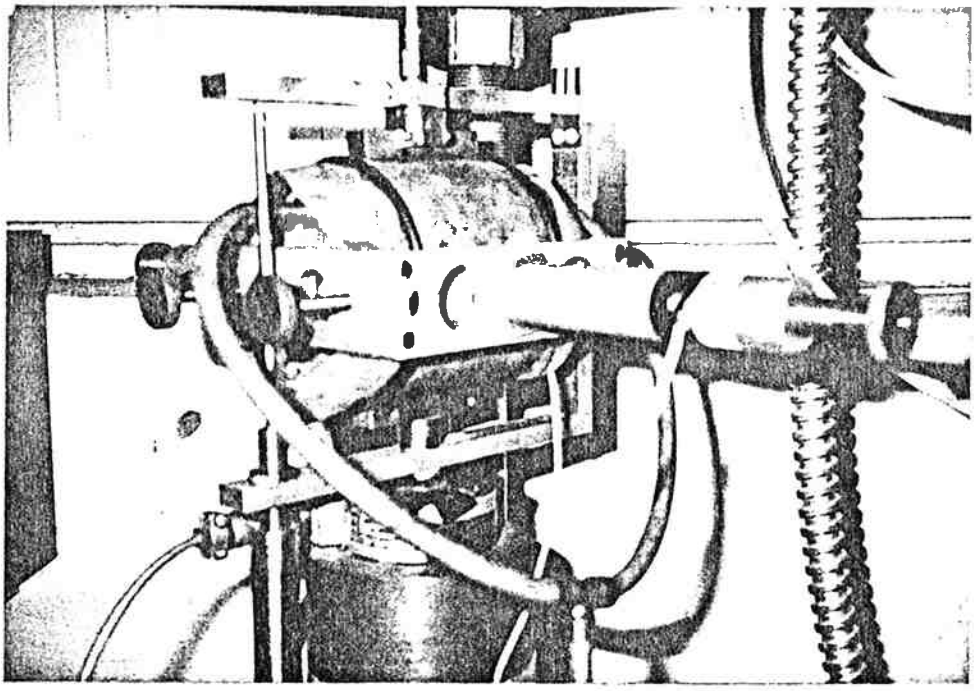

b) Side View

Fig. 3.15 Close-Up of Repeated Load Diametral Test System

(plane stress). The force applied to mount the horizontal transducer yoke on the bounding plane of the specimen and the stresses on the bounding plane induced by the repeated diametral load undoubtedly would reduce the deformations measured and may be treated as a plane strain problem.

A preliminary test program was conducted to examine the effect of the transducer yoke, rubber membranes, aluminum plates and teflon sheets on the measured vertical and horizontal deformations. A hard rubber specimen was used in the study. The test results indicate: (1) the use of the transducer yoke apparently has little influence on the measurement of vertical deformation, (2) the use of aluminum plates, teflon sheets and rubber membranes apparently reduces the vertical deformation measured but has little influence on the measurement of horizontal deformation, and (3) the resilient moduli associated with higher values of vertical deformation are about 10% to 25% lower than those associated with lower values of vertical deformation (refer to Appendix A).

Based upon these test results, it seems reasonable to conclude that the violations associated with simplifying the repeated load diametral test systems employed in the study to two dimensional problems will lead to slightly higher values of resilient modulus and higher values of Poisson's ratio. However, at present, it appears reasonable to adopt this test system for evaluation of resilient properties of unbound materials.

3.4.3 Hveem Stabilometer Resistance Value Test

This section briefly describes the test procedures for the "R" value test. Additional details may be found in the following references: ODOT Test Method 105-72 (1978), AASHTO T190-74 (1978), and California Test Method No. 301-F (1971). The procedure employed in the study is as follows:

(1) Prepare and Compact Specimen - A cylindrical specimen 100 mm (4 in.) in diameter and 64 mm (2.5 in.) in height is prepared at the desired water content. Normally, four water contents are used for a complete test. The specimens are compacted with a tamping-foot kneading compactor.

(2) Test for Exudation Pressure - The compacted specimen is compressed in a standard mold until water exudes from the specimen. The water closes several electric circuits wired in parallel through the base plate of the exudation measuring device. The exudation pressure is the pressure associated with five of the six circuits closed.

(3) Test for Expansion Pressure - After the exudation pressure test is complete, the specimen is subjected to the expansion pressure test. A perforated brass plate is placed on the specimen and the specimen is covered with 200 ml (200 CC) of water and allowed to stand for 16 to 20 hours. The expansion of the specimen during this period is measured with a dial gage.

(4) Stabilometer Resistance Value Test - After the expansion pressure test is complete, the specimen is placed in the stabilometer. The vertical pressure is applied slowly at a speed of 1.3 mm/min. (0.05 in./min.) until it reaches 1120 kpa (160 psi). The horizontal pressure developed is read immediately. The vertical pressure is reduced to 550 kPa (80 psi) and the horizontal pressure is reduced to 34 kPa (5 psi) with the displacement pump. Finally, the turns of the displacement pump required to bring the horizontal pressure to 690 kPa (100 psi) are determined.

The resistance value of the material is computed from the following expression:

$$R = 100 - \frac{100}{(2.5/D)\ ((P_v/P_h) - 1\ ) + 1} \qquad (3.1)$$

in which, R = Hveem stabilometer resistance value

P_v = vertical pressure in psi, 1100 kpa (160 psi)

P_h = horizontal pressure in psi at P_v = 1100 kPa (160 psi)

D = turns of the displacement pump to increase pressure from 34 kPa to 69 kPa (5 to 100 psi)

The "R" value test equipments employed in the study is shown in Figure 3.16.

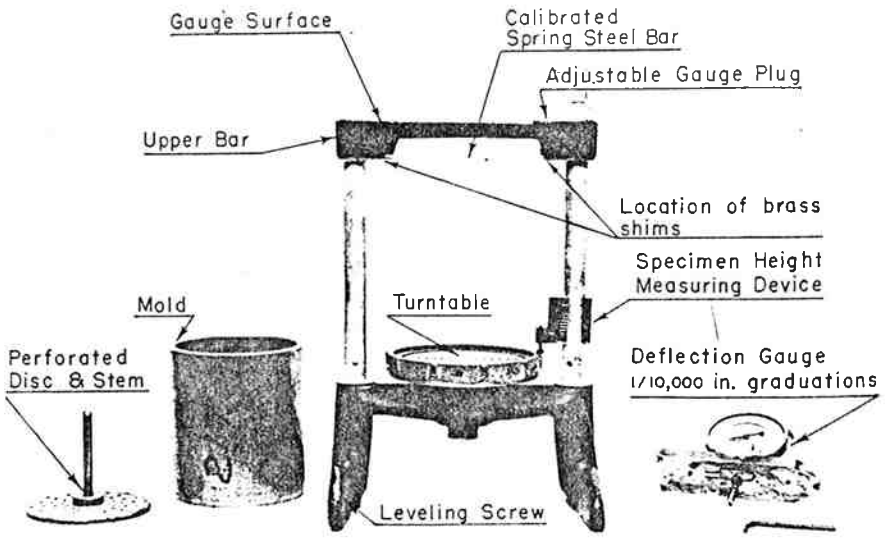

a) Expansion Pressure Device and Accessories

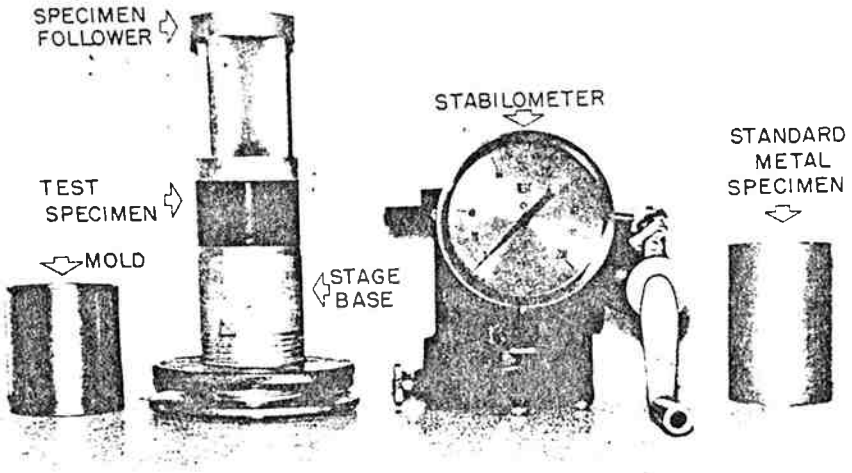

b) Stabilometer and Accessories

Fig. 3.16 "R" VALUE TEST SET UP (AFTER AASHTO)

CHAPTER 4

TEST RESULTS

4.1 Hveem Stabilometer Resistance Value Test Results

The "R" value test results presented in this section include: (1) comparisons of the "R" values for the "Dry specimen" (refer to section 3.1), (2) the "R" value test results over a range of water contents for each material, and (3) the determination of the design "R" value for each material.

4.1.1 Comparison of the "R" Value Test Results for the "Dry Specimen"

Tables 4.1 and 4.2 present the test results for the materials investigated in the study. Two McKenzie subgrade soils at water contents of 9.0% and 13.0% were tested. The inital dry densities[1] are about 70 kg/m^3 (4.5 pcf) (w/c = 9.0%) and 40 kg/m^3 (2.7 pcf)(w/c = 13.0%) less than the final dry densities[2]. The "R" values associated with the initial dry densities are about 7.5 (w/c = 9.0%) and 6.3 (w/c = 13.0%) less than those associated with the final dry densities. Two Fremont subgrade soil specimens at water contents of 10% and 20% were tested. The initial dry densities are about 70 kg/m^3 (4.4 pcf) and 60 kg/m^3 (3.9 pcf)(w/c = 10% and 20% respectively) less than the final dry densities. The "R" values associated with the initial dry densities are about 7.0 (w/c = 10%) and 6.0 (w/c = 20%) less than those associated with the final dry densities.

---

[1] Initial dry density is the density associated with the specimen thickness measured after kneading compaction.

[2] Final dry density is the density associated with the specimen thickness measured after the exudation pressure test.

Table 4.1 "R" VALUE TEST RESULTS FOR THE SUBGRADE SOILS

McKenzie Subgrade	Water Content (%)	9.0	13.0	16.5	17.0	18.2	19.0
	Dry Density (pcf)	100.6[1] 105.9[2]	105.3[1] 108.6[2]	106.1	103.1	101.0	98.5
	Exudation Pressure (psi)	-- +800	-- +800	138.7	183.0	94.0	0.0
	"R" Value	72[3] 79.5[4]	75[3] 82[4]	66	64	63	59
Fremont Subgrade	Water Content (%)	10.0	20.0	25.0	26.4	29.7	31.0
	Dry Density (pcf)	81[1] 86[2]	82[1] 86[2]	84	82	81	80
	Exudation Pressure (psi)	-- +800	-- +800	606	480	14.3	0.0
	"R" Value	76[3] 83[4]	79[3] 85[4]	84	81	67	63

1 psi = 6.9 kPa, 1 pcf = .16 0 kN/m^3

Note: 1 Dry density is calculated based on the thickness of the specimen measured after the kneading compaction.

2 Dry density is calculated based on the thickness of the specimen measured after the exudation pressure test.

3 "R" value is corrected based on the thickness of the specimen measured after the kneading compaction.

4 "R" value is corrected based on the thickness of the specimen measured after the exudation pressure test.

TABLE 4.2 "R" VALUE TEST RESULTS FOR CINDER BASE MATERIALS

Gray Cinder Base	Water Content (%)	10.0	32.6	36.9	41.1	50.0	55.0
	Dry Density (pcf)	44.3[a] 51.8[b]	49.5	51.9	49.8	45.3	45.1
	Exudation Pressure (psi)	-- +800	788	676	557	484	0
	"R" Value	73[c] 84[d]	80	80	77	79	73
Red Cinder Base	Water Content (%)	15.0	17.3	19.1	20.0	20.9	25.0
	Dry Density (pcf)	69[a] 74[b]	68	69	69	68	67
	Exudation Pressure (psi)	-- +800	298.4	115.4	119.4	119.4	16
	"R" Value	78[c] 75[d]	72	75	73	72	72

1 psi = 6.9 kPa, 1 pcf = .16 0 kN/m^3

Note: a Dry density is calculated based on the thickness of the specimen measured after the kneading compaction.

b Dry density is calculated based on the thickness of the specimen measured after the exudation pressure test.

c "R" value is corrected based on the thickness of the specimen measured after the kneading compaction.

d "R" value is corrected based on the thickness of the specimen measured after the exudation pressure test.

One Gray cinder base specimen at a water content of 10% was tested. The initial dry density is 120 kg/m^3 (7.5 pcf) less than the final dry density. The "R" value associated with the initial dry density is about 11.0 less than that associated with the final dry density. One Red cinder base specimen at a water content of 15% was tested. The initial dry density is about 80 kg/m^3 (4.8 pcf) less than the final dry density. The "R" value associated with the final dry density is about 3.3 less than that associated with the initial dry density. Obviously, the dry densities and "R" values for those specimens subjected to 5500 kPa (800 psi) axial pressure were higher than those specimens which omitted the exudation pressure test.

4.1.2 "R" Value Test Results Over a Range of Water Contents

The "R" value test results over a range of water contents for each material are given in Tables 4.1 and 4.2. Eight McKenzie subgrade soil specimens were tested at water contents ranging from 9% to 19%. The "R" value test results range from 59 to 82. Eight Fremont subgrade soil specimens were tested at water contents ranging from 10% to 31%. The "R" value test results range from 63 to 85. Seven Gray cinder base specimens at water contents ranging from 10% to 55% were tested. The "R" value test results range from 73 to 80. Seven Red cinder base specimens at water contents ranging from 15% to 25% were tested. The "R" value test results range from 72 to 78.

Figures 4.1 to 4.4 demonstrate the sensitivity of the "R" value to the water content and dry density. Generally speaking, the "R" value increases with increasing dry density and decreases with increasing water content. The ODOT "R" value test results are summarized in Appendix C. Four McKenzie subgrade soil specimens were tested at water contents ranging from 19.2% to 24.5%. The "R" value test results range from 66 to 80. Four Fremont subgrade

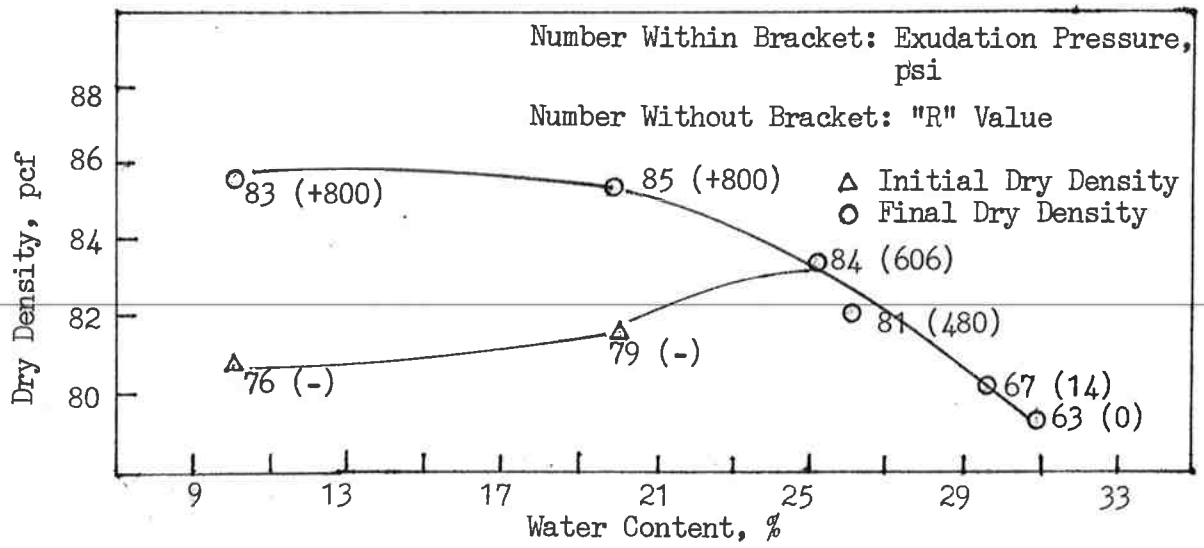

FIG. 4.1 "R" VALUE TEST RESULTS - FREMONT SUBGRADE SOILS

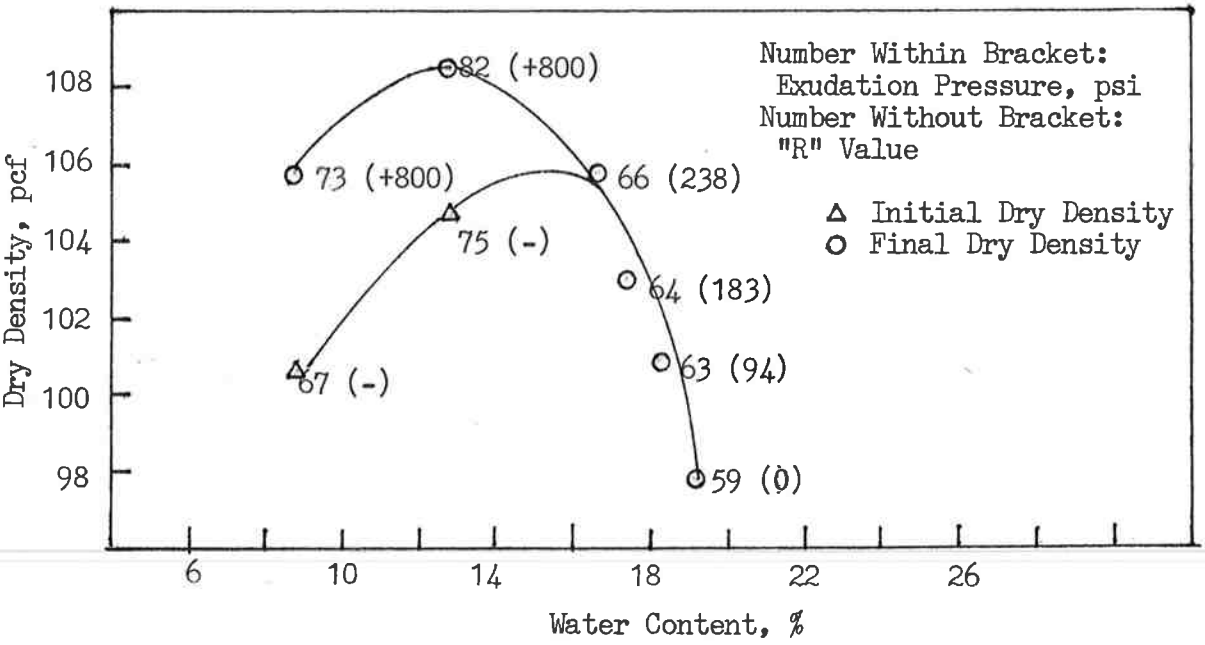

FIG. 4.2 "R" VALUE TEST RESULTS - MCKENZIE SUBGRADE SOILS

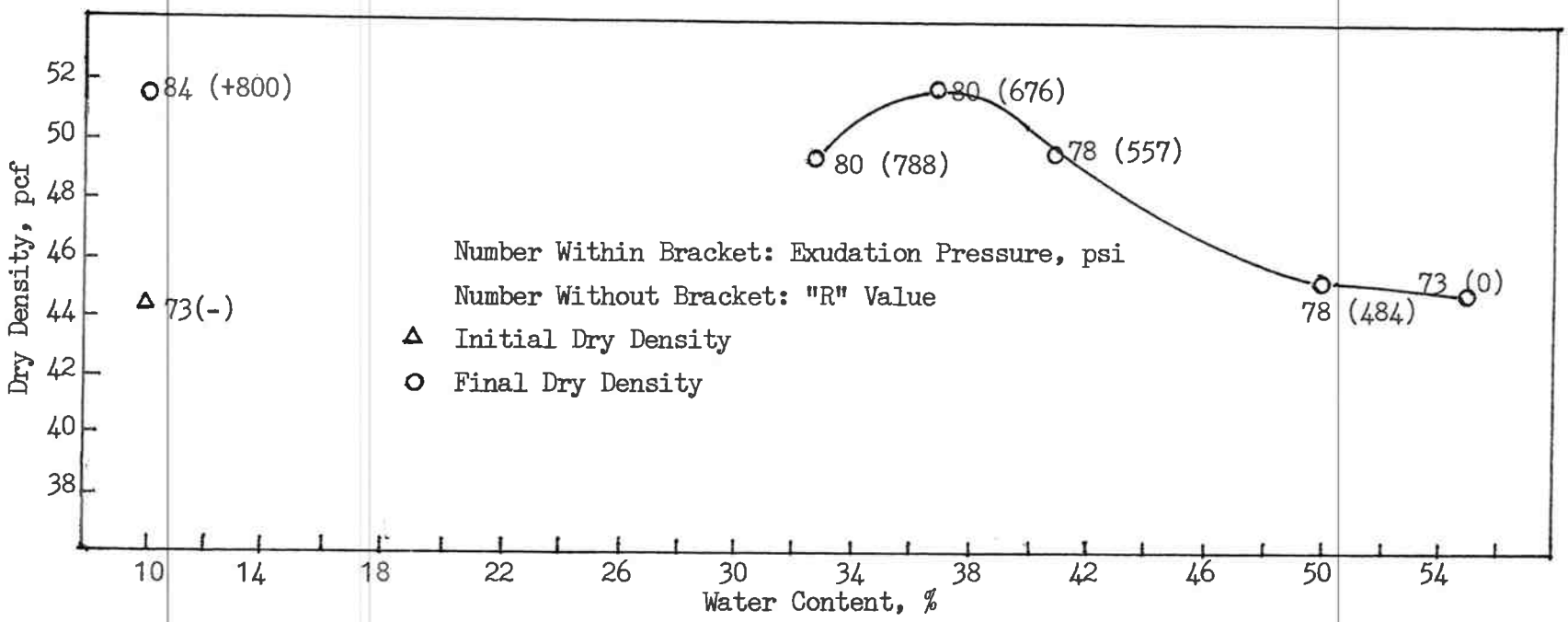

FIG. 4.3 "R" VALUE TEST RESULTS - GRAY CINDER BASE MATERIALS

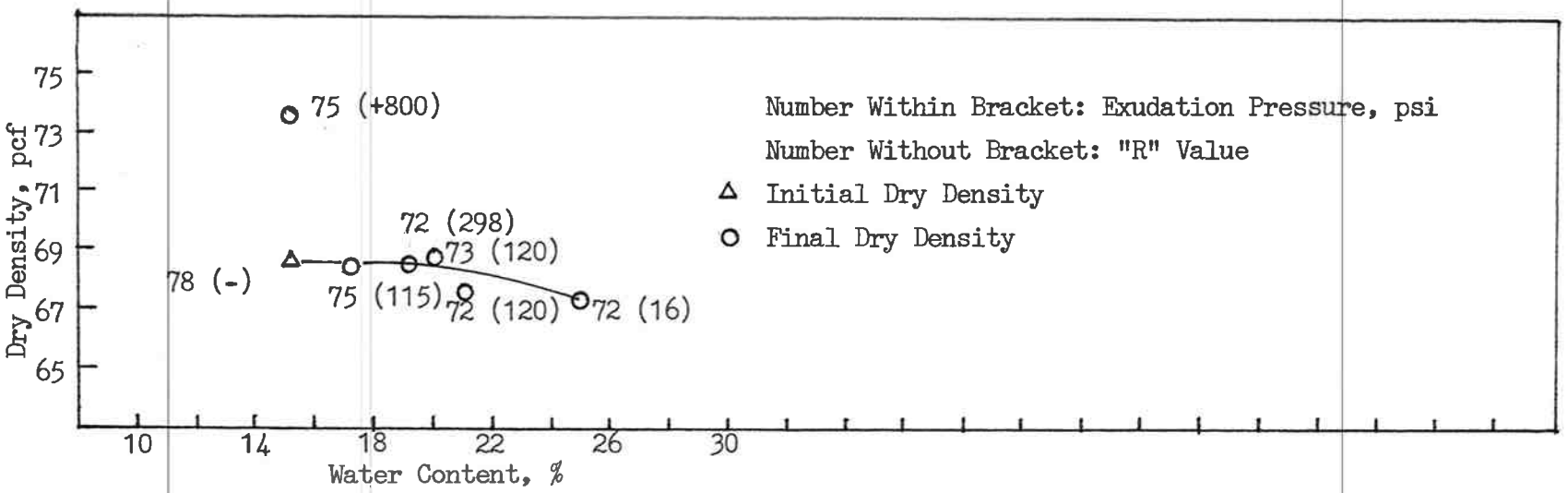

FIG. 4.4 "R" VALUE TEST RESULTS - RED CINDER BASE MATERIALS

soil specimens were tested at water contents ranging from 24.1% to 32.1%. The "R" value test results range from 72 to 85. Four McKenzie base specimens were tested at water contents ranging from 15.7% to 19.8%. The "R" value test results range from 77 to 87. Four Fremont base specimens were tested at water contents ranging from 10.7% to 15.8%. The "R" value test results range from 67 to 80.

4.1.3 Determination of the Design "R" Value for Each Material

The determination of the design "R" value based on the ODOT flexible pavement design procedure is as follows:

(1) The "R" value at 2100 kPa (300 psi) exudation pressure is selected as the design value for soils containing less than 90% passing the 6 mm (No. 4) sieve.

(2) The design "R" value for other soils is the value at the "wet side" water content corresponding to 95% maximum dry density determined from the standard Proctor compaction test (T-99).

The design "R" value for each material is listed in Table 4.3. It should be noted that a design "R" value for the Fremont subgrade soils was selected at 2100 kPa (300 psi) exudation pressure even though it contains more than 95% passing 6 mm (No. 4) sieve materials. This is owing to the fact that the specimen which had 95% maximum dry density according to the Proctor compaction test result corresponds approximately to a water content of 33.5%. At this water content the material is too wet to conduct the "R" value test. The criteria described above are applicable to cohesive soils. All other materials met the first requirement; hence, the design "R" values are determined at an exudation pressure of 2070 kPa (300 psi).

The design "R" values for each material based on ODOT "R" value test results are also summarized in Appendix C. These design "R" values are

TABLE 4.3 Design "R" Values for Test Materials

	Fremont Subgrade	McKenzie Subgrade	Gray Cinder	Red Cinder
Design "R" Value	77	68	77	73

determined based on the criteria associated with an exudation pressure of 2100 kPa (300 psi). The design "R" values determined by ODOT for McKenzie base and subgrade soil are 70 and 70, respectively. The design "R" values for Fremont base aggregate is 86 and for subgrade soil is 70.

4.2 Resilient Modulus Test Results

The resilient moduli determined with the repeated load triaxial and diametral test systems are presented in this section. Also included is (1) an examination of the change of water content before and after the modulus test, and (2) an interpretation of the test results, including the influence of the stress level and of water content and dry density.

4.2.1 Change of Water Content of Test Specimen

The water content of the test specimens measured before and after the modulus test are summarized in Tables 4.4 to 4.7. The water contents and dry densities for the "dry" subgrade soil specimens (refer to section 3.1) do not change significantly in both the triaxial and diametral test. However, for the "wet" specimens (refer to section 3.1), the differences of water content in the diametral test are more pronounced than in the triaxial test. The major water loss is due to the suction associated with the vacuum used to apply the confining pressure. The application of vacuum pressure removed water from the specimen; however, the water removed is the free water (water retained in the pores and channels or the surface of the particle) and not the held water. Some highly saturated subgrade specimens were prepared, however, the specimens apparently liquefied at the base during cyclic loading Apparently, the triaxial resilient modulus test system employed in the study is not suitable for highly saturated cohesionless soils.

Water loss for the Red cinder base materials was observed during the compaction and modulus test. The major water loss is due to the high perme-

TABLE 4.4 Comparison of Water Content and Dry Density of Triaxial and Diametral Resilient Modulus Tests - Fremont Subgrade Soil Specimens

Sample No.		A-Dry	B-Dry	C-Wet
Initial Water Content (%)	Triaxial	10.3	20.8	26.8
	Diametral	10.0	20.0	26.8
Final Water Content (%)	Triaxial	9.8	19.9	26.7
	Diametral	9.6	20.2	22.0
Initial Dry Density (pcf)	Triaxial	81.8	82.1	83.1
	Diametral	81.0	82.1	82.9

1 pcf = 16.0 kg/m^3

TABLE 4.5 Comparison of Water Content and Dry Density of Triaxial and Diametral Resilient Modulus Tests - McKenzie Subgrade Soil Specimens

Sample No.		A-Dry	B-Dry	C-Wet
Initial Water Content (%)	Triaxial	8.5	12.9	16.0
	Diametral	9.0	13.0	16.5
Final Water Content (%)	Triaxial	9.0	12.0	15.8
	Diametral	8.9	12.9	14.7
Initial Dry Density (pcf)	Triaxial	100.7	106.3	105.7
	Diametral	100.2	106.5	105.7

1 pcf = 16.0 kg/m^3

TABLE 4.6 Comparison of Water Content and Dry Density of Triaxial and Diametral Resilient Modulus Tests - Gray Cinder Base

Sample No.		A-Dry	B-Dry	C-Wet
Initial Water Content (%)	Triaxial	10.9	32.4	49.5
	Diametral	10.0	32.5	50.0
Final Water Content (%)	Triaxial	9.9	32.2	47.2
	Diametral	10.9	32.7	49.8
Initial Dry Density (pcf)	Triaxial	44.9	49.4	43.7
	Diametral	44.0	48.9	42.8

1pcf= 16.0 kg/m^3

TABLE 4.7 Comparison of Water Content and Dry Density of Triaxial and Diametral Resilient Modulus Tests - Red Cinder Base

Sample No.		A-Dry	B-Dry	C-Wet
Initial Water Content (%)	Triaxial	15.0	20.7	26.1
	Diametral	15.0	20.0	25.0
Final Water Content (%)	Triaxial	13.2	14.7	25.6
	Diametral	14.3	18.9	20.9
Initial Dry Density (pcf)	Triaxial	68.1	70.9	67.8
	Diametral	67.5	69.5	67.0

1pcf= 16.0 kg/m^3

ability of the coarse materials. No significant water losses were observed during the test for the Gray cinder base material. This is owing to the fact that the Gray cinder base materials are very porous. The water added before compaction appeared to be completely absorbed in the particles.

The dry density of the test specimens were not measured after the modulus test and were assumed equal to the initial dry density. Therefore, the following presentations concerning the influence of water content and dry density on resilient modulus and correlations between the triaxial and diametral resilient modulus are based on the initial water content and dry density values.

4.2.2 Interpretation of the Resilient Modulus Test Results

The triaxial resilient modulus test results are generally expressed in terms of the sum of the principal stresses for untreated aggregate materials. The advantages of expressing the test results in this form include: (1) emphasizing the importance of accounting for the variation of the stress states within the base layer of asphalt concrete pavements, and (2) providing a simplified basis to examine factors which may affect the resilient modulus for the materials considered. The disadvantages of this expression include (1) neglecting the importance of the effect of the principal stress ratio on the resilient modulus, and (2) increasing the difficulty associated with the comparisons between the triaxial and diametral resilient modulus.

In the diametral resilient modulus test, the deviator stresses are not distributed uniformly either along the vertical or horizontal diameter of the test specimen. Equations 2.42 and 2.43 employed in the study to compute resilient modulus and Poisson's ratio are based upon linear elasticity for an idealized material. The values of resilient modulus and Poisson's ratio should be constant for a homogeneous, isotropic and linear elastic material.

However, the values of resilient modulus and Poisson's ratio for unbound materials would not be constant owing, in part, to the nonlinear and heterogeneous properties associated with unbound materials. Based on this fact, it is suggested that the diametral test results should be termed "Equivalent" diametral resilient modulus and "Equivalent" diametral Poisson's ratio to emphasize that these values are determined and computed based upon linear elasticity and do not take into account nonlinear and heterogeneous properties associated with unbound materials.

The comparisons between resilient moduli determined with triaxial and diametral test systems may be examined assuming (1) the initial states of stress of the test specimens are identical both in the triaxial and diametral test systems, and (2) the states of biaxial deviator stress of the diametral test specimen do not affect the resilient modulus and Poisson's ratio, i.e., assuming the diametral test specimen is an idealized homogeneous, isotropic and linear elastic material. Based upon these assumptions, the comparisons between triaxial resilient modulus and diametral resilient modulus may be examined in terms of comparable states of stress. Specifically, the triaxial test results are plotted in terms of the axial compressive deviator stress, and the diametral test results are plotted in terms of the compressive deviator stress at the center of test specimen.

4.2.3 Influence of the Stress Level

4.2.3.1 Triaxial Resilient Modulus Test Results

The effect of the axial deviator stress and confining pressure on the resilient modulus for two subgrade soil specimens and two cinder base materials are shown in Figures 4.5 to 4.16. In general, the resilient modulus increased considerably with increasing confining pressure but only slightly with increasing axial compressive deviator stress.

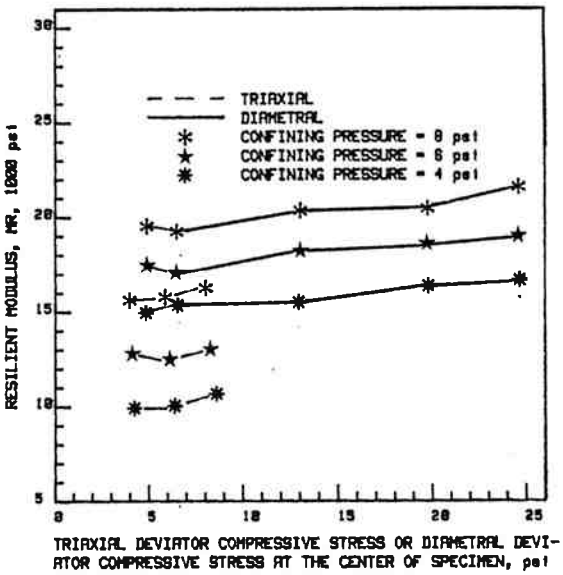

FIG.4.5 COMPARISON OF TRIAXIAL AND DIAMETRAL RESILIENT MODULUS - FREMONT SUBGRADE SOIL A-DRY, 1psi=6.9kPa

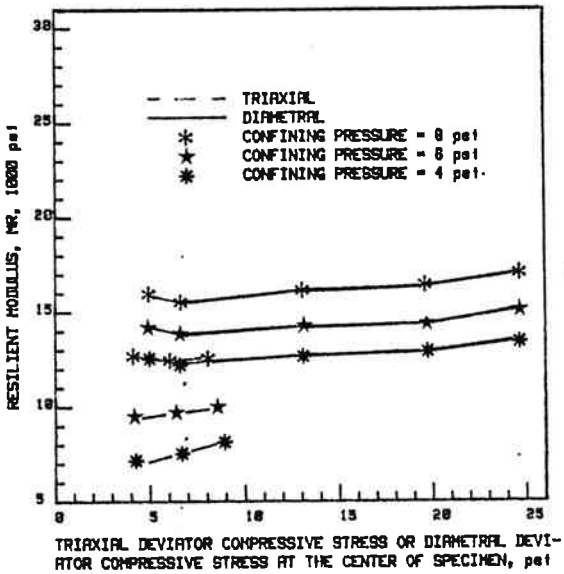

FIG.4.6 COMPARISON OF TRIAXIAL AND DIAMETRAL RESILIENT MODULUS - FREMONT SUBGRADE SOIL B-DRY, 1psi=6.9kPa

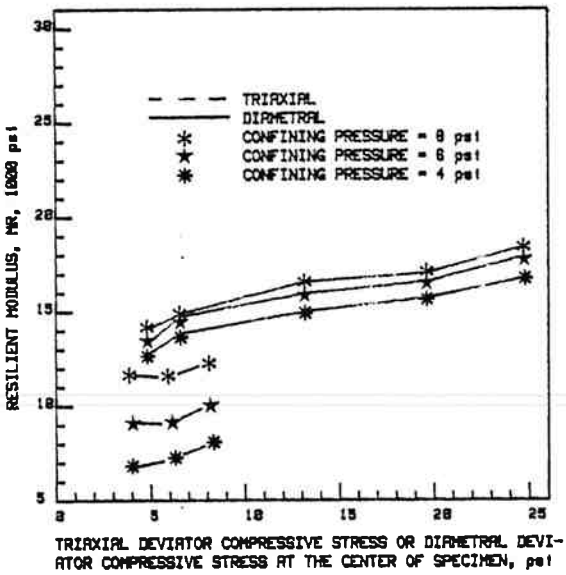

FIG.4.7 COMPARISON OF TRIAXIAL AND DIAMETRAL RESILIENT MODULUS - FREMONT SUBGRADE SOIL C-WET, 1psi=6.9kPa

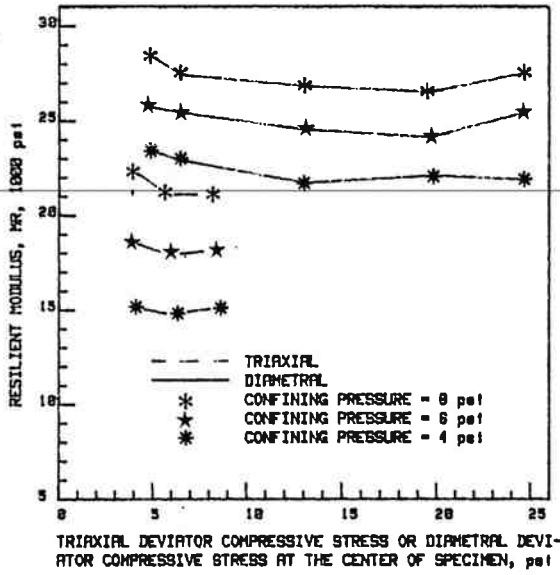

FIG.4.8 COMPARISON OF TRIAXIAL AND DIAMETRAL RESILIENT MODULUS - MCKENZIE SUBGRADE SOIL A-DRY, 1psi=6.9kPa

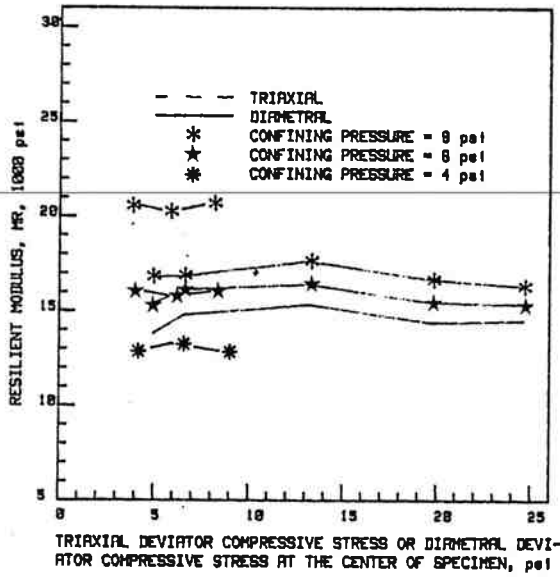

FIG.4.9 COMPARISON OF TRIAXIAL AND DIAMETRAL RESILIENT MODULUS - MCKENZIE SUBGRADE SOIL B-DRY, 1psi=6.9kPa

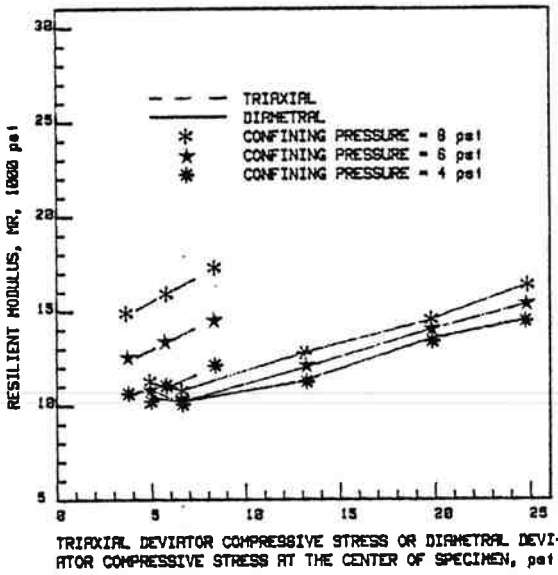

FIG.4.10 COMPARISON OF TRIAXIAL AND DIAMETRAL RESILIENT MODULUS - MCKENZIE SUBGRADE SOIL C-WET, 1psi=6.9kPa

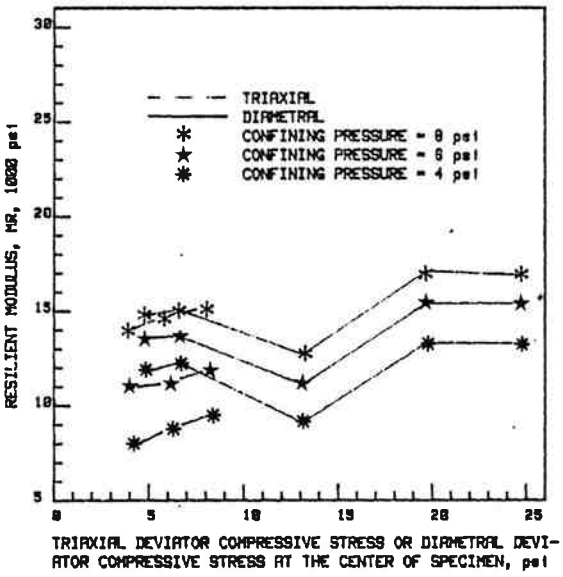

FIG.4.11 COMPARISON OF TRIAXIAL AND DIAMETRAL RESILIENT MODULUS - GRAY CINDER BASE A-DRY, 1psi=6.9kPa

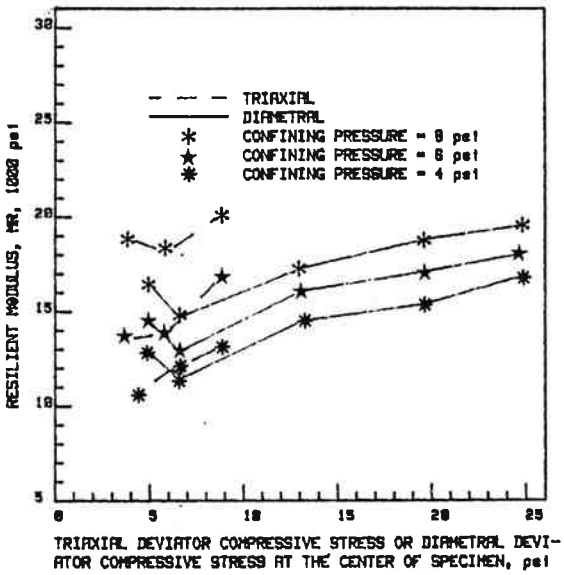

FIG.4.12 COMPARISON OF TRIAXIAL AND DIAMETRAL RESILIENT MODULUS - GRAY CINDER BASE B-DRY, 1psi=6.9kPa

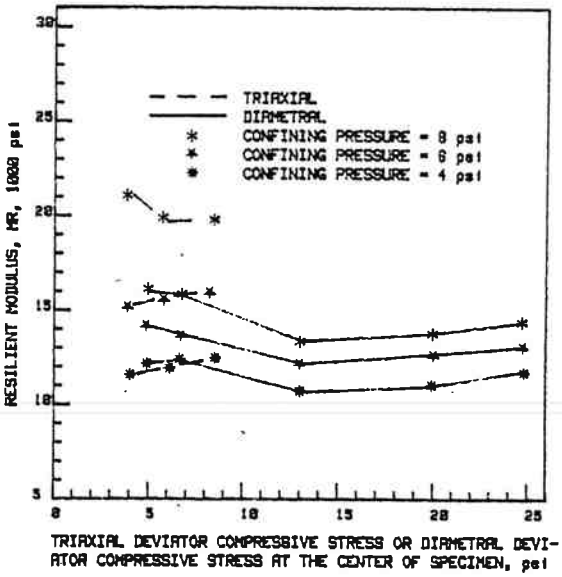

FIG.4.13 COMPARISON OF TRIAXIAL AND DIAMETRAL RESILIENT MODULUS - GRAY CINDER BASE C-WET, 1psi=6.9kPa

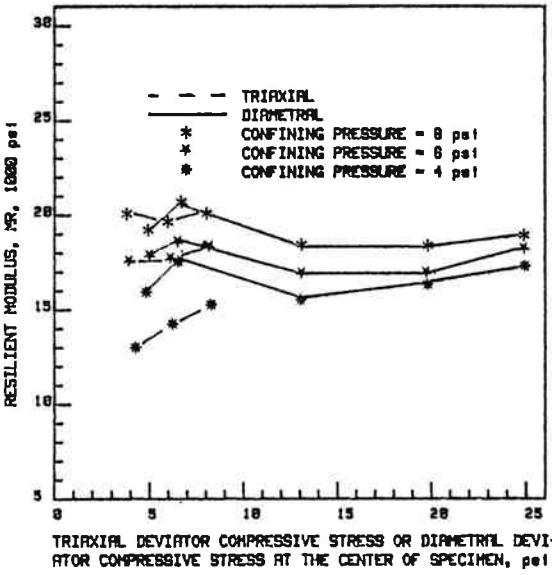

FIG.4.14 COMPARISON OF TRIAXIAL AND DIAMETRAL RESILIENT MODULUS - RED CINDER BASE A-DRY, 1psi=6.9kPa

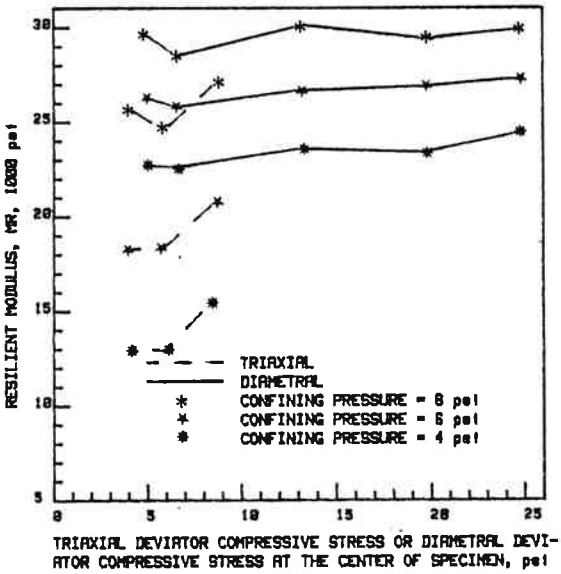

FIG.4.15 COMPARISON OF TRIAXIAL AND DIAMETRAL RESILIENT MODULUS - RED CINDER BASE B-DRY, 1psi=6.9kPa

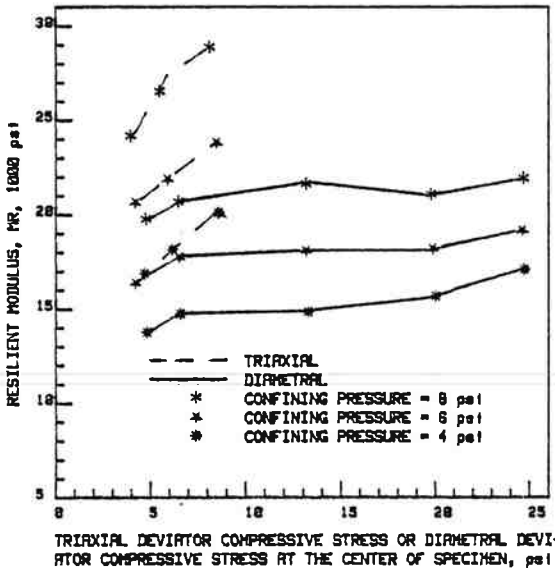

FIG.4.16 COMPARISON OF TRIAXIAL AND DIAMETRAL RESILIENT MODULUS - RED CINDER BASE C-WET, 1psi=6.9kPa

The effect of sum of the principal stresses on resilient modulus for two cinder base materials is shown in Figures 4.17 and 4.18. As shown, modulus increases greatly with increasing sum of the principal stresses.

4.2.3.2 Diametral Resilient Modulus Test Results

The effect of the deviator compressive stress at the center of the specimen and confining vacuum pressure on the resilient modulus for the four test materials are also shown in Figures 4.5 to 4.16. The effect is about the same as for the triaxial test results. In general, the resilient modulus increased considerably with increasing confining pressure but only slightly with increasing deviator compressive stress.

The diametral resilient moduli based on equations 2.42.a and 2.43.a for a plane strain problem are presented in Appendix B. The effect of the deviator compressive stress at the center of the specimen and confining pressure on the resilient modulus associated with the plane strain condition are shown in Figures B.1 to B.12. In general, the resilient modulus increased with increasing confining pressure but decreased with increasing deviator compressive stress (increasing diametral load or increasing deviator tensile stress).

4.2.4 Influence of Water Content and Dry Density

4.2.4.1 Triaxial Resilient Modulus Test Results

The effect of water content on the resilient modulus for the four test materials are shown in Table 4.8 and Figures 4.19 to 4.22. The effect of dry density on the resilient modulus for the four test materials are shown in Tables 4.9. In general, the resilient modulus decreases with increasing water content at constant value of confining pressure and axial deviator stress. It appears that water content is the major factor influencing the triaxial resilient modulus for the subgrade soils.

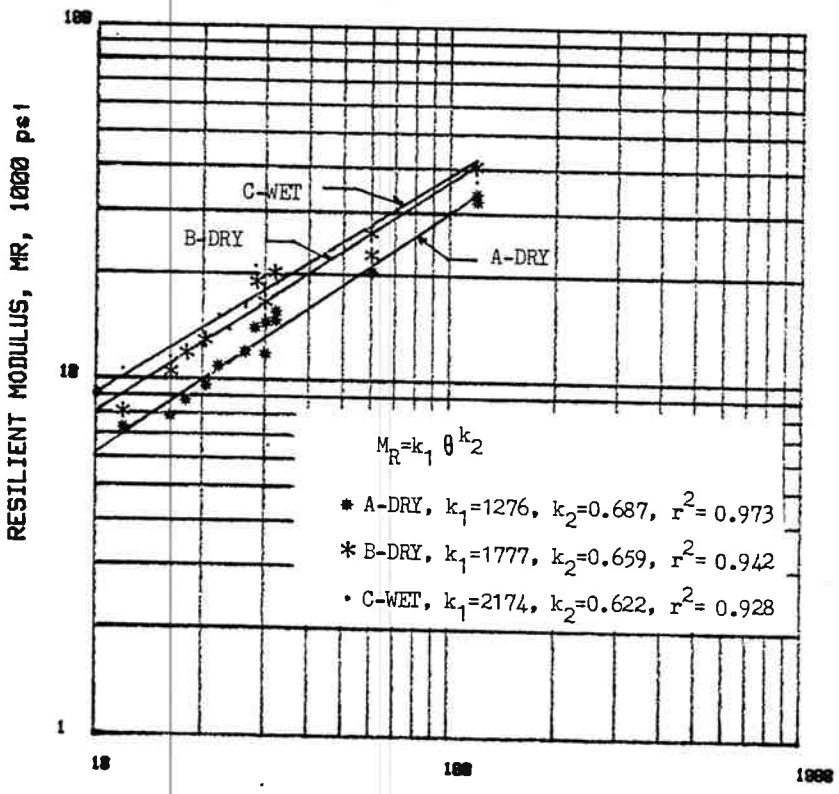

FIG.4.17 TRIAXIAL RESILIENT MODULUS VS. SUM OF PRINCIPAL STRESSES - GRAY CINDER BASE
1 psi= 6.9 kPa

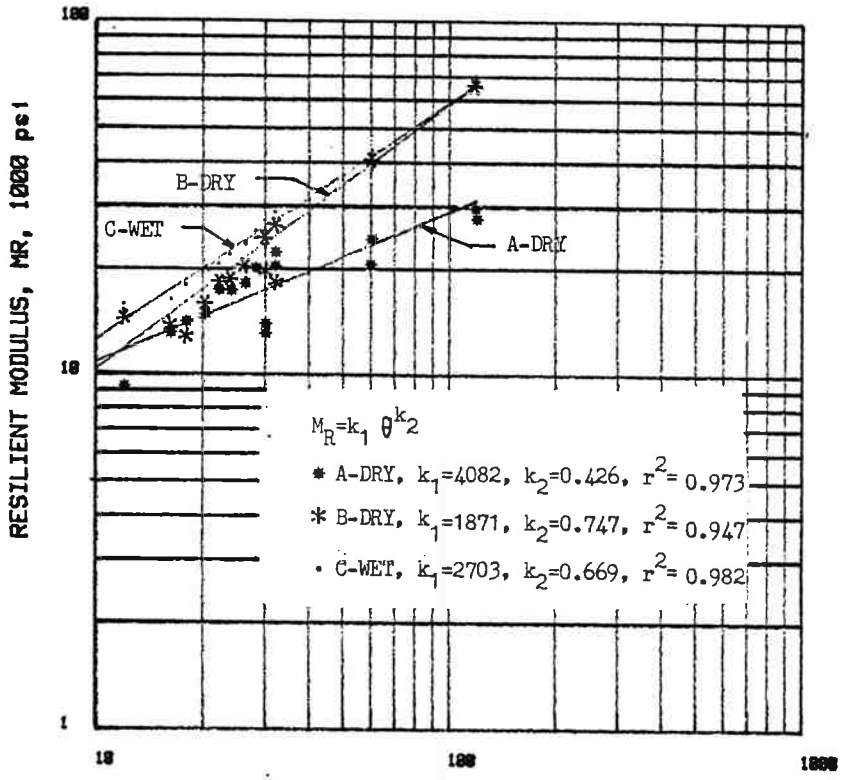

FIG.4.18 TRIAXIAL RESILIENT MODULUS VS. SUM OF PRINCIPAL STRESSES - RED CINDER BASE
1 psi= 6.9 kPa

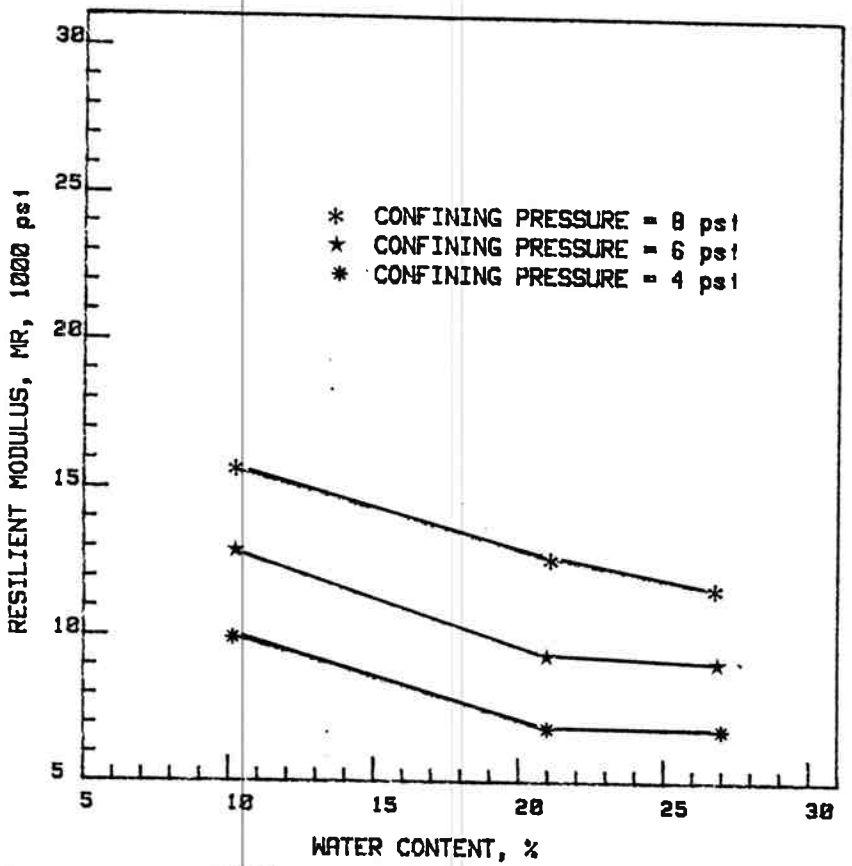

FIG.4.19 EFFECT OF WATER CONTENT ON TRIAXIAL RESILIENT MODULUS - FREMONT SUBGRADE SOIL, DEVIATOR STRESS=4.2psi, 1psi=6.9kPa

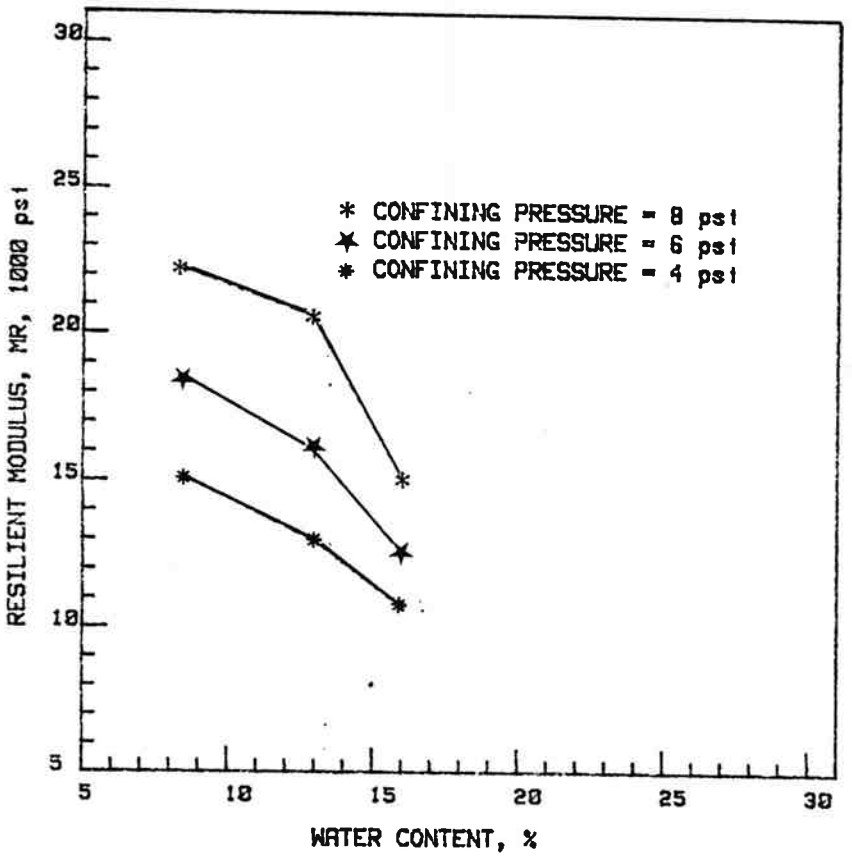

FIG.4.20 EFFECT OF WATER CONTENT ON TRIAXIAL RESILIENT MODULUS - MCKENZIE SUBGRADE SOIL, DEVIATOR STRESS=4.2psi, 1psi=6.9kPa

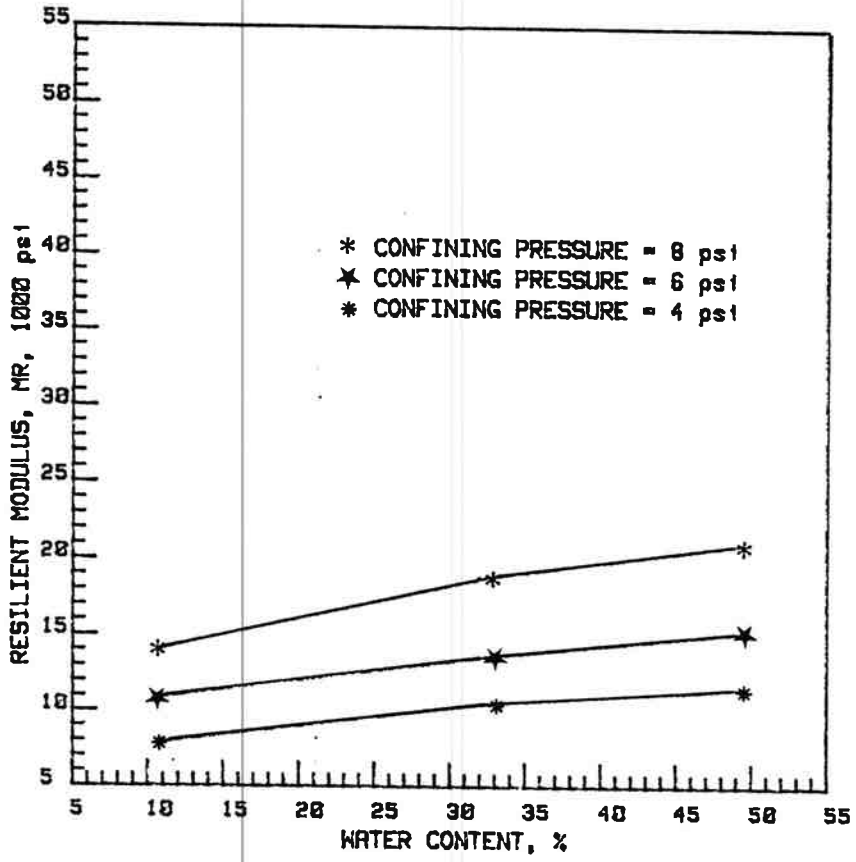

FIG.4.21 EFFECT OF WATER CONTENT ON TRIAXIAL RESILIENT MODULUS - GRAY CINDER BASE DEVIATOR STRESS=4.2 psi, 1psi=6.9kPa

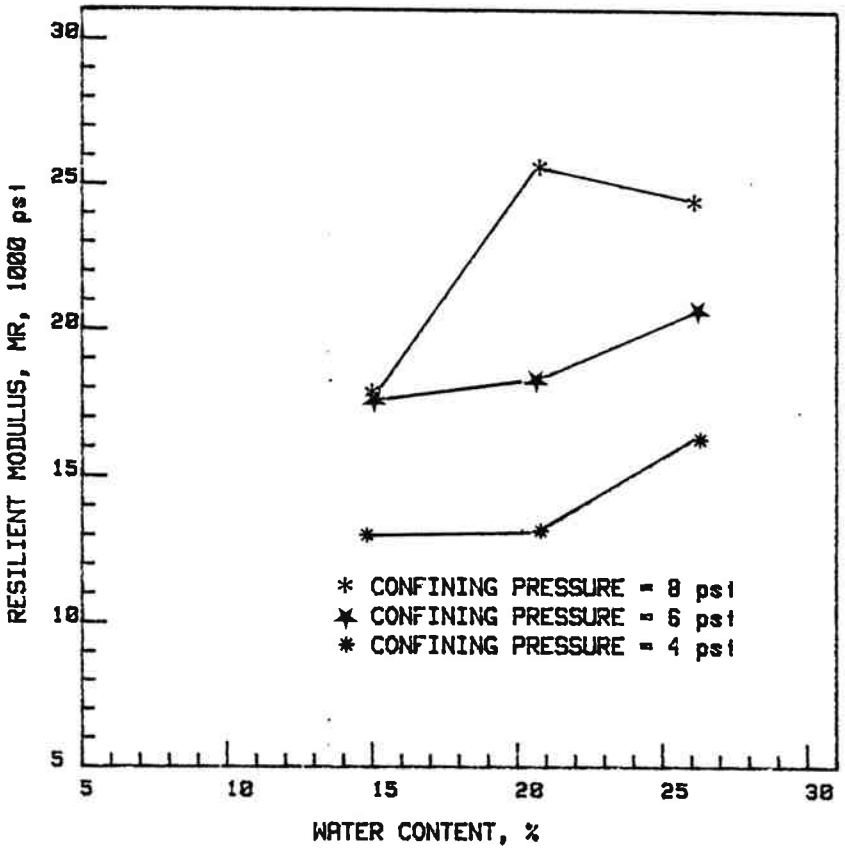

FIG.4.22 EFFECT OF WATER CONTENT ON TRIAXIAL RESILIENT MODULUS - RED CINDER BASE DEVIATOR STRESS=4.2psi, 1psi=6.9kPa

TABLE 4.8 EFFECT OF WATER CONTENT ON TRIAXIAL RESILIENT MODULUS

			Confining Pressure (psi)	4			6			8		
Fremont Subgrade	Water Content (%)			10.3	20.8	26.8	10.3	20.8	26.8	10.3	20.8	26.8
	Resilient Modulus (1000 psi)	Deviator Stress (psi)	4.2	9.9	6.9	6.8	12.8	9.4	9.1	15.6	12.7	11.6
			5.9	9.9	7.4	7.2	12.4	9.6	9.1	15.7	12.4	11.5
			8.4	10.6	8.0	8.1	13.1	9.9	10.2	16.5	12.7	12.5
McKenzie Subgrade	Water Content (%)			8.5	12.9	16.0	8.5	12.9	16.0	8.5	12.9	16.0
	Resilient Modulus (1000 psi)	Deviator Stress (psi)	4.2	15.2	13.0	10.7	18.5	16.1	12.6	22.2	20.6	15.1
			5.9	14.8	13.1	11.0	17.9	16.9	13.4	21.1	19.7	16.0
			8.4	15.1	13.0	11.6	18.2	16.1	14.1	21.1	20.8	16.1
Gray Cinder	Water Content (%)			10.9	32.4	49.5	10.9	32.4	49.5	10.9	32.4	49.5
	Resilient Modulus (1000 psi)	Deviator Stress (psi)	4.2	7.9	10.5	11.6	10.9	13.6	15.3	14.1	18.8	21.1
			5.9	8.7	11.8	12.0	11.2	13.9	15.8	14.8	18.1	19.7
			8.4	9.6	13.0	12.5	12.1	16.5	16.1	15.0	19.9	19.9
Red Cinder	Water Content (%)			15.0	20.7	26.1	15.0	20.7	26.1	15.0	20.7	26.1
	Resilient Modulus (1000 psi)	Deviator Stress (psi)	4.2	13.0	13.1	16.3	17.6	18.3	20.6	17.6	25.6	24.4
			5.9	14.1	12.9	17.9	17.6	18.4	21.9	19.7	24.6	27.4
			8.4	15.3	15.5	20.1	18.4	20.6	23.8	20.3	26.9	29.1

1psi=6.89kPa, 1pcf= 16.0 kg/m^3

TABLE 4.9 EFFECT OF DRY DENSITY ON TRIAXIAL RESILIENT MODULUS

Confining Pressure (psi)				4			6			8		
Fremont Subgrade	Dry Density (pcf)			82.0	83.1	83.1	82.0	83.1	83.1	82.0	83.1	83.1
	Resilient Modulus (1000 psi)	Deviator Stress (psi)	4.2	6.9	9.9	6.8	9.4	12.8	9.1	12.7	15.6	11.6
			5.9	7.4	9.9	7.2	9.6	12.4	9.1	12.4	15.7	11.5
			8.4	8.0	10.6	8.1	9.9	13.1	10.2	12.7	16.5	12.5
McKenzie Subgrade	Dry Density (pcf)			100.7	105.7	106.3	100.7	105.7	106.3	100.7	105.7	106.3
	Resilient Modulus (1000 psi)	Deviator Stress (psi)	4.2	15.2	10.7	13.0	18.5	12.6	16.1	22.2	15.1	20.6
			5.9	14.8	11.0	13.1	17.9	13.4	16.9	21.1	16.0	19.7
			8.4	15.1	11.6	13.0	18.2	14.1	16.1	21.1	16.1	20.8
Gray Cinder Base	Dry Density (pcf)			43.7	44.9	49.4	43.7	44.9	49.4	43.7	44.9	49.4
	Resilient Modulus (1000 psi)	Deviator Stress (psi)	4.2	11.6	7.9	10.5	15.3	10.9	13.6	21.1	14.1	18.8
			5.9	12.0	8.7	11.8	15.8	11.2	13.9	19.7	14.8	18.1
			8.4	12.5	9.6	13.0	16.1	12.1	16.5	19.9	15.0	19.9
Red Cinder Base	Dry Density (pcf)			67.8	68.1	70.9	67.8	68.1	70.9	67.8	68.1	70.9
	Resilient Modulus (1000 psi)	Deviator Stress (psi)	4.2	16.3	13.0	13.1	20.6	17.6	18.3	24.4	17.6	25.6
			5.9	17.9	14.1	12.9	21.9	17.6	18.4	27.4	19.7	24.6
			8.4	20.1	15.3	15.5	23.8	18.4	20.6	29.1	20.3	26.9

1psi=6.89kPa, 1pcf= 16.0 kg/m^3

The effect of water content or dry density on the resilient modulus for the cinder base material is not well defined as shown in Tables 4.8 and 4.9. An alternative expression of the resilient modulus in terms of the sum of the principal stresses could be employed as shown in Figures 4.17 and 4.18. The regression consant k_1 increased with increasing water content and k_2 increased with increasing dry density.

4.2.4.2 Diametral Resilient Modulus Test Results

The effect of water content and dry density on the resilient modulus for the four test materials is shown in Table 4.10, Figures 4.23 to 4.26 and Table 4.11. It is difficult to draw conclusions based on the limited data set. However, it is interesting to note: (1) the range of the subgrade soils resilient moduli are greater than the range of the cinder base resilient moduli, and (2) the vacuum confining pressure plays an important role in the investigation of the effect of water content and dry density on the diametral resilient modulus.

4.3 Comparison Between Triaxial and Diametral Resilient Modulus

The resilient modulus and Poisson's ratio for a homogeneous, isotropic, linear elastic material, whether determined with a triaxial test system or determined with a diametral test system should be identical. Soils are generally recognized as highly nonlinear, anisotropic, heterogenous material. The diametral loading response will undoubtedly differ from the triaxial loading response owing to these factors alone.

Experimental test results and example calculations for the diametral resilient modulus and Poisson's ratio computed based on equations 2.42 and 2.43 are given in Appendix B. According to the information given in Appendix B, it is interesting to note that for the plane stress case:
(1) Poisson's ratio varies from -0.007 to 1.52 for subgrade soils, and from

TABLE 4.10 EFFECT OF WATER CONTENT ON DIAMETRAL RESILIENT MODULUS

Confining Pressure (psi)				4			6			8	
Fremont Subgrade	Water Content (%)			10.3	20.8	26.8	10.3	20.8	26.8	10.3	20.8	26.8
	Resilient Modulus (1000 psi)	Diametral Load (lb)	26.2	15.0	12.6	12.8	17.4	14.2	13.4	19.6	15.9	14.2
			34.6	15.4	12.3	13.8	17.0	13.8	14.8	19.3	15.5	14.9
			69.2	15.5	12.7	15.0	18.2	14.2	16.0	20.3	16.2	16.6
			103.8	16.4	12.9	15.7	18.5	12.9	16.6	20.5	16.4	17.0
			129.8	16.6	13.5	16.7	19.0	15.2	17.9	21.3	17.1	18.4
McKenzie Subgrade	Water Content (%)			8.5	12.9	16.0	8.5	12.9	16.0	8.5	12.9	16.0
	Resilient Modulus (1000 psi)	Diametral Load (lb)	26.2	23.4	13.8	10.4	25.7	15.4	10.8	28.4	16.8	11.2
			34.6	22.9	14.8	10.2	25.4	16.1	10.2	27.4	16.9	10.8
			69.2	21.7	15.3	11.3	24.5	16.4	12.0	26.8	17.6	12.8
			103.8	22.1	14.4	13.5	24.1	15.5	14.0	26.5	16.7	14.5
			129.8	21.9	14.5	14.5	25.4	15.4	15.3	27.5	16.3	16.3
Gray Cinder Base	Water Content (%)			10.9	32.4	49.5	10.9	32.4	49.5	10.9	32.4	49.5
	Resilient Modulus (1000 psi)	Diametral Load (lb)	26.2	11.8	12.9	12.2	13.6	14.5	14.2	14.8	16.5	16.0
			34.6	12.3	11.4	12.4	13.7	12.9	13.8	15.1	14.7	15.9
			69.2	9.1	14.5	10.7	11.1	16.1	12.2	12.7	17.3	13.4
			103.8	13.3	15.4	11.0	15.4	17.1	12.7	17.1	18.8	13.8
			129.8	13.3	16.8	11.8	15.4	18.0	13.1	16.9	19.5	14.4
Red Cinder Base	Water Content (%)			15.0	20.7	26.1	15.0	20.7	26.1	15.0	20.7	26.1
	Resilient Modulus (1000 psi)	Diametral Load (lb)	26.2	16.1	22.7	13.8	17.9	26.3	16.9	19.2	29.6	19.8
			34.6	17.7	22.6	14.8	18.7	25.8	17.8	20.6	28.5	20.7
			69.2	15.6	23.6	14.9	16.9	26.7	18.1	18.3	30.1	21.7
			103.8	16.4	23.4	15.6	16.9	26.9	18.1	18.3	29.4	21.0
			129.8	17.2	24.4	17.1	18.2	27.3	19.2	18.9	29.9	21.9

1psi=6.89kPa, 1lb=4.45N

TABLE 4.11 EFFECT OF DRY DENSITY ON DIAMETRAL RESILIENT MODULUS

Confining Pressure (psi)				4			6			8		
Fremont Subgrade	Dry Density (pcf)			82.1	82.9	83.1	82.1	82.9	83.1	82.1	82.9	83.1
	Resilient Modulus (1000 psi)	Diametral Load (lb)	26.2	12.6	12.8	15.0	14.2	13.4	17.4	15.9	14.2	19.6
			34.6	12.3	13.8	15.4	13.8	14.8	17.0	15.5	14.9	19.3
			69.2	12.7	15.0	15.5	14.2	16.0	18.2	16.2	16.6	20.3
			103.8	12.9	15.7	16.4	12.9	16.6	18.5	16.4	17.0	20.5
			129.8	13.5	16.7	16.6	15.2	17.9	19.0	17.1	18.4	21.3
McKenzie Subgrade	Dry Density (pcf)			100.2	105.7	106.5	100.2	105.7	106.5	100.2	105.7	106.5
	Resilient Modulus (1000 psi)	Diametral Load (lb)	26.2	23.4	10.4	13.8	25.7	10.8	15.4	28.4	11.2	16.8
			34.6	22.9	10.2	14.8	25.4	10.2	16.1	27.4	10.8	16.9
			69.2	21.7	11.3	15.3	24.5	12.0	16.4	26.8	12.8	17.6
			103.8	22.1	13.5	14.4	24.1	14.0	15.5	26.5	14.5	16.7
			129.8	21.9	14.5	14.5	25.4	15.3	15.4	27.5	16.3	16.3
Gray Cinder Base	Dry Density (pcf)			42.8	44.0	48.9	42.8	44.0	48.9	42.8	44.0	48.9
	Resilient Modulus (1000 psi)	Diametral Load (lb)	26.2	12.2	11.8	12.9	14.2	13.6	14.5	16.0	14.8	16.5
			34.6	12.4	12.3	11.4	13.8	13.7	12.9	15.9	15.1	14.7
			69.2	10.7	9.1	14.5	12.2	11.1	16.1	13.4	12.7	17.3
			103.8	11.0	13.3	15.4	12.7	15.4	17.1	13.8	17.1	18.8
			129.8	11.8	13.3	16.8	13.1	15.4	18.0	14.4	16.9	19.5
Red Cinder Base	Dry Density (pcf)			67.0	67.5	69.5	67.0	67.5	69.0	67.0	67.5	69.0
	Resilient Modulus (1000 psi)	Diametral Load (lb)	26.2	13.8	16.1	22.7	16.9	17.9	26.3	19.8	19.2	29.6
			34.6	14.8	17.7	22.6	17.8	18.7	25.8	20.7	20.6	28.5
			69.2	15.6	16.4	23.4	18.1	16.9	26.9	21.0	18.3	29.4
			103.8	14.9	15.6	23.6	18.1	16.9	26.7	21.7	18.3	30.1
			129.8	17.1	17.2	24.4	19.2	18.2	27.3	21.9	18.9	29.9

1psi=6.89kPa, 1lb=4.45N, 1pcf=, 16.0 kg/m^3

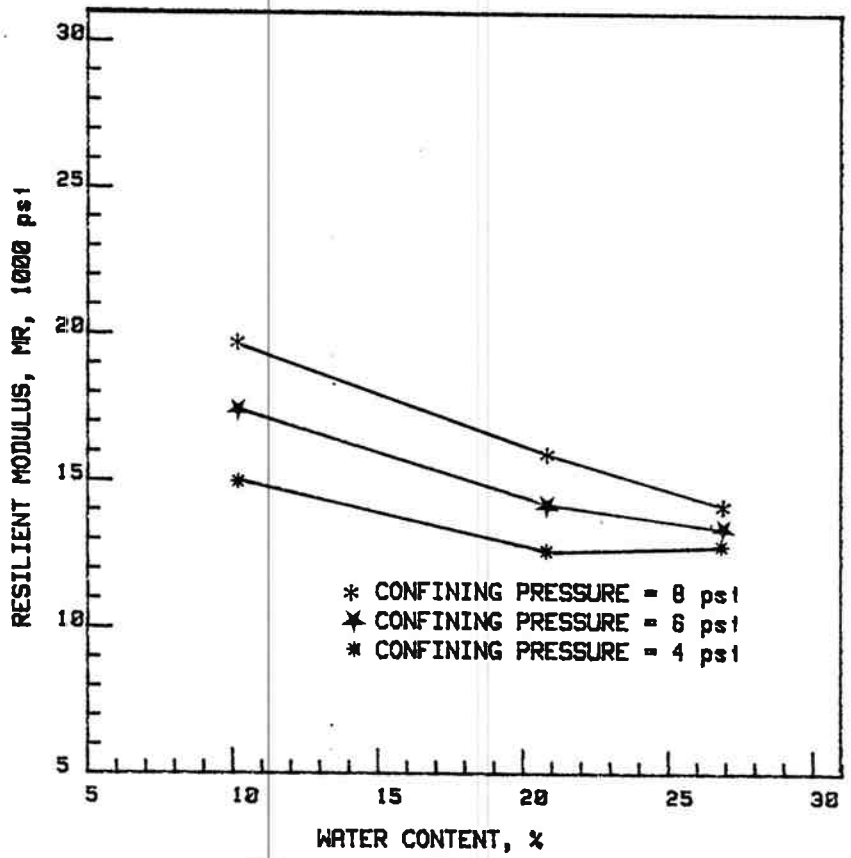

FIG.4.23 EFFECT OF WATER CONTENT ON DIAMETRAL RESILIENT MODULUS - FREMONT SUBGRADE SOIL DIAMETRAL LOAD=116N (26lb), 1psi=6.9kPa

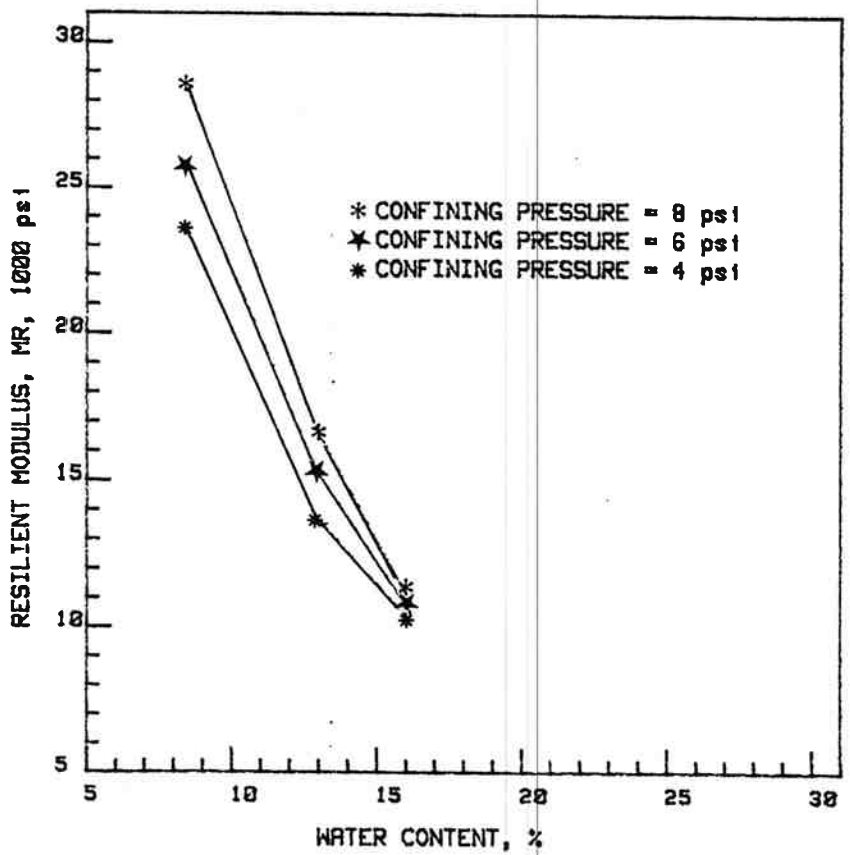

FIG.4.24 EFFECT OF WATER CONTENT ON DIAMETRAL RESILIENT MODULUS - MCKENZIE SUBGRADE SOIL DIAMETRAL LOAD=116N (26lb), 1psi=6.9kPa

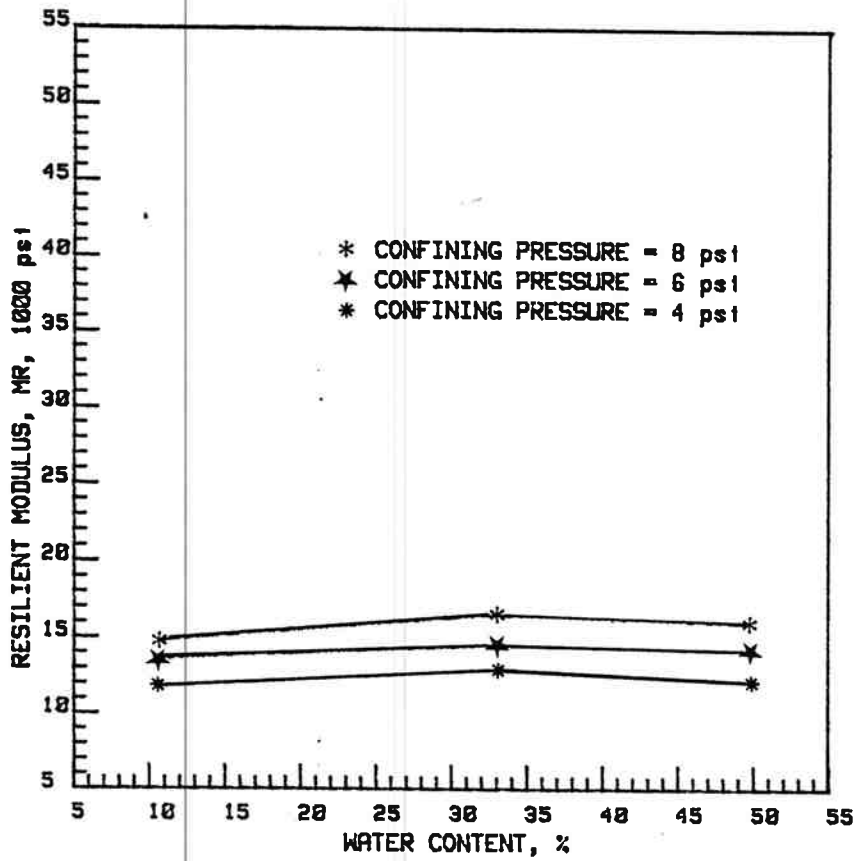

FIG.4.25 EFFECT OF WATER CONTENT ON DIAMETRAL RESILIENT MODULUS - GRAY CINDER BASE
DIAMETRAL LOAD=116N (26lb) 1psi=6.9kPa

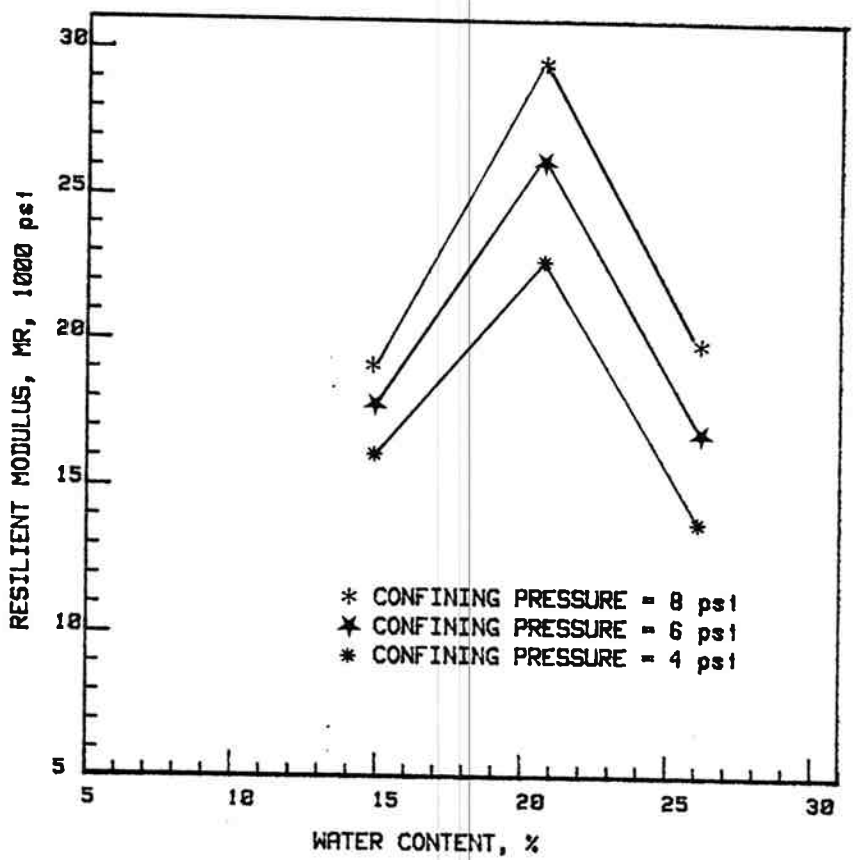

FIG.4.26 EFFECT OF WATER CONTENT ON DIAMETRAL RESILIENT MODULUS - RED CINDER BASE
DIAMETRAL LOAD=116N (26lb), 1psi=6.9kPa

0.06 to 1.78 for cinder base materials, (2) Poisson's ratio decreased with increasing confining pressure or with decreasing diametral load, (3) a low Poisson's ratio is associated with low diametral load while a high Poisson's ratio is associated with high diametral load, and (4) while there are substantial variations for Poisson's ratio, calculated resilient moduli based on the computed Poisson's ratio over the diametral load range of 110 N to 578 N (26 lb to 130 lb) do not vary significantly. For the plane strain case 1) Poisson's ratio varies from -0.007 to 0.62 for the subgrade soils, and from 0.07 to 0.59 for the cinder base materials, (2) Poisson's ratio decreases slightly with increasing confining pressure, and (3) Poisson's ratio increases with increasing diametral load. Apparently, the plane strain solutions (re. Appendix B) give more reasonable values for Poisson's ratio than plane stress solutions. The deviations of values of Poisson's ratio from the theoretical upper limit may indicate the test specimens dilate when subjected to high levels of diametral loading.

The stress regimes within each layer comprising the pavement structure subjected to traffic loading are very complicated. The theoretical analysis indicates the subgrade soils in a full-depth pavement or an aggregate base layer in a conventional pavement structure may be subjected to lateral tensile stress. The question is thus raised as to how unbound materials such as those investigated in the study are able to exhibit a positive modulus value when subjected to lateral tensile stress.

Apparently, if the initial confining stress at the point considered within the pavement structure is greater than the lateral tensile stress induced by traffic loading, the material will not fail and may be characterized using a diametral test system. Undoubtedly, there are some discrepencies associated with the diametral system employed in the study and the working

formula to calculate the resilient modulus and Poisson's ratio. The equations which permit the calculations of resilient modulus and Poisson's ratio should be modified to incorporate the nonlinearity and heterogeneous characteristics of unbound materials.

The comparisons between resilient moduli determined with triaxial and diametral test system as discussed in section 4.2.2 may be examined in terms of comparable states of stress. Specifically, the triaxial test results are plotted in terms of the axial compressive deviator stress, and the diametral test results are plotted in terms of the compressive deviator stress at the center of the test specimen. The comparison between resilient moduli determined with triaxial and diametral test system presented in this section are the diametral resilient modulus computed based on equations 2.42 and 2.43 (associated with the plane stress problem). The comparison between triaxial resilient moduli and diametral resilient moduli computed based on equations 2.42a and 2.43a (associated with the plane strain problem) are given in Appendix B.

Figures 4.5 to 4.10 present a comparison between diametral and triaxial resilient moduli for subgrade soils. The resilient moduli ratio (diametral/triaxial) of Fremont subgrade soil for comparable states of stress vary from 1.26 to 1.83. The resilient modulus ratio (diametral/triaxial) of McKenzie subgrade soil for comparable states of stress varies from 0.74 to 1.06. In general, the resilient modulus ratio increased with decreasing confining pressure and was slightly affected by deviator compressive stress. It should be noted that the effects of confining pressure on diametral moduli decreased with increasing water content but the effects of confining pressure on triaxial moduli are consistent over the range of water content and dry density considered.

Figures 4.11 to 4.16 present a comparison between diametral and triaxial resilient moduli for cinder base materials. The resilient modulus ratio (diametral/triaxial) for comparable states of stress vary from 0.89 to 1.44 for Gray cinder and 0.79 to 1.74 for Red cinder. In general, the resilient modulus ratio increased with decreasing confining pressure and was slightly affected by deviator compressive stress in the range from 27 kPa to 62 kPa (4 to 9 psi). The effects of confining pressure are consistent for both diametral and triaxial moduli over the range of water content and dry density considered.

Apparently, it is not possible to establish general correlation factors between resilient modulus determined with diametral or triaxial test system. The differences between triaxial and diametral resilient moduli for comparable states of stress were ± 80%. The comparisons between triaxial resilient modulus and diametral resilient modulus indicate the effects of initial states of stress are consistent for both diametral and triaxial moduli over the range of water content and dry density considered. Quantitatively, the effects of initial states of stress on triaxial resilient moduli are greater than diametral resilient moduli. This is owing to the differences associated with the application of the confining pressure. The effects of deviator compressive stress for both triaxial resilient modulus and diametral resilient modulus are not significant at least for the range of stress levels considered. The values of Poisson's ratio were not measured in the triaxial test, therefore, no comparisons between triaxial Poisson's ratio and diametral Poisson's ratio could be made.

4.4 Correlations Between "R" Value and Resilient Modulus

As shown in Table 4.12, no distinct relationships between "R" value and resilient modulus could be found over the range of material conditions con-

TABLE 4.12 COMPARISON OF "R" VALUE AND RESILIENT MODULUS

Sample No.		A-Dry	B-Dry	C-Wet
Fremont Subgrade	"R" Value	76	79	81
	Triaxial Resilient Modulus (1000 psi)	9.9	6.9	6.8
	Diametral Resilient Modulus (1000 psi)	15.3	12.6	12.8
McKenzie Subgrade	"R" Value	72	75	66
	Triaxial Resilient Modulus (1000 psi)	15.2	13.0	10.7
	Diametral Resilient Modulus (1000 psi)	23.4	13.8	10.4
Gray Cinder Base	"R" Value	73	80	79
	Triaxial Resilient Modulus (1000 psi)	7.9	10.5	11.6
	Diametral Resilient Modulus (1000 psi)	11.8	12.9	12.2
Red Cinder Base	"R" Value	69	69	72
	Triaxial Resilient Modulus (1000 psi)	13.0	13.1	16.3
	Diametral Resilient Modulus (1000 psi)	16.1	22.7	13.8

Note: 1 Triaxial resilient modulus values are associated with a confining pressure of 28 kPa (4 psi) and a deviator stress of 29 kPa (4.2 psi)

2 Diametral resilient modulus values are associated with a confining pressure of 28 kPa (4 psi) and a deviator compressive stress at the center of specimen of 35 kPa (5 psi)

sidered. This is owing to the substantial differences between the nature of each test method with respect to the stress levels, the confinement of the test specimen, the geometry of the test specimen and the rate of loading. Although, the correlation factors between "R" value and resilient modulus could not be found, the "R" values for all the materials tested in the study and previous works done by Hull, et al (1980) indicate very strong materials, which should be equivalent to good quality aggregates.

CHAPTER 5

FLEXIBLE PAVEMENT THICKNESS DESIGN IMPLICATIONS

The purpose of this chapter is to present a comparison between a flexible pavement designed with (1) the ODOT procedure, and (2) the MET procedure and the test data generated in the project.

5.1 Hveem Stabilometer Resistance Value Design Method

Flexible pavement thickness based on Hveem stabilometer "R" values may be computed from:

$$CBE = 0.03546\ (TC)\ (100-R) \qquad (5.1)$$

in which, CBE (crushed base equivalent): an equivalent thickness for various materials complying with the Standard Specifications and Special Provisions required by ODOT.

TC (traffic coefficient): $TC = 1.3\ (EWL)^{0.119}$ or

$TC = 1.746\ (EAL)^{0.119}$

EWL is an average 22 kN (5 kip) equivalent wheel load and EAL is an average 80 kN (18 kip) equivalent axle load. Since the failure criteria employed in the analytical pavement thickness design is related to the EAL, the TC in terms of a 80 kN (18 kip) EAL is adopted in the study.

R: Hveem stabilometer value

Fig. 5.1 shows the relationships between CBE, TC and R over the range of TC from 5 to 16 (EAL from 10^4 to 10^8) and "R" values ranging from 30 to 60. The materials investigated in the study had "R" values ranging from 55 to 80, indicating very strong materials.

A provision required minimum thickness based on the construction, maintenance and under-design problems for various traffic volumes is employed by

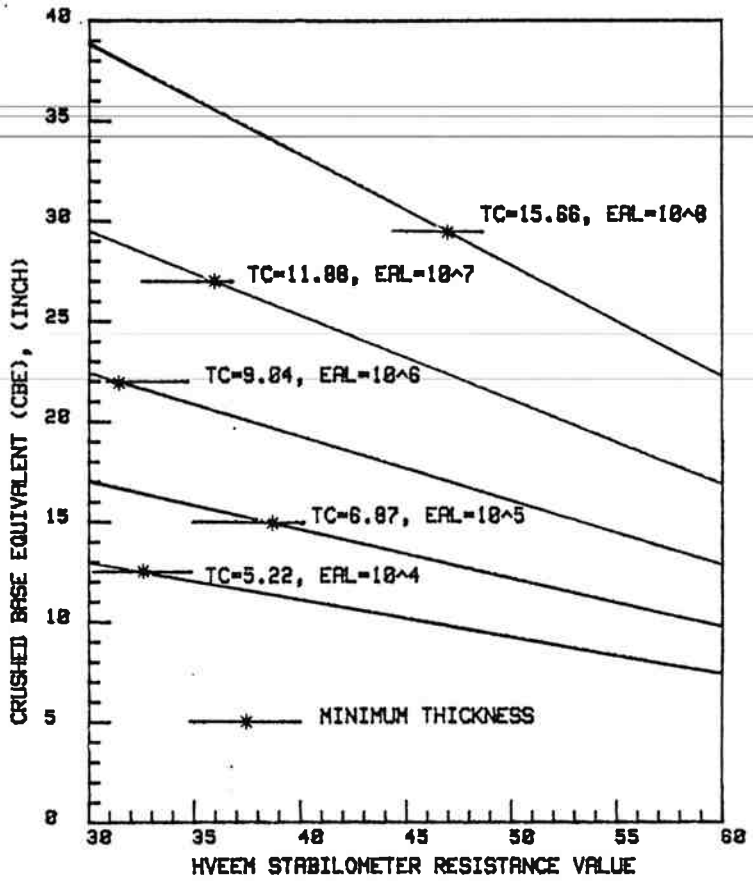

FIG.5.1 RELATIONSHIP BETWEEN 'R' VALUE, TC AND CBE

ODOT. The provision required minimum thickness for the TC's and EAL's selected in the study are illustrated in Figure 5.1. If a pavement is designed based upon the "R" values of the materials investigated in the study, resulting thickness is less than the minimum. For example, given TC = 15.7, and the design "R" value of 68 for McKenzie Subgrade soils, the thickness computed from equation 5.1 is 452 mm (17.8 in.) CBE. The minimum thickness required associated with TC = 15.7 is 750 mm (29.5 in.) CBE; hence the minimum requirements control in all cases.

5.2 Analytical Pavement Thickness Design Based on Multilayer Elastic Theory (MET)

The stresses and strains in the pavement structure under traffic loads may be determined using available computer algorithms based on MET. Hull, et al (1980) employed computer program PSAD2A to analyze the stresses, strains and deflections in the pavement structure under traffic loads. The predicted surface deflections caused by an 80 kN (18000 lb) single axle load compared favorable with the average measured Benkleman beam deflections.

Two computer programs, ELSYM5 and PSAD2A, were employed in the study to determine the critical elastic strains under a dual wheel load (80 kN (18 kip) axle load and 550 kPa (80 psi) tire pressure. ELSYM5 was used to analyze a two-layer or full-depth pavement structure. PSAD2A was employed to analyze a conventional pavement structure (AC surface layer plus untreated aggregate base and subgrade soils). PSAD2A accounts for the stress-dependent characteristics of untreated base materials.

In the two-layer pavement structure analysis, a constant modulus and Poisson's ratio were assumed for each layer. Moduli values of 275,600 kPa (40,000 psi) and 2,067,000 kPa (300,000 psi) and Poisson's ratio equal to 0.35 were selected for the asphalt concrete layer. Four values of resilient

moduli (34,400, 51,700, 69,000 and 17,200 kPa (5,000, 7,500, 10,000 and 25,000 psi)) and two values of Poisson's ratio (0.1 and 0.4) were selected for the subgrade soils (see Figure 5.2).

Two critical elastic strains are used to determine the design pavement thickness. The tensile strain at the bottom of the AC layer must be less than an allowable value to minimize pavement cracking under traffic load. The allowable value of tensile strain suggested by Santucci (1977) is shown in Figure 5.3. Further, the vertical strain at the surface of subgrade layer must be less than an allowable value to minimize pavement surface rutting. The allowable value of vertical subgrade strain suggested by Monismith and Mclean (1971) is shown in Figure 5.4.

Three locations in the pavement structure are checked for critical strains as shown in Figure 5.5: (1) midway between the tires, (2) directly beneath one of the tires, and (3) under the edge of one of the tires. The greatest strain value obtained at three locations is used in the design procedure.

The results of the computer analysis allow design charts to be constructed, as shown in Figures 5.6 to 5.13. Two conclusions can be drawn from the charts as follows: (1) the tensile strain increases with decreasing stiffness of AC layer and with decreasing modulus of subgrade soil layer, and (2) the vertical subgrade strain increases with decreasing stiffness of AC layer and with decreasing modulus of subgrade soil layer. The influence of Poisson's ratio for the subgrade soil layer on the tensile strain and on the vertical subgrade strain are opposite, that is, the tensile strain decreases with increasing Poisson's ratio, while the vertical subgrade strain increases with decreasing Poisson's ratio of subgrade soil layer (see Figures 5.14 to 5.17).

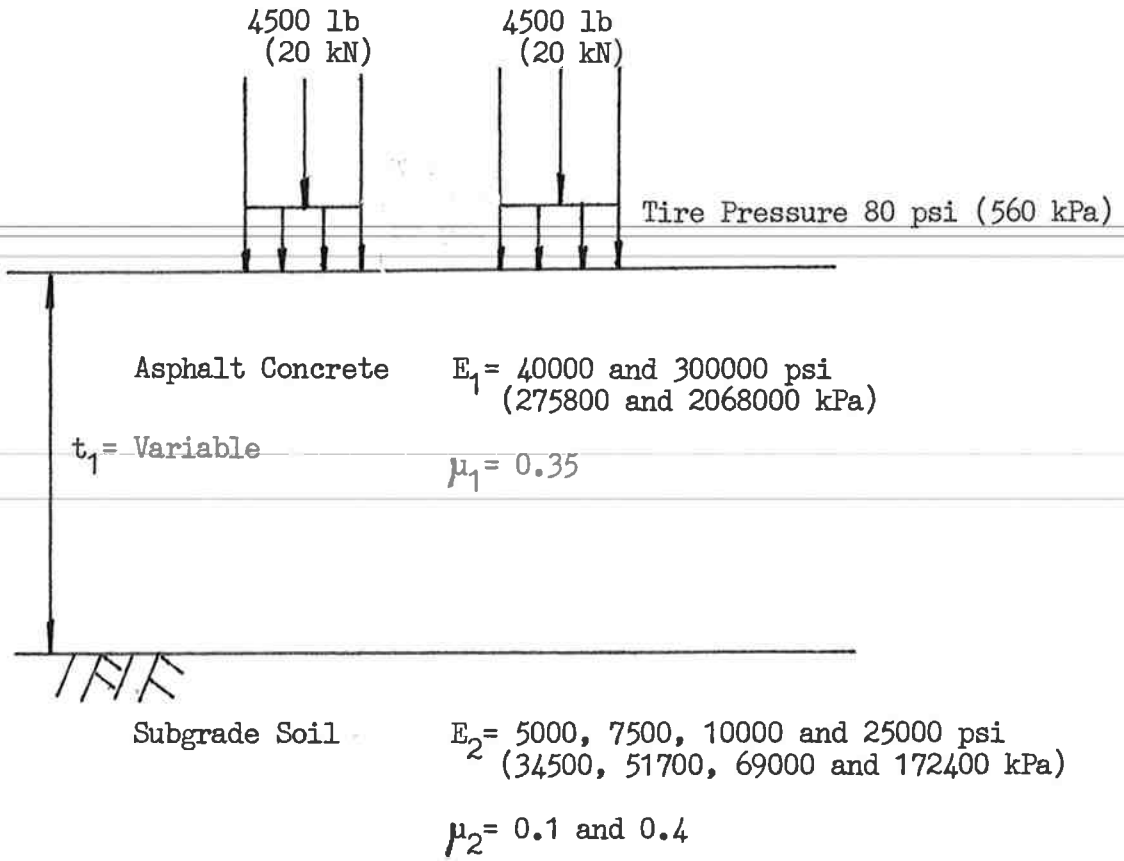

FIG. 5.2 FULL-DEPTH PAVEMENT STRUCTURE, LOADING CONDITIONS AND MATERIAL PROPERTIES

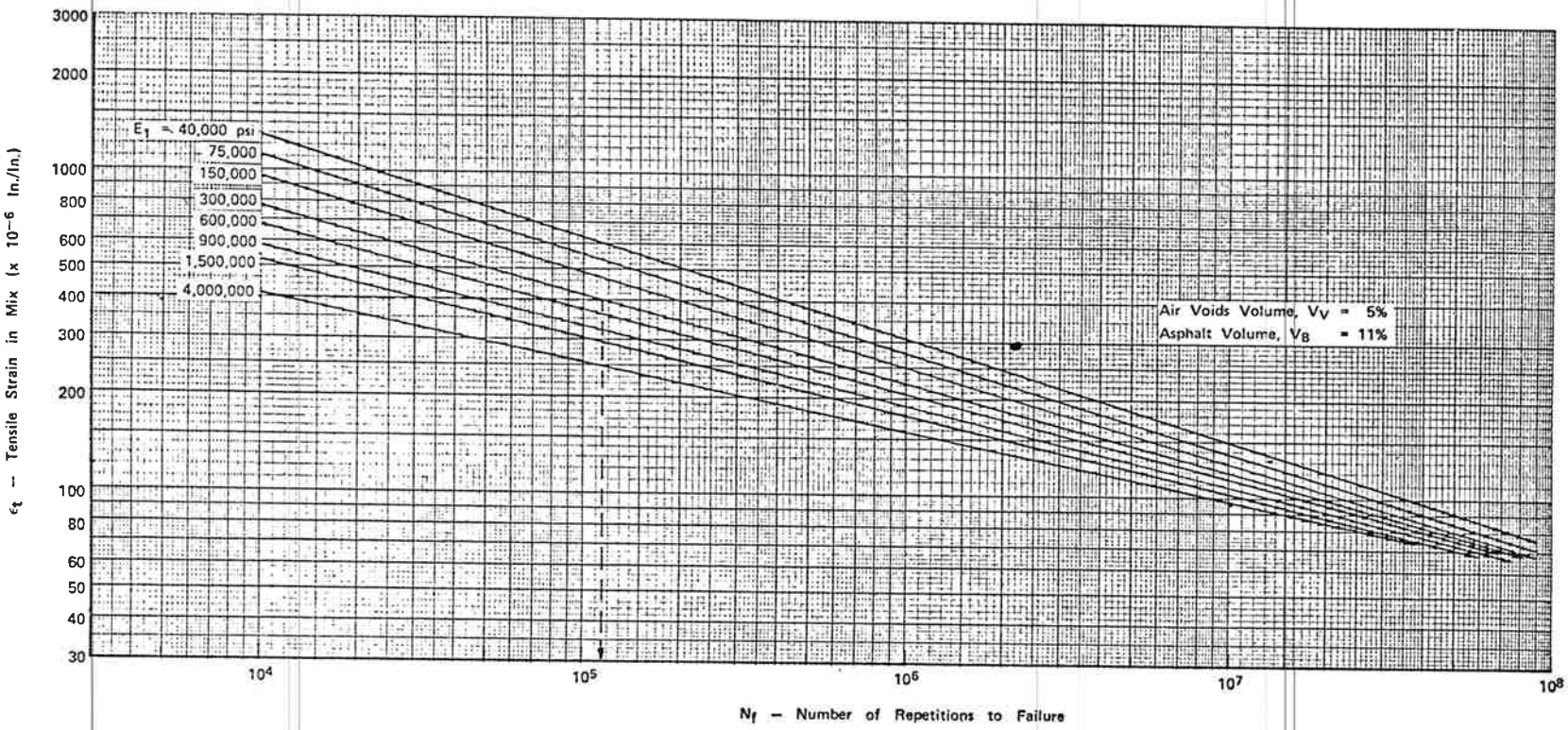

FIG. 5.3 FATIGUE CRITERIA FOR ASPHALT AND EMULSIFIED ASPHALT MIXES (after Santucci, 1977)

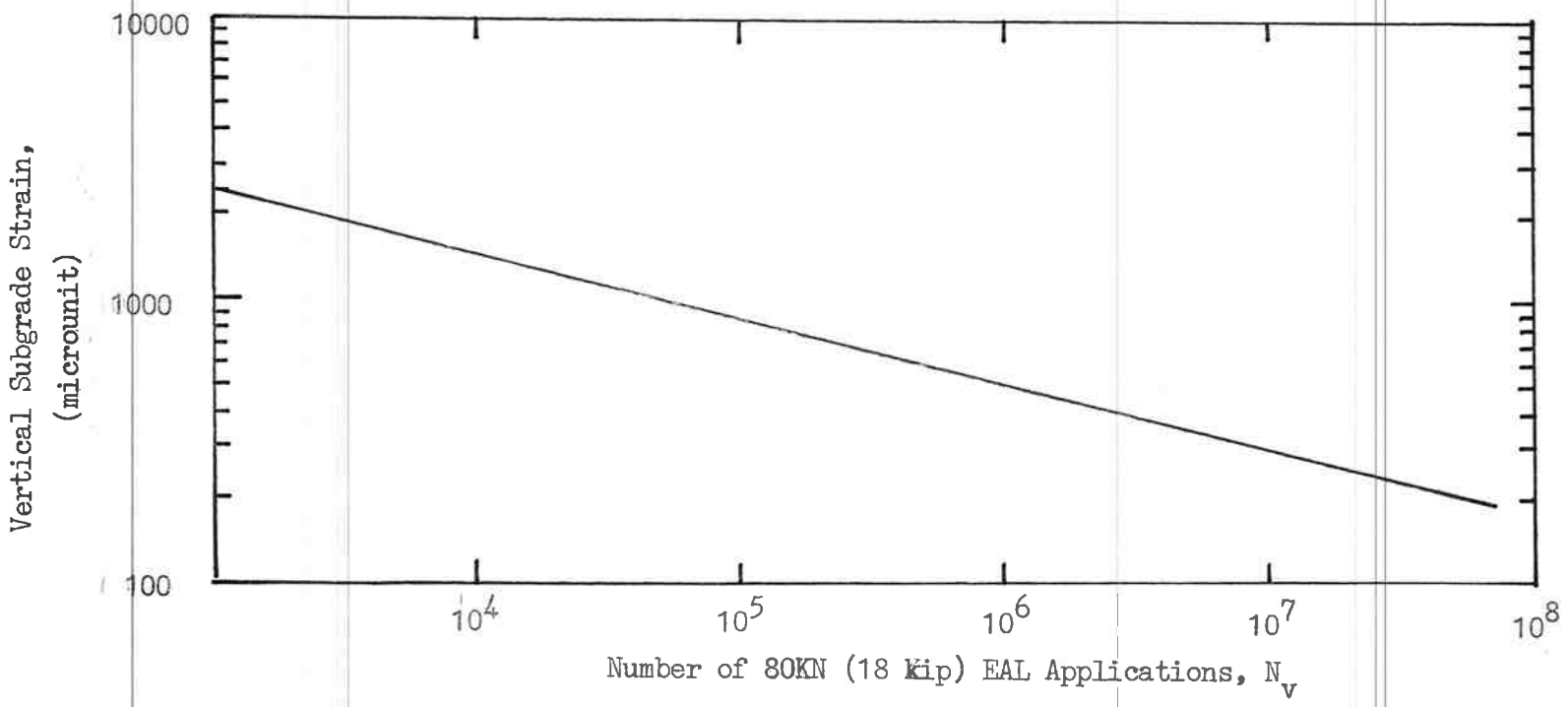

FIG. 5.4 LIMITING SUBGRADE STRAIN CRITERIA (after Monismith and Mclean, 1971)

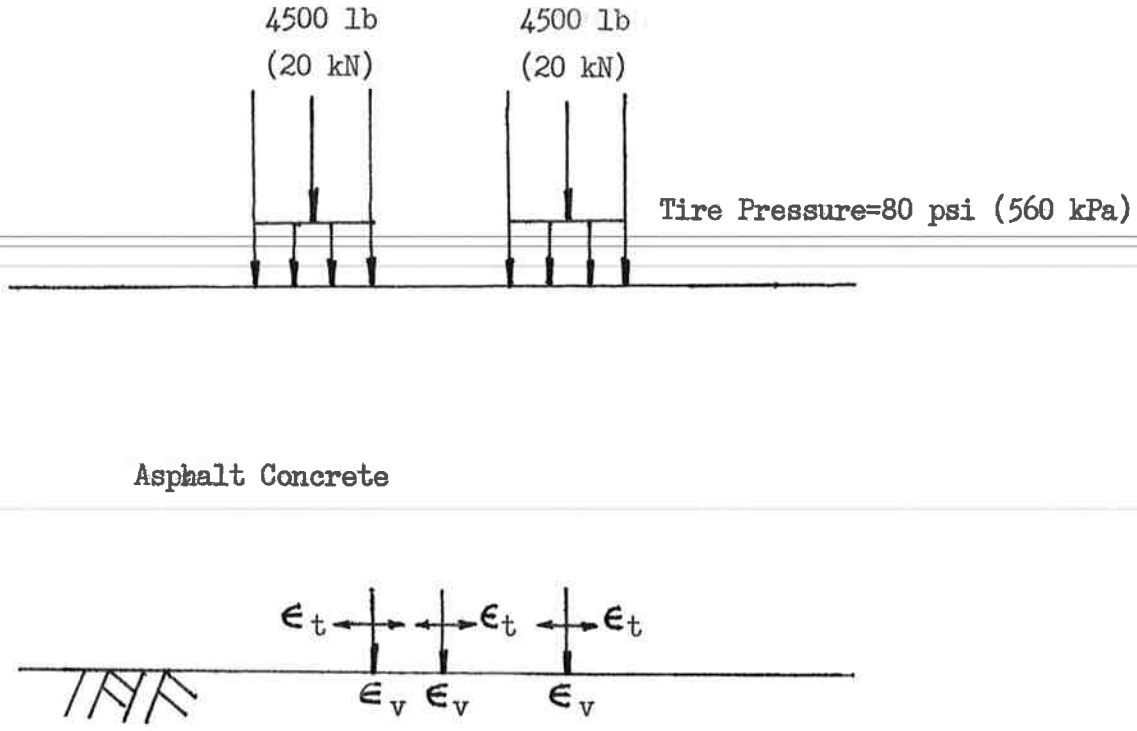

FIG. 5.5 LOCATIONS OF MAXIMUM HORIZONTAL TENSILE (ϵ_t) AND VERTICAL COMPRESSIVE SUBGRADE (ϵ_v) STRAINS IN FULL-DEPTH PAVEMENT STRUCTURE

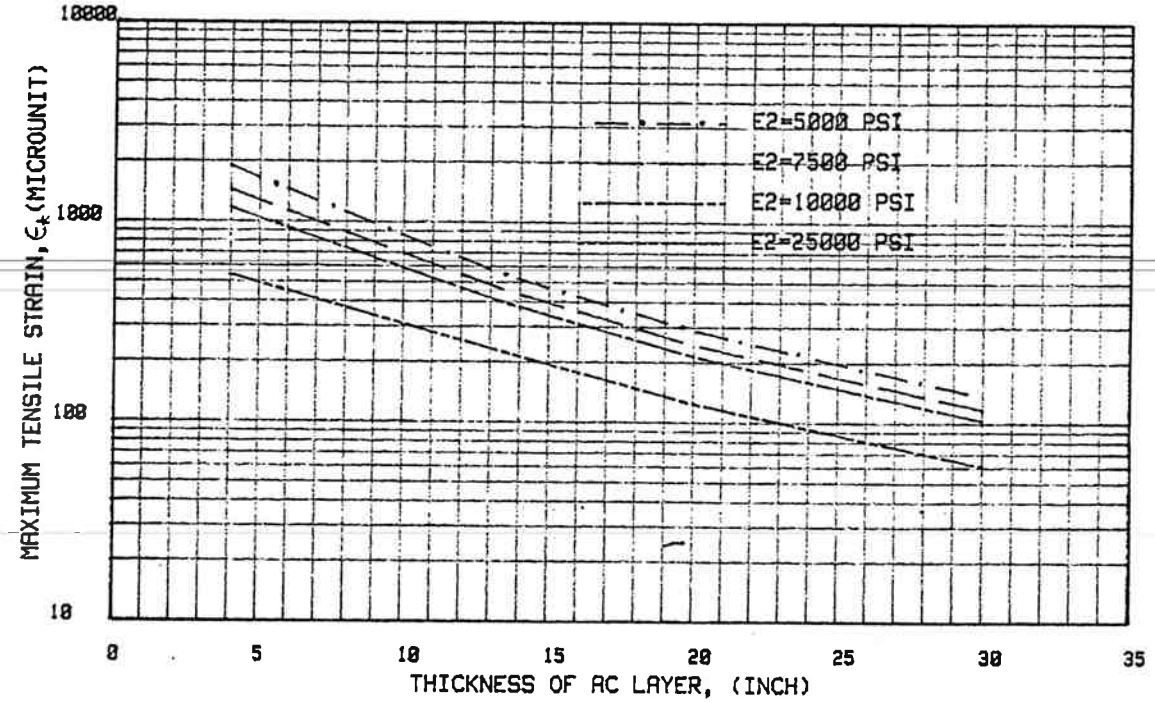

FIG.5.6 DESIGN CHART, MAXIMUM TENSILE STRAIN VS. AC THICKNESS, E1=40000 PSI, μ1=0.35 ,μ2=0.4

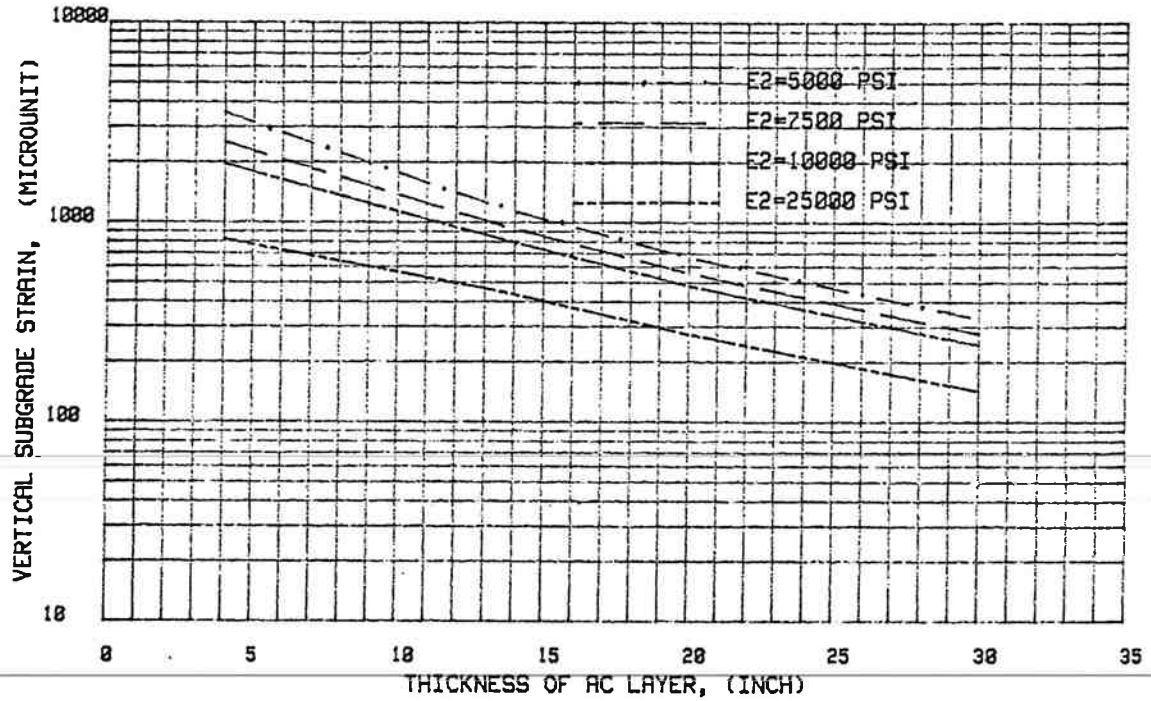

FIG.5.7 DESIGN CHART, VERTICAL SUBGRADE STRAIN VS. AC THICKNESS, E1=40000 PSI, μ1=0.35 ,μ2=0.4

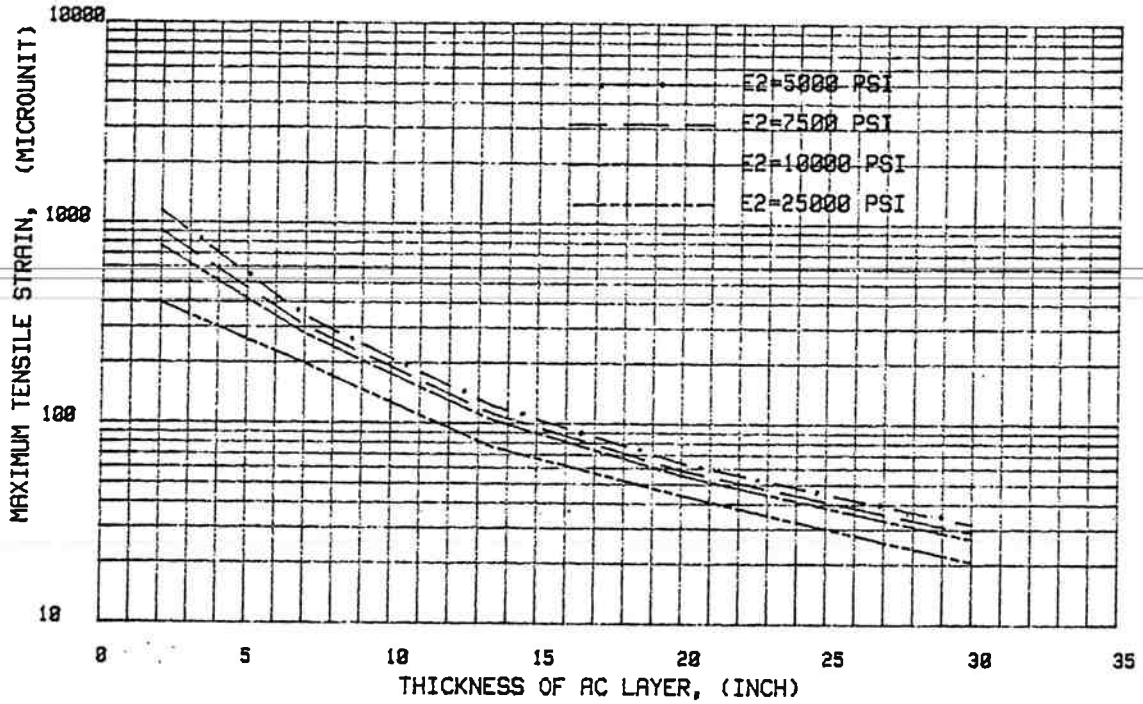

FIG.5.8 DESIGN CHART, MAXIMUM TENSILE STRAIN VS. AC THICKNESS, E1=300000 PSI, U1=0.35, U2=0.4

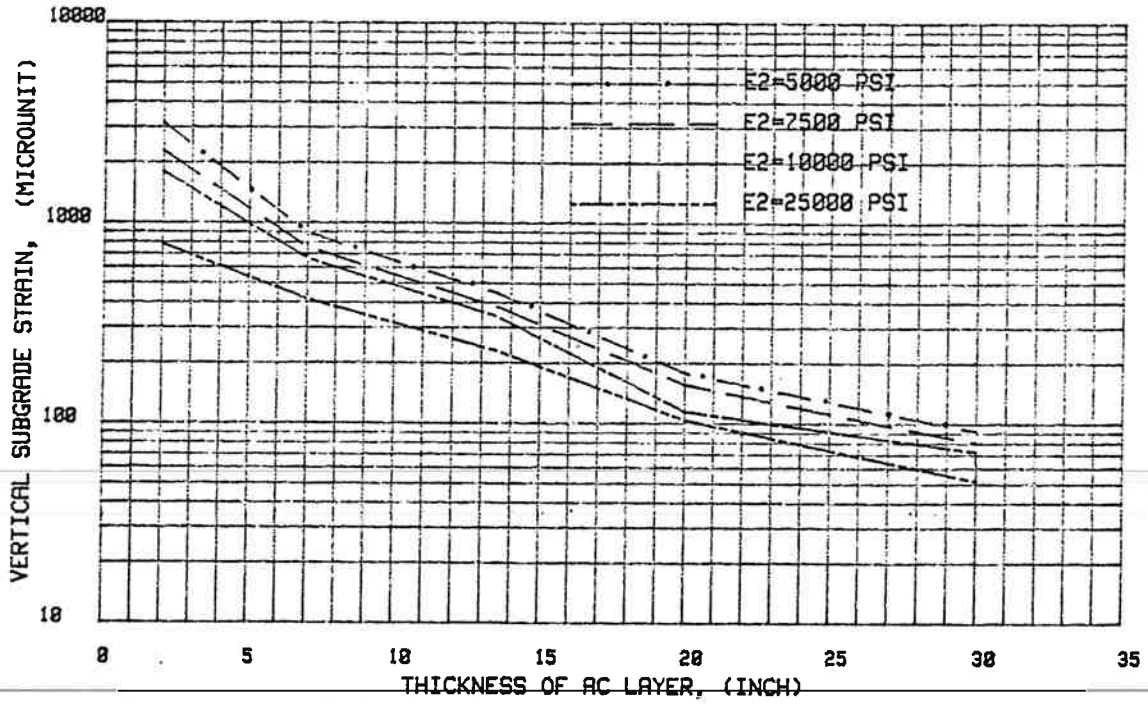

FIG.5.9 DESIGN CHART, VERTICAL SUBGRADE STRAIN VS. AC THICKNESS, E1=300000 PSI, U1=0.35, U2=0.4

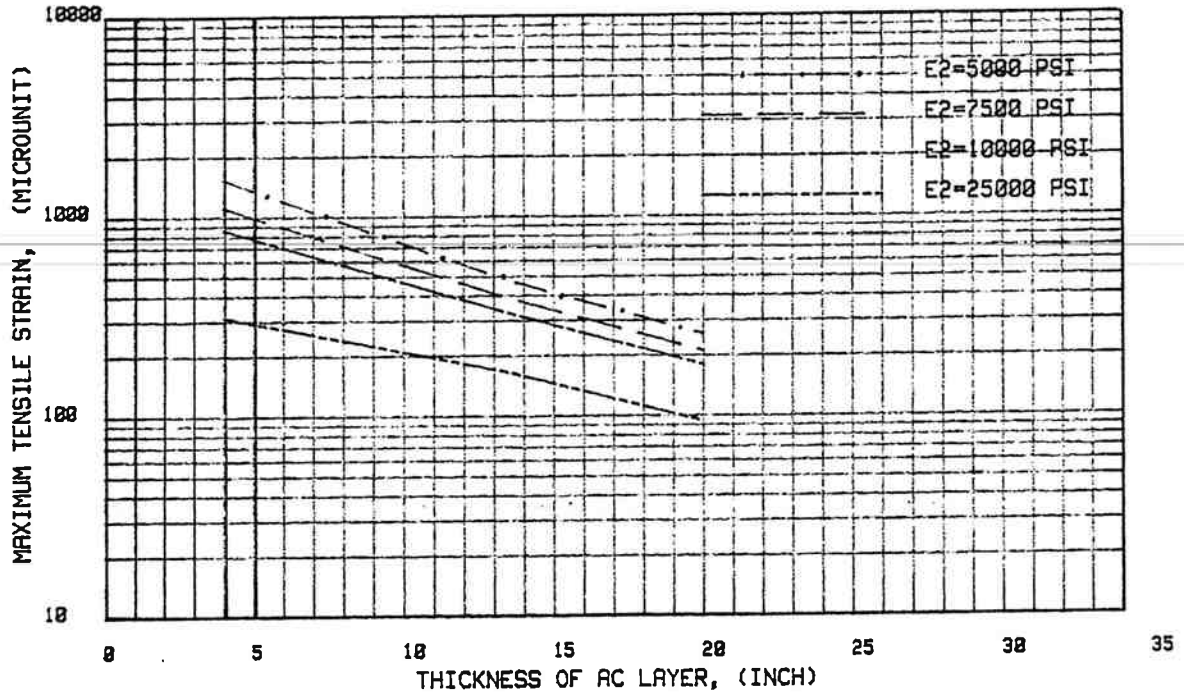

FIG.5.10 DESIGN CHART, MAXIMUM TENSILE STRAIN VS. AC THICKNESS, E1=40000 PSI, U1=0.35, U2=0.1

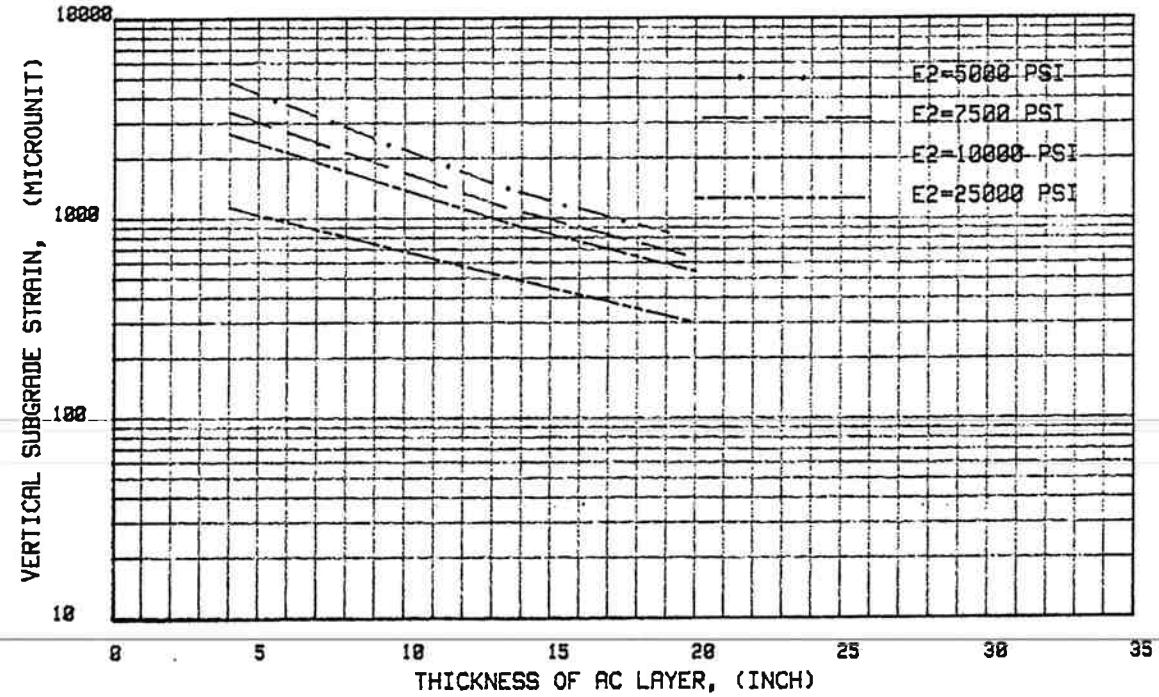

FIG.5.11 DESIGN CHART, VERTICAL SUBGRADE STRAIN VS. AC THICKNESS, E1=40000 PSI, U1=0.35, U2=0.1

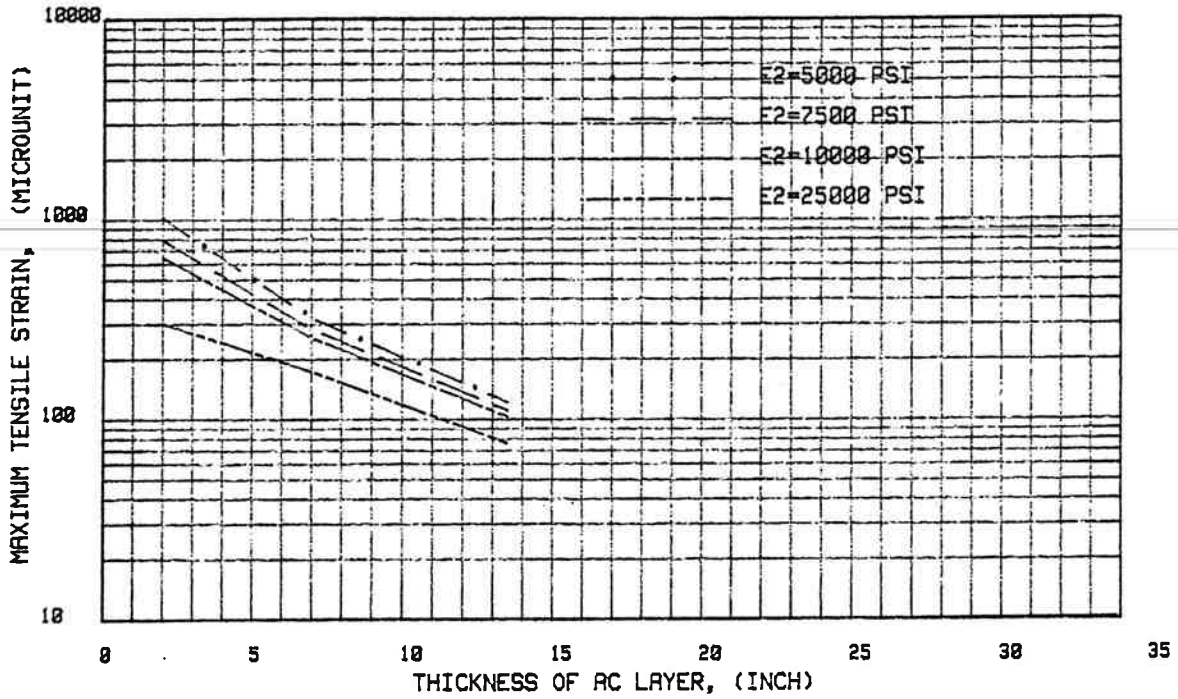

FIG.5.12 DESIGN CHART,MAXIMUM TENSILE STRAIN VS. AC THICKNESS, E1=300000 PSI,U1=0.35, U2=0.1

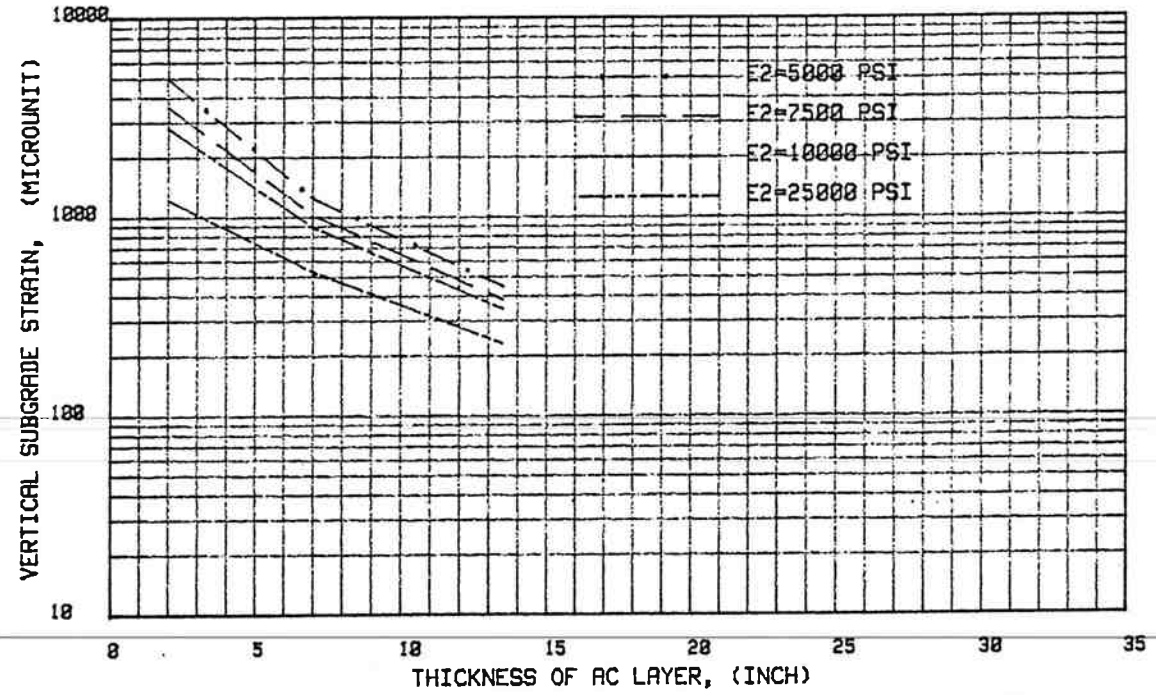

FIG.5.13 DESIGN CHART, VERTICAL SUBGRADE STRAIN VS. AC THICKNESS, E1=300000 PSI,U1=0.35, U2=0.1

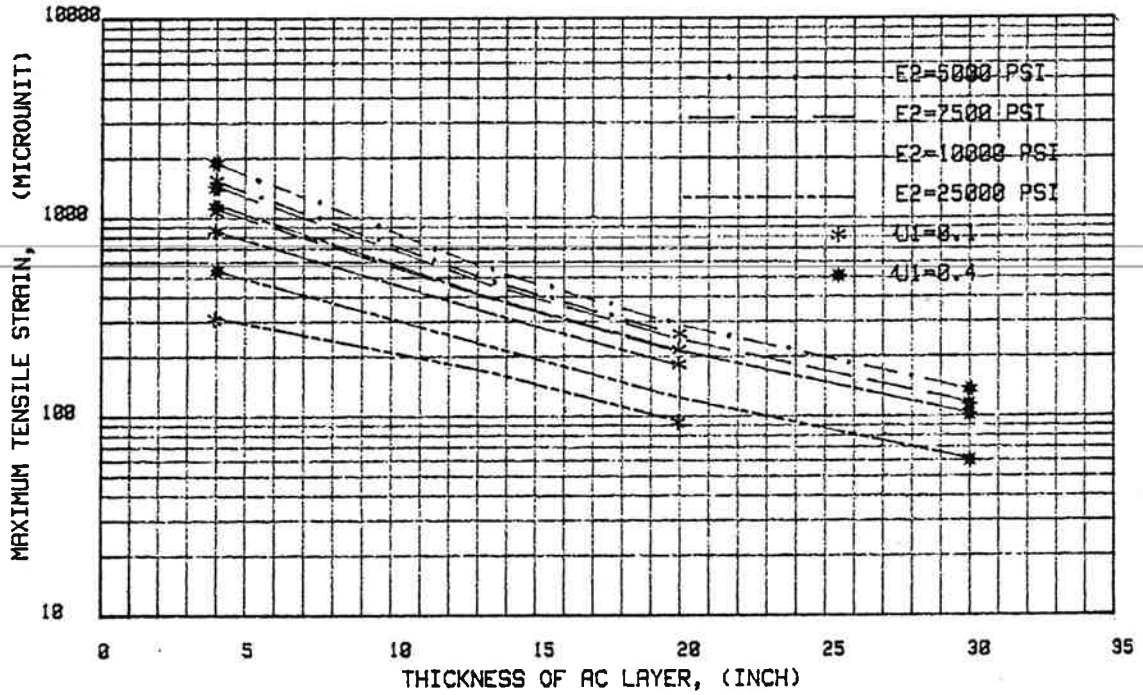

FIG.5.14 EFFECT OF SUBGRADE POISSON'S RATIO ON THE MAXIMUM TENSILE STRAIN, E1=40000 PSI

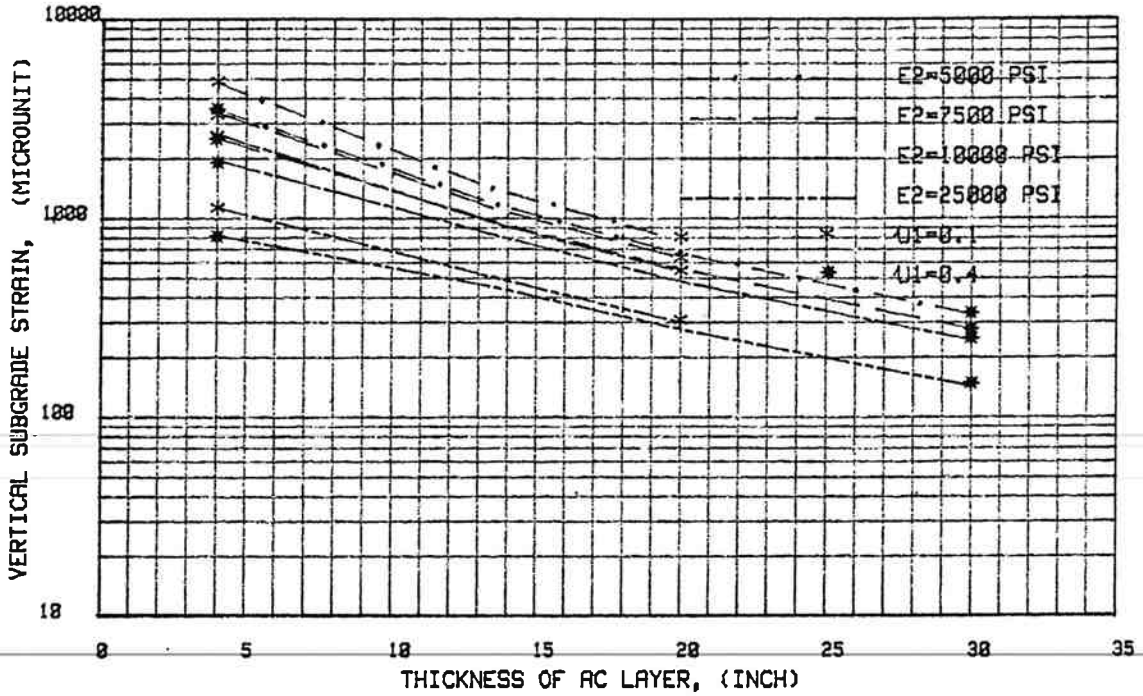

FIG.5.15 EFFECT OF SUBGRADE POISSON'S RATIO ON THE VERTICAL SUBGRADE STRAIN, E1=40000 PSI

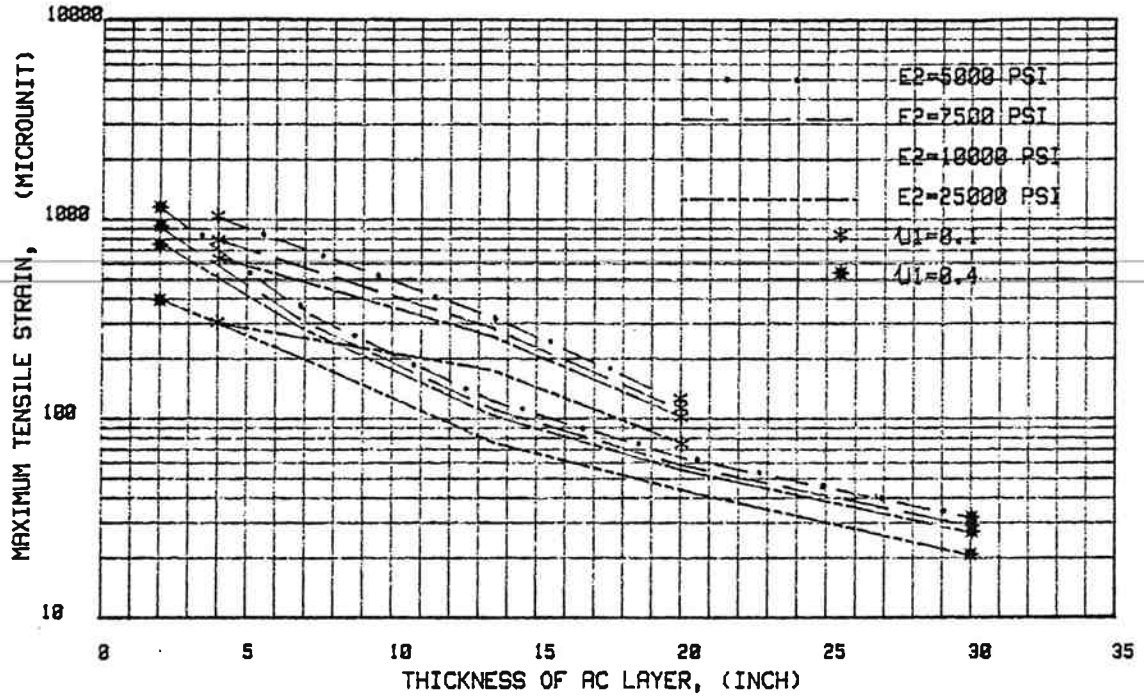

FIG.5.16 EFFECT OF SUBGRADE POISSON'S RATIO ON THE MAXIMUM TENSILE STRAIN, E1=300000 PSI

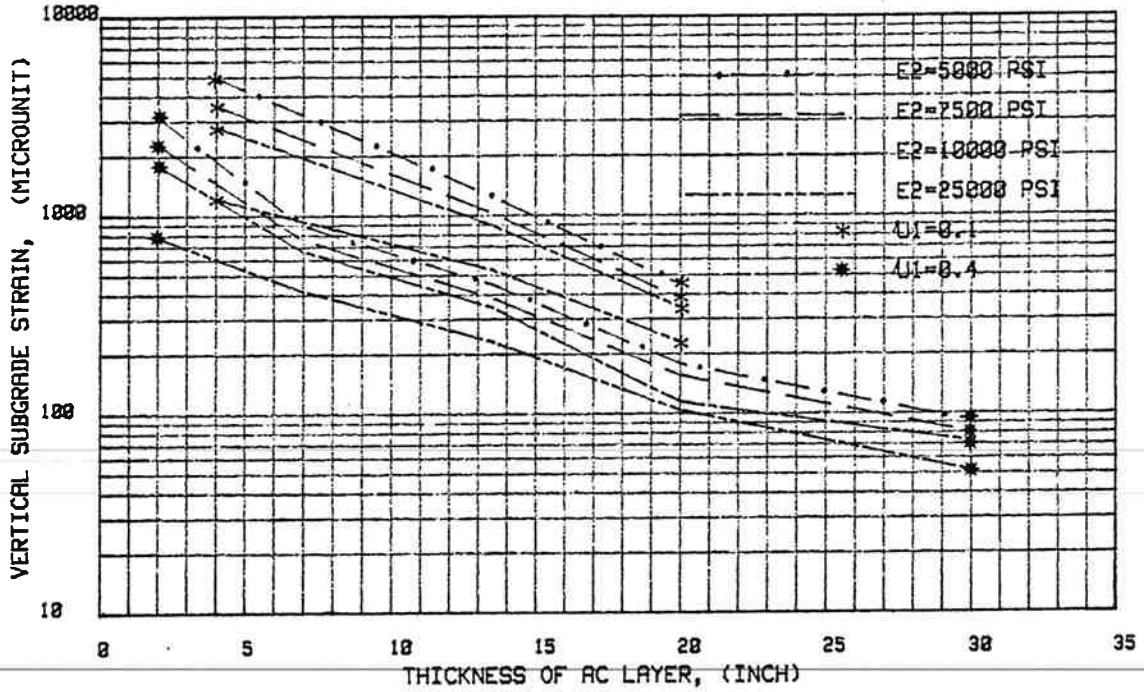

FIG.5.17 EFFECT OF SUBGRADE POISSON'S RATIO ON THE VERTICAL SUBGRADE STRAIN, E1=300000 PSI

Eight analyses were performed using the program PSAD2A for a conventional pavement structure (AC surface layer plus untreated base aggregate and subgrade soil. A pavement section consisting of a 229 mm (9 inch surface asphalt concrete layer, 229 mm (9 inch) aggregate base and subgrade soil was selected. This section is equivalent to the minimum requirement 689 mm (27 inch) CBE associated with a TC = 12 (EAL = 10^7). Each analysis was performed assuming a constant value of modulus 275,600 kPa (40,000 psi) or 2,067,000 kPa (300,000 psi) and Poisson's ratio 0.35 for the asphalt concrete layer. A stress-dependent modulus obtained from the repeated load triaxial test was assigned to the aggregate base layer and a constant value of Poisson's ratio 0.2. A constant value of modulus 34,500 kPa (5,000 psi) and Poisson's ratio 0.4 was selected for the subgrade soil layer (see Figure 5.18). The loading configuration is the same as that used in a full-depth pavement structure analysis. Two critical strains were examined: (1) maximum tensile strain at the bottom of the surface asphalt concrete layer, and (2) the vertical subgrade strain at the top of the subgrade layer.

Table 5.1 lists the results for each analysis. It is interesting to note that although the stress-dependent characteristics of aggregate base materials are different in the "dry" and "wet" conditions, the critical strains obtained for a specific aggregate base are not substantially different, at least for the range of modulus ratio, depth of surface asphalt concrete layer considered.

5.3 Comparison of Pavement Thickness Design Based on Multilayer Elastic Theory and "R" Value

Comparison of pavement thickness design based on the MET and failure criteria presented in section 5.2 and thickness design based on the "R" value may be made assuming the composite asphalt structure, such as an asphalt con-

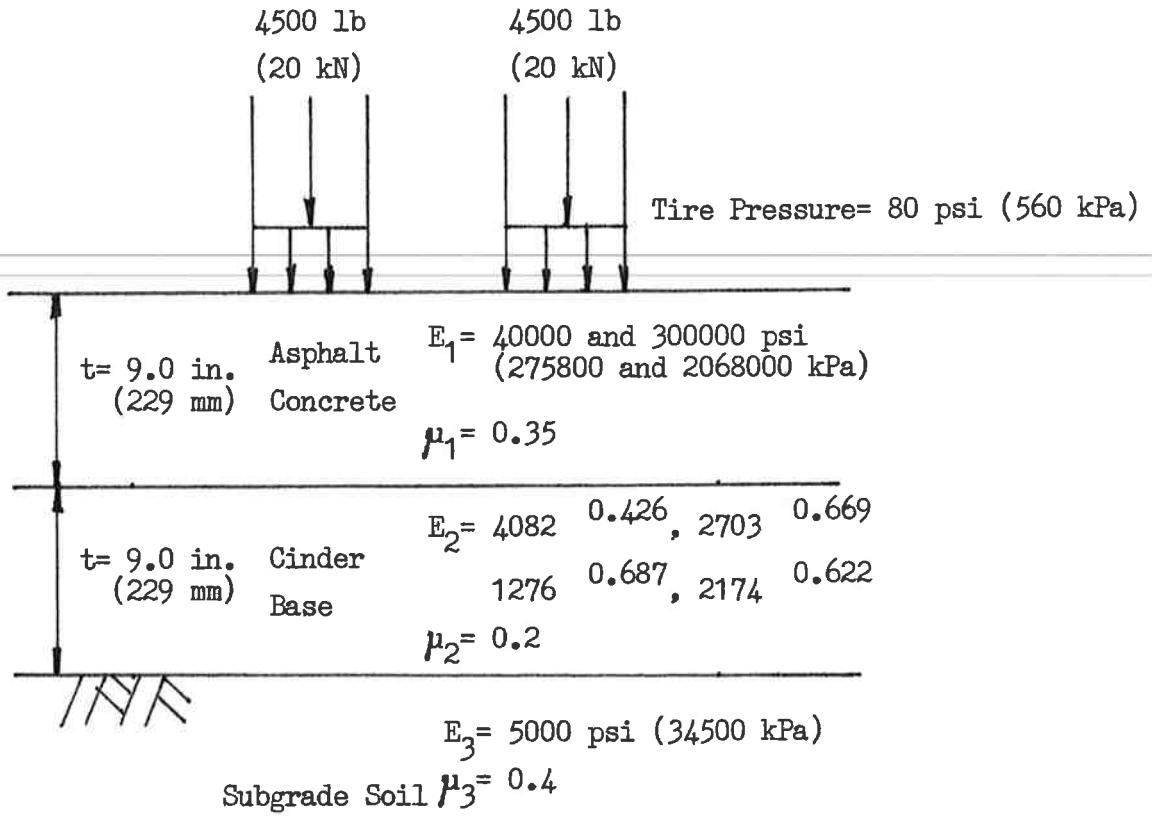

FIG. 5.18 CONVENTIONAL PAVEMENT STRUCTURE, LOADING CONDITIONS AND MATERIAL PROPERTIES

TABLE 5.1 ANALYSIS OF CONVENTIONAL PAVEMENT STRUCTURE

Material		Gray Cinder Base				Red Cinder Base			
Sample No.		A-Dry		C-Wet		A-Dry		C-Wet	
Triaxial Resilient Modulus $M_R = k_1^{k_2}$	k_1	1276.2		2174.2		4082		2703	
	k_2	0.687		0.622		0.426		0.669	
Asphalt Concrete Stiffness (1000 psi)		40	300	40	300	40	300	40	300
Average Base Modulus, After Iteration (1000 psi)		4.6	3.4	6.3	5.1	8.0	6.9	7.7	6.0
Vertical Subgrade Strain (microunit)		1051	403	1080	450	1086	479	1086	472
Maximum Tensile Strain (microunit)		874	249	757	237	673	227	675	229

1 psi=6.9 kPa

Note: Poisson's ratio of Asphalt concrete layer, cinder base layer and subgrade soil layer equals 0.35,0.2 and 0.4 respectively.

Modulus of subgrade layer equals 5000 psi.

crete mix in the surface over a treated base plus untreated aggregate base, can be transformed to a full-depth pavement structure. The transformation to a full-depth pavement structure requires the use of appropriate substitution ratios employed by the ODOT (see Table 5.2).

The differences between the two design methods following this approach are illustrated in Figure 5.19 and 5.20. In general, a full-depth pavement section design based on MET associated with the low stiffness asphalt concrete surface layer (275,600 kPa (40,000 psi)) results in thicknesses greater than the minimum thickness associated with the "R" value design method. The thickness based on MET associated with the high modulus asphalt concrete surface layer (2,067,000 kPa (300,000 psi)) is thinner than the minimum thickness associated with "R" value design method.

5.4 Comparisons of Thickness Design Based on MET with Material Properties Determined with Repeated Load Triaxial Test System to Diametral Test System

The initial confining pressure within a pavement structure increased with increasing depth and unit weight of the materials above the point in a pavement structure considered. Normally, the initially confining pressure may not be as high as 28 kPa (4 psi), and are not equal in three Cartesian directions. The deviator stresses within each layer comprising the pavement structure subjected to traffic loading are very complicated. The computer analysis indicates the subgrade soils in a full-depth pavement structure or the aggregate base layer in a conventional pavement structure may be subjected to lateral tensile deviator stresses. The question is thus raised as to how unbound materials such as those investigated in the study are able to exhibit a positive modulus value when subjected to lateral tensile deviator stress.

TABLE 5.2 CRUSHED BASE EQUIVALENT FACTORS

1.0 in. Asphalt Concrete Wearing Surface & Base	= 2.0 in. Aggregate Base
1.0 in. Cement Treated Base	= 1.8 in. Aggregate Base
1.0 in. Plant Mix Bituminous Base	= 1.8 in. Aggregate Base
1.0 in. Emulsion Treated Wearing Surface & Base	= 1.8 in. Aggregate Base
1.0 in. Oil Mat	= 1.1 in. Aggregate Base
1.0 in. Aggregate Subbase	= 0.8 in. Aggregate Base

iinch=25.4mm

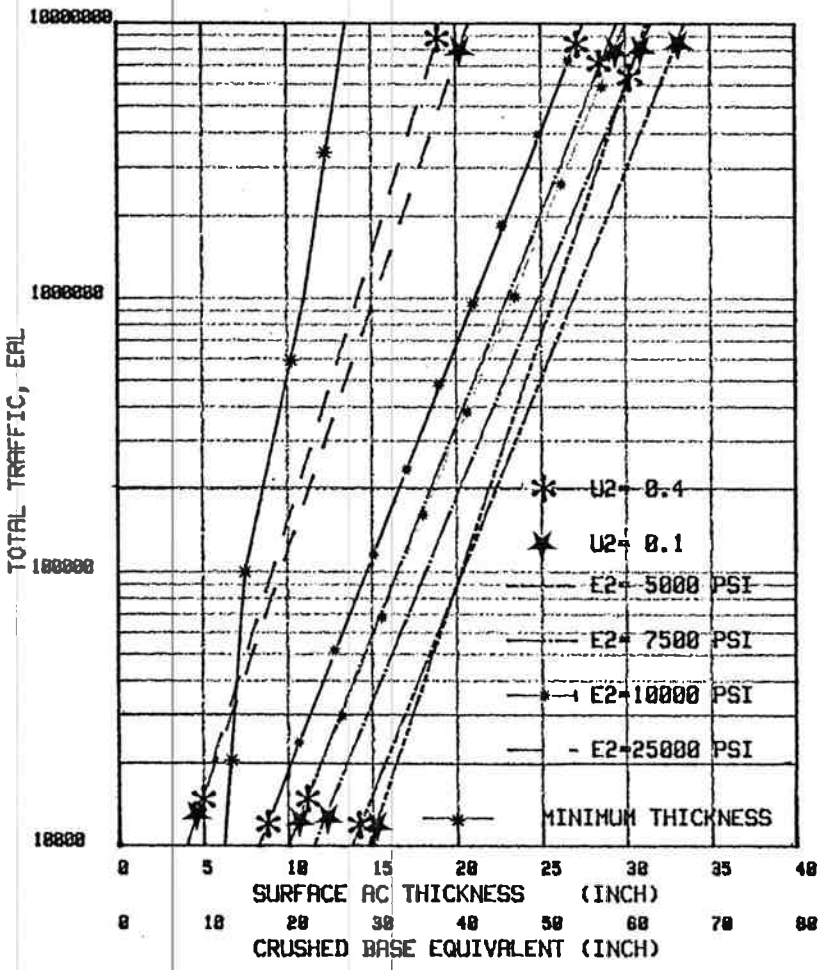

FIG.5.19 COMPARISON OF PAVEMENT THICKNESS DESIGN BASED ON MET AND 'R' VALUE,E1=40000 PSI

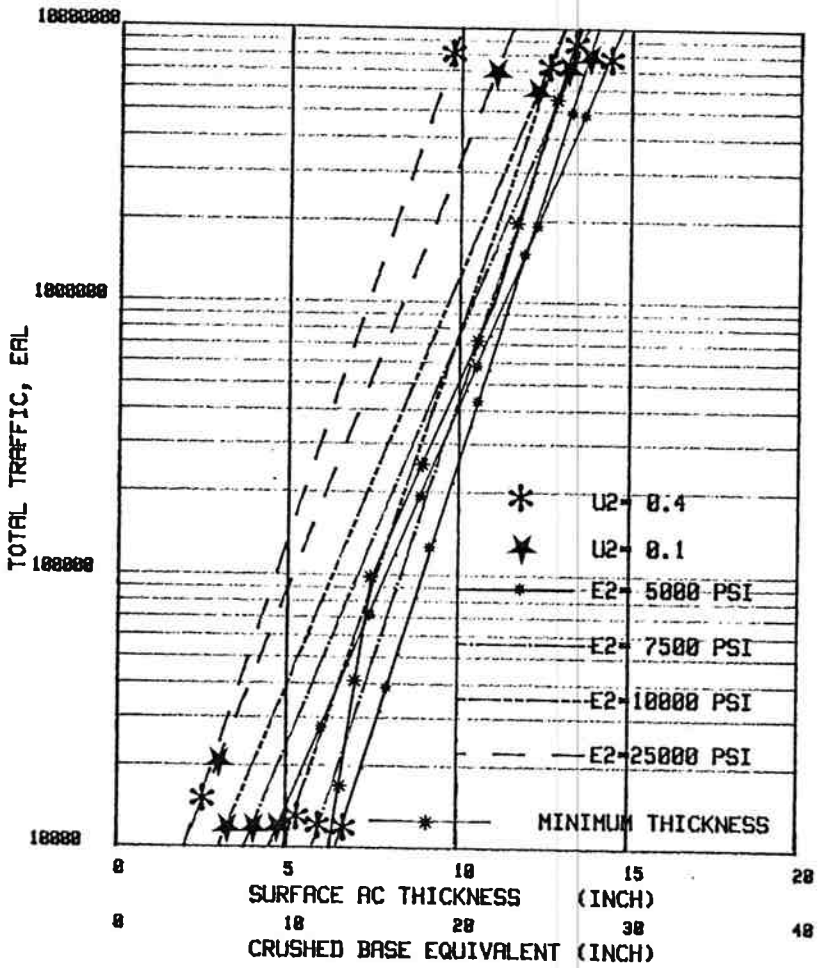

FIG.5.20 COMPARISON OF PAVEMENT THICKNESS DESIGN BASED ON MET AND 'R' VALUE,E1=300000 PSI

Apparently, if the initial confining pressure at the point considered within the pavement structure is greater than the lateral tensile deviator stress induced by traffic loading, the materials may not fail and be characterized using a diametral test system.

Undoubtedly, either the repeated load triaxial test systems or the diametral test systems employed in the study have their advantages and disadvantages with respect to simulating the actual states of stress within the pavement structure.

The laboratory test results discussed in Chapter 4 indicate the resilient properties of noncohesive subgrade soils, either determined with triaxial test systems or diametral test systems, depend largely on the initial confining pressure. The "Equivalent" diametral resilient moduli of subgrade soils are in the range of 71,600 to 161,000 kPa (10,400 to 23,400 psi) or 0.9 to 1.8 times the triaxial resilient moduli, and the "Equivalent" diametral Poisson's ratio are in the range of 0.02 to 0.17 at a confining pressure of 28 kPa (4 psi) and diametral load levels of 116 N to 154 N (26 to 34.6 lb).

The resilient properties of cinder base materials undoubtedly are highly stress-dependent. The diametral test results demonstrate the effect of initial confining pressure on the resilient modulus but do not reflect the influence of sum of the principal stress as that in the triaxial test results. The "Equivalent" diametral resilient moduli of cinder base materials are in the range of 81,300 to 156,000 kPa (11,800 to 22,700 psi) or 0.8 to 1.7 times the triaxial resilient moduli, and the "Equivalent" diametral Poisson's ratio are in the range of 0.07 to 0.28 at a confining pressure of 28 kPa (4 psi) and diametral load levels of 116 N to 154 N (26 to 34.6 lb).

To compare thickness designs based on MET and material properties determined with the repeated load triaxial test system and diametral test system.

an average resilient modulus ratio (diametral/triaxial) and lower diametral Poisson's ratio are used. The Poisson's ratio in the triaxial test was not measured, therefore an assumed value of 0.4 was selected for the subgrade soils and 0.2 was selected for the cinder base materials.

For the full-depth pavement structure, the design thickness associated with higher values of diametral resilient modulus and lower values of Poisson's ratio was approximately equivalent to that associated with lower values of triaxial resilient modulus and higher values of Poisson's ratio. For example, given TC = 12, asphalt concrete stiffness of 2,067,000 kPa (300,000 psi) and Poisson's ratio of 0.35, the design thickness for a subgrade modulus value of 34,000 kPa (5,000 psi) and Poisson's ratio, 0.4, is 376 mm (14.8 in.), and for the subgrade modulus value of 69,000 kPa (10,000 psi) and Poisson's ratio, 0.1, is 330 mm (13 in.). Given TC = 12, asphalt concrete stiffness, 275,000 kPa (40,000 psi), and Poisson's ratio, 0.35, the design asphalt concrete thickness for a subgrade modulus value of 34,000 kPa (5,000 psi) and Poisson's ratio, 0.4, is 800 mm (31.5 in.). For subgrade modulus value of 69,000 kPa (10,000 psi), the design asphalt concrete thickness is 762 mm (30 in.).

To compare the differences of the pavement thickness design between the resilient properties of cinder base materials determined with repeated load triaxial test systems to diametral test systems, a pavement thickness of 686 mm (27 in.) CBE associated with the TC = 12 was assumed. The computer analysis for the conventional pavement structure using triaxial resilient modului (see Table 5.1) indicates the two critical strains do not vary significantly over the material properties considered. Since the relationship between diametral resilient modulus and sum of principal stresses cannot be obtained, the comparison can only be made based on the modulus ratio (diame-

tral/triaxial) as discussed in previous sections. For example, given an asphalt concrete stiffness of 2,067,000 kPa (300,000 psi), Poisson's ratio, 0.35, subgrade modulus, 34,000 kPa (5,000 psi), Poisson's ratio, 0.4, average aggregate base modulus, 48,000 kPa (7,000 psi), Poisson's ratio, 0.2, the critical tensile strain is 227 microunit, and the critical subgrade vertical strain is 478 microunit. With an average aggregate base modulus, 23,000 kPa (3,300 psi) Poisson's ratio, 0.2 and other conditions keep constant, the critical tensile strain is 249 microunit, and the critical subgrade vertical strain is 403 microunit.

The pavement thickness design based on MET apparently is affected by the material properties, the failure criteria selected and the design traffic volume expected. The vertical subgrade strain controls the pavement thickness design over the range of material properties considered in the study (see Table 5.3). It may be expected that the tensile strain at the bottom of asphalt concrete layer would control the thickness design with increasing subgrade resilient modulus or thickness and stiffness of asphalt concrete layer. Santucci (1977) indicated that the limiting vertical subgrade strain criteria selected in his study was developed for asphalt concrete mixes with stiffness of about 1,722,000 kPa (250,000 psi) or less. For asphalt concrete mixes with moduli greater than 1,722,000 kPa (250,000 psi), a value of asphalt concrete stiffness of 1,722,000 kPa (250,000 psi) should be used in the design. Yoder and Witczak (1975) indicate that it is important to use a value of asphalt concrete stiffness, Poisson's ratio and assumed aggregate base to subgrade soil modulus ratio identical to those associated with the development of the limiting vertical subgrade strain criteria. Hull, et al (1980) indicate that the failure criteria based on the limiting vertical subgrade strain may not be appropriate for a thin oil mat surface layer which

TABLE 5.3 DESIGN THICKNESS OF FULL-DEPTH PAVEMENT STRUCTURE

Equivalent Axle Load (EAL)	10^4				10^7			
Asphalt Concrete Poisson's Ratio	0.35	0.35	0.35	0.35	0.35	0.35	0.35	0.35
Asphalt Concrete Stiffness (1000 psi)	40	300	40	300	40	300	40	300
Subgrade Soil Resilient Modulus (1000 psi)	5	10	5	10	5	10	5	10
Subgrade Soil Poisson's Ratio	0.4	0.4	0.4	0.4	0.4	0.4	0.4	0.4
Design Thickness of Asphalt Concrete Layer, t_1 (in.)	12.7	8.0	5.5	3.5	31.0	28.0	16.8	11.0
Design Thickness of Asphalt Concrete Layer, t_2 (in.)	7.0	4.0	3.5	2.0	29.5	26.0	13.3	10.0
Subgrade Soil Poisson's Ratio	0.2	0.2	0.2	0.2	0.2	0.2	0.2	0.2
Design Thickness of Asphalt Concrete Layer, t_1 (in.)	14.0	10.0	7.0	5.5	27.5	23.0	14.3	12.5
Design Thickness of Asphalt Concrete Layer, t_2 (in.)	5.0	0.0	3.0	1.0	25.5	22.0	14.0	12.8

1 psi= 6.9 kPa, 1 1n.= 25.4mm

Note: t_1 is the design thickness based on limiting subgrade strain
t_2 is the design thickness based on limiting tensile strain at the bottom of asphalt concrete layer

has low stiffness value overlying volcanic cinder base and noncohesive subgrade soils such as the McKenzie Highway pavement structure investigated in the study. It is possible that the materials investigated in the study can sustain substantial vertical subgrade strain without permanent deformation. The limiting vertical subgrade strain criteria for a thin surface asphalt concrete which has low stiffness value overlying the highly resilient materials investigated in the study should be developed in the future.

CHAPTER 6

CONCLUSIONS AND RECOMMENDATIONS

With the laboratory data set developed in the study and discussions presented in previous chapters, several conclusions and recommendations were made.

6.1 Conclusions

(1) The Hveem stabilometer resistance value test results for cinder base materials and cohesionless subgrade soils investigated in the study are greater than 65 indicating these materials, when characterized in terms of "R" value, should be equivalent to a good quality aggregate base or subbase.

(2) No distinct relationships between "R" value and triaxial or diametral resilient modulus could be found. This is owing to the substantial differences between the nature of each test method with respect to the stress levels, the confinement of the test specimen, the geometry of test specimen and the rate of loading.

(3) The triaxial resilient modulus test results obtained in the study demonstrate the stress-dependent characteristics associated with cinder base materials and the significant effect of the confining pressure on the resilient modulus associated with cohesionless subgrade soils.

(4) The diametral test system employed in the study offers great potential in providing information associated with the response of unbound materials subjected to lateral tensile deviator stresses induced by traffic loading. The test results indicate, however, the materials considered in the test program deviate from an idealized linear elastic, homogeneous, isotropic material. Further, slight errors are introduces by simplifying

the diametral test system to a two dimensional problem.

(5) The limiting vertical subgrade strain criteria selected in the study may not be appropriate for a thin asphalt concrete surface layer (which has low stiffness value) overlying the highly resilient materials such as those investigated in the study. It is possible that the materials investigated in the study can sustain substantial vertical subgrade strain without permanent deformation.

6.2 Recommendations

Recommendations for further research include:

(1) The diametral test systems may be modified to satisfy the boundary conditions for a two dimensional problem and the equations which permit the calculations of resilient modulus and Poisson's ratio should be modified to incorporate the nonlinearity and heterogeneous characteristics of unbound materials.

(2) The failure criterion based on limiting vertical subgrade strain may not be appropriate for a thin surface asphalt concrete layer which has low stiffness value overlying the highly resilient materials. A failure criteria based on limiting vertical subgrade strain should be developed for the use of volcanic cinder base and cohesionless subgrade soils.

(3) Non-traffic associated distress of pavement structures, including frost action and precipitation deserve further studying for the highway in eastern Oregon.

REFERENCES

1. AASHTO Test Method T-190, "Standard Method of Test for Resistance R-Value and Expansion Pressure of Compacted Soils", AASHTO Materials Part II, 12th edition, 1978.
2. Adedimila, A. S. and Kennedy, T. W., "Fatigue and Resilient Characteristics of Asphalt Mixtures by Repeated-Load Indirect Tensile Test", Research Report 183-5, Center for Highway Research, The University of Texas at Austin, August 1975.
3. Barksdale, R. D., "Compressive Stress Pulse Times in Flexible Pavements for Use in Dynamic Testing", Highway Research Record No. 345, Highway Research Board, Washington, D.C., 1971, pp. 32-44.
4. Clemmons, G. H., "An Evaluation of Coastal Oregon's Marginal Aggregate", Transportation Research Report 79-5, Oregon State University, 1979.
5. California Test Method No. 301-F, "Method of Test for Determination of Resistance "R" Value of Treated and Untreated Base, Subbase and Basement Soils by Stabilometer", State of California, Department of Public Works, Division of Highways.
6. Deacon, J. A., "Materials Characterization-Experimental Behavior", Highway Research Board, Special Report 126, Highway Research Board, Washington, D.C., 1970.
7. Evans, G. L., "Properties of Marginal Aggregates Treated With Asphalt Emulsion," Masters Thesis, Department of Civil Engineering, Oregon State University, 1980.
8. Filz, G., "Resilient Modulus Testing with MTS Electrohydraulic Closed Loop Test System at Oregon State University", August 1978.

9. Frocht, M. M., "Photoelasticity", Vol. 2, John Wiley and Sons, Inc., New York, 1948.

10. Hicks, R. G., Swait, J. D., Jr., Chastain, E. O., "Use of Layered Theory in the Design and Evaluation of Pavement System", Transportation Research Report, Oregon State University, Jan. 1978.

11. Hicks, R. G. and Monismith, C. L., "Factors Influencing the Resilient Response of Granular Materials", Highway Research Record No. 345, Highway Research Board, Washington, D.C., 1971, pp. 14-31.

12. Hondros, G., "The Evaluation of Poisson's Ratio and Modulus of Material of a Low Tensile Resistance by the Brazilian (Indirect Tensile) Test with Particular Reference to Concrete", Australian Journal of Applied Science, Vol. 10, No. 3, 1956.

13. Hull, T., Vinson, T. S. and Hicks, R. G., "Resilient Properties of Volcanic Materials", Proceedings, 18th Annual Symposium on Engineering Geology and Soil Engineering, Boise, Idaho, April 1980.

14. Kennedy, T. W., "Characterization of Asphalt Pavement Material Using the Indirect Tensile Test", Proceedings, Association of Asphalt Paving Technologists, Vol. 46, 1977.

15. Kennedy, T. W. and Hudson, W. R., "Application of the Indirect Tensile Test to Stabilized Materials", Highway Research Record No. 235, Highway Research Board, Washington, D.C., 1968, pp. 36-48.

16. Kennedy, T. W., "Practical Use of the Indirect Tensile Test for the Characterization of Pavement Materials", Proceedings, Vol. 9, Part 3, Australian Road Research Board, 9th ARRB Conference, University of Queensland, August 1978.

17. Kalcheff, I V. and Hicks, R. G., "A Test Procedure for Determining the Resilient Properties of Granular Materials", Journal of Testing and Exaluation, Vol. 1, No. 6, Nov. 1973, pp. 472-479.

18. Monismith, C. L., "Alternatives for Pavements in the 1980's", Keynote Address, 18th Paving Conference, University of New Mexico, Albuquerque, New Mexico, Jan. 1981, pp. 83-125.

19. Monismith, C. L. and McLean, D. B., "Design Considerations for Asphalt Pavements", Report No. TE71-8, University of California, Berkeley, 1971.

20. Monismith, C. L. and McLean, D. B. and Ogawa, N., "Design Considerations for Asphalt Pavements," Report No. TE73-5, University of California, Berkeley, Dec. 1973.

21. Wallace, Keith and C.L. Monismith, "Diametral Modulus Testing on Non-linear Pavement Methods," Proceedings, Assocation of Asphalt Paving Technologists, 1980.

22. OSHD Test Method, Materials Section, State of Oregon, Department of Transportation, Highway Division, 1978.

23. Pong, S. J., "Comparison of Resilient Characteristics of Asphalt Con-Create Using Diametral and Triaxial Test Methods", Transportation Research Report 81-1, Oregon State University, March 1981.

24. Santucci, L. E., "Thickness Design Procedure for Asphalt and Emulsified Asphalt Mixes," Proceedings, Fourth International Conference on the Structural Design of Pavements, Vol. I, University of Michigan, Aug. 1977, pp. 424-456.

25. Schmidt, R. J., "A Practical Method for Measuring the Resilient Modulus of Asphalt-Treated Mixes," Highway Research Record No. 404, Highway Research Board, Washington, D.C., 1972, pp. 22-32.

26. Yoder, E. J. and Witczak, M. W., Principal of Pavement Design, 2nd Edition, John Wiley and Sons, Inc., 1975.

APPENDIX A

ADEQUACY OF DIAMETRAL TEST SYSTEM

The objective of this initial phase of investigation was to evaluate the effect of the transducer yoke, rubber membrane and aluminum plates on the measured vertical and horizontal deformations.

A 100 mm (4 in.) diameter, 64 mm (2.5 in.) in height hard rubber specimen was chosen as the test material. A rubber membrane was cut out and sealed with cellophane tape in the regions where vertical and horizontal deformations were measured. Therefore, the deformations measured did not reflect deformations in the rubber membrane.

The test program, as shown in Fig. A.1, includes five test series: (1) the specimen was tested without the rubber membrane and transducer yoke, and vertical deformations were measured (V1), (2) with the transducer yoke on the horizontal (H2) and vertical (V2) deformation were measured, (3) with the specimen enclosed with rubber membrane, aluminum plate and teflon sheets, the horizontal (H3) and vertical (V3) deformation were measured, (4) with transducer yoke removed and the vertical deformation (V4) was measured, (5) with the rubber membrane, aluminum plates and teflon sheets removed the vertical (V5) deformation was measured.

The test results are shown in Tables A.1 and A.2. Some conclusions may be drawn from these data sets: (1) the use of transducer yoke apparently has little influence on the measurement of vertical deformation, (2) the use of aluminum plates, teflon sheets and rubber membranes apparently reduced the vertical deformation measured but has little influence on the measurement of horizontal deformation, and (3) however, the resilient moduli associated with higher values of vertical deformation are about 10% to 25% lower than

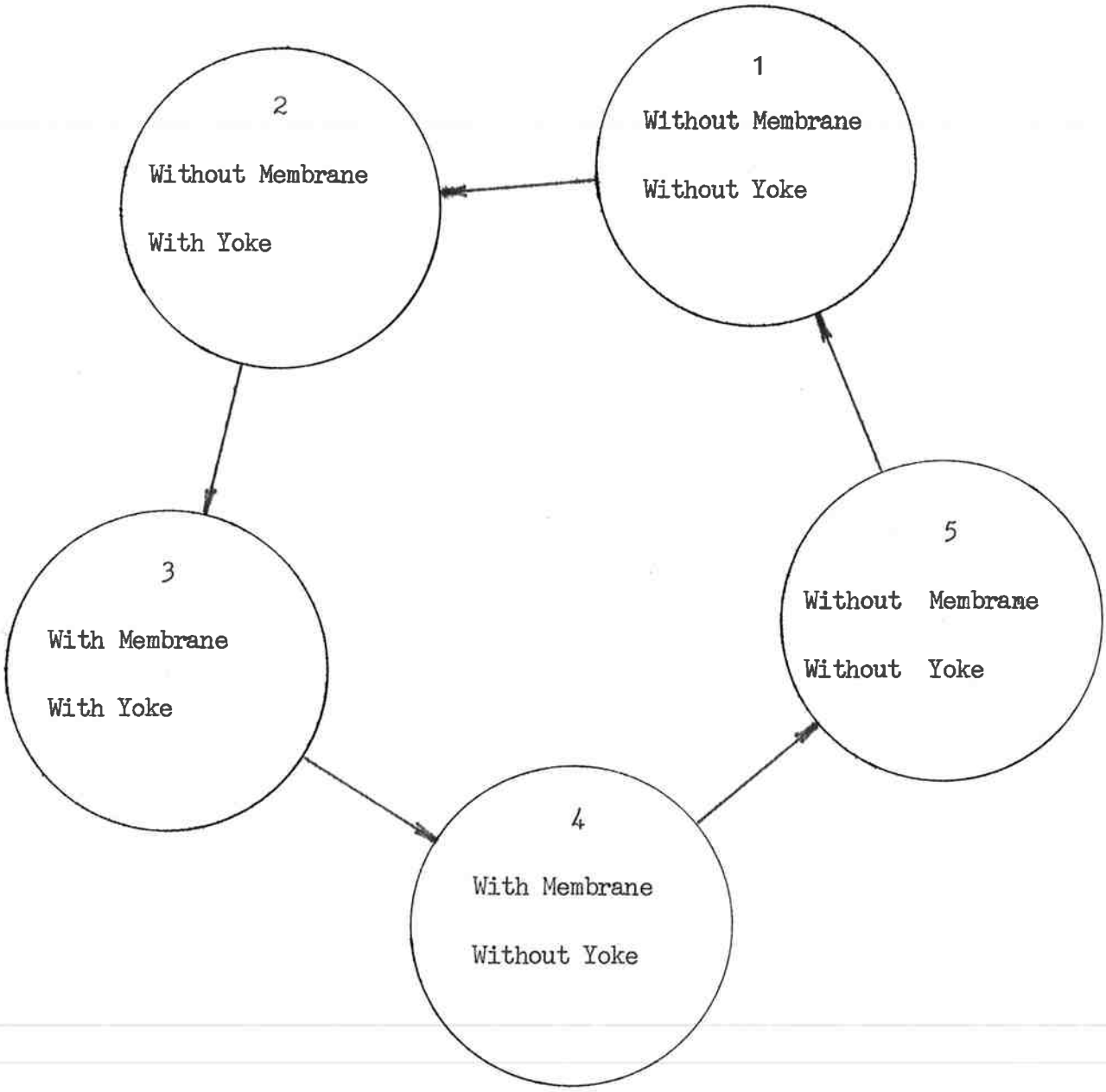

FIG. A.1 TEST PROGRAM

TABLE A.1 TEST RESULTS 1

Diametral Load (lb)	Vertical Deformation (microinch)					Vertical Deformation Ratio				
	V1	V2	V3	V4	V5	V2/V1	V3/V1	V4/V1	V5/V1	V3/V2
20	2083	1875	1528	1528	2083	0.90	0.73	0.73	1.00	0.81
40	3749	3056	2639	2777	3680	0.81	0.70	0.73	0.98	0.86
70	5832	4722	4028	4513	5555	0.81	0.69	0.77	0.95	0.85
90	7360	5694	4999	5832	6388	0.77	0.68	0.79	0.87	0.88
120	9026	7222	6249	7360	7499	0.80	0.69	0.81	0.83	0.86
200	12776	11111	10000	11943	11109	0.87	0.78	0.93	0.87	0.90

1lb=4.45N, 1inch=25.4mm

TABLE A.2 TEST RESULTS 2

Diametral Load (lb)	Vertical Deformation (microinch)		Horizontal Deformation (microinch)		Poisson's Ratio			Resilient Modulus (1000 psi)		
	V2	V3	H2	H3	2	3a	3b	2	3a	3b
20	1875	1528	173	170	0.06	0.13	0.12	15.3	18.7	18.5
40	3056	2639	324	322	0.11	0.17	0.14	18.7	21.6	21.2
70	4722	4028	535	485	0.14	0.16	0.14	21.2	24.8	24.3
90	5694	4999	702	734	0.17	0.25	0.20	22.6	25.7	24.6
120	7222	6249	937	976	0.19	0.29	0.22	23.7	27.4	26.0
200	11111	10000	1628	1738	0.25	0.35	0.26	25.9	28.5	26.6

Note: 2 were computed based on plane stress equation
3a were computed based on plane stress equation
3b were computed based on plane strain equation
1lb=4.45N, 1psi=6.89kPa, 1inch=25.4mm

those associated with lower values of vertical deformation.

Based on these test results, it seems reasonable to conclude that the diametral test system employed in the study will lead to slightly higher values of resilient modulus and Poisson's ratio due to interaction between the end plates and test specimen. However, at present, it appears reasonable to adopt this test system for evaluation of resilient properties of unbound materials.

APPENDIX B

DIAMETRAL TEST RESULTS

This appendix presents the experimental test results and example calculations for the diametral resilient modulus and Poisson's ratio.

The vertical diametral load was measured with a strainsert load cell. Horizontal deformations were measured with two horizontal transducer. Vertical deformations were measured with a gage head LVDT. The voltage output from the load cell, transducers and LVDT were input to a Hewlett-Packard two channel strip chart recorder. All measurement devices should be calibrated to determine the calibration factors. The actual loads and deformations were determined multiplying the reading of strip chart recorder by the calibration factors. It should be noted that the vertical deformations should be corrected by a linear relationship factor which depends on the geometry relationship between the pivot and the position where the vertical deformation LVDT was placed. The Poisson's ratio was computed by the equation 2.42. The resilient modulus was computed by the equation 2.43.

For example, the calibration factors of each measurement device is determined as follows:

Load cell - 3.87 N/mm (0.87 lb/mm) at sensitivity = 0.1

Horizontal transducer 1 - 168×10^{-6} mm/mm (6.62 microinch/mm) at sensitivity = 1.0

Horizontal transducer 2 - 175×10^{-6} mm/mm (6.88 microinch/mm) at sensitivity = 1.0

Vertical deformation LVDT - 6350×10^{-6} mm/mm (250 microinch/mm) at sensitivity = 1.0

the readings from the strip chart recorder are as follows:

Load cell - 30.0 mm

Horizontal transducer 1 - 22.5 mm

Horizontal transducer 2 - 27.0 mm

Vertical deformation LVDT - 19.5 mm

the actual load and deformations are determined multiplying the readings of strip chart recorder by the calibration factors as follows:

Load - 116 N (26.2 lb)

Total horizontal deformations - 8500 x 10^{-6} mm (335 microinch)

Vertical deformation - 0.124 mm (4900 microinch) x 0.5556 (geometry factor) = 0.069 mm (2710 microinch)

The diametral Poisson's ratio and resilient modulus when computed according to the equations 2.42 and 2.43 are as follows:

Poisson's ratio - 0.1725

Resilient modulus - 95,000 kPa (13,800 psi).

The diametral Poisson's ratio and resilient modulus where computed according to the equations 2.42.a and 2.43.a are as follows:

Poisson's ratio - 0.149

Resilient Modulus - 93,500 kPa (13,600 psi)

Tables B.1 through B.12 present the diametral test results for all of the materials considered in the study. Figures B.1 through B.12 show a comparison of the triaxial to the diametral resilient moduli for all of the materials considered in the study.

TABLE B.1 DIAMETRAL TEST RESULTS - FREMONT SUBGRADE SOIL, A-DRY

Confining Pressure, (psi)	Diametral Load (lb)	Vertical Deformation (microinch)	Horizontal Deformation (microinch)	Poisson's Ratio		Resilient Modulus (1000 psi)	
				Plane Stress	Plane Strain	Plane Stress	Plane Strain
4	26.2	2500	206	0.025	0.025	15.0	15.0
6	26.2	2153	179	0.028	0.274	17.4	17.4
8	26.2	1917	157	0.023	0.023	19.6	19.6
4	34.6	3292	287	0.050	0.048	15.4	15.3
6	34.6	2917	249	0.036	0.035	17.0	17.0
8	34.6	2570	227	0.046	0.044	19.3	19.2
4	69.2	6389	805	0.181	0.153	15.5	15.1
6	69.2	5417	672	0.174	0.148	18.2	17.8
8	69.2	4861	571	0.151	0.131	20.3	20.0
4	103.8	9028	1636	0.376	0.274	16.4	15.1
6	103.8	7986	1342	0.330	0.248	18.5	17.4
8	103.8	7222	1121	0.285	0.222	20.5	19.5
4	129.8	11111	2504	0.532	0.347	16.6	14.6
6	129.8	9722	2060	0.484	0.326	18.9	16.9
8	129.8	8680	1728	0.439	0.305	21.3	19.3

1lb=4.45N, 1psi=6.89kPa, 1inch=25.4mm

TABLE B.2 DIAMETRAL TEST RESULTS - FREMONT SUBGRADE SOIL, B-DRY

Confining Pressure (psi)	Diametral Load (lb)	Vertical Deformation (microinch)	Horizontal Deformation (microinch)	Poisson's Ratio		Resilient Modulus (1000 psi)	
				Plane Stress	Plane Strain	Plane Stress	Plane Strain
4	26.2	2986	240	0.018	0.018	12.6	12.6
6	26.2	2639	199	0.001	0.001	14.2	14.2
8	26.2	2361	173	-0.007	-0.007	15.9	15.9
4	34.6	4027	337	0.031	0.030	12.3	12.3
6	34.6	3583	276	0.007	0.007	13.8	13.8
8	34.6	3194	236	-0.005	-0.005	15.5	15.5
4	69.2	7777	982	0.183	0.154	12.7	12.4
6	69.2	6944	786	0.136	0.120	14.2	14.0
8	69.2	6110	639	0.105	0.095	15.7	16.0
4	103.8	11457	2223	0.422	0.297	12.9	11.7
6	103.8	10276	1781	0.349	0.258	14.4	13.4
8	103.8	9027	1433	0.297	0.229	16.4	15.5
4	129.8	13609	3345	0.603	0.376	13.5	11.6
6	129.8	12151	2681	0.515	0.340	15.2	13.4
8	129.8	10762	2345	0.505	0.336	17.1	15.2

1lb=4.45N, 1psi=6.89kPa, 1inch=25.4mm

TABLE B.3 DIAMETRAL TEST RESULTS - FREMONT SUBGRADE SOIL, C-WET

Confining Pressure (psi)	Diametral Load (lb)	Vertical Deformation (microinch)	Horizontal Deformation (microinch)	Poisson's Ratio		Resilient Modulus (1000 psi)	
				Plane Stress	Plane Strain	Plane Stress	Plane Strain
4	26.2	2916	276	0.069	0.065	12.8	12.8
6	26.2	2777	257	0.062	0.059	13.5	13.5
8	26.2	2638	252	0.073	0.068	14.2	14.0
4	34.6	3555	369	0.102	0.093	13.8	13.6
6	34.6	3333	357	0.114	0.102	14.8	14.7
8	34.6	3305	333	0.092	0.084	14.9	14.9
4	69.2	6499	1092	0.330	0.248	15.0	14.2
6	69.2	6110	1017	0.324	0.245	16.0	15.2
8	69.2	5888	953	0.308	0.235	16.6	15.8
4	103.8	9221	2288	0.611	0.380	15.7	14.8
6	103.8	8749	2110	0.587	0.370	15.7	14.8
8	103.8	9527	1963	0.549	0.354	17.0	15.1
4	129.8	10832	2866	0.669	0.401	16.7	14.2
6	129.8	10138	2697	0.674	0.403	17.8	15.2
8	129.8	9860	2448	0.612	0.380	18.4	16.0

1lb=4.45N, 1psi=6.89kPa, 1inch=25.4mm

TABLE B.4 DIAMETRAL TEST RESULTS - MCKENZIE SUBGRADE SOIL, A-DRY

Confining Pressure (psi)	Diametral Load (lb)	Vertical Deformation (microinch)	Horizontal Deformation (microinch)	Poisson's Ratio		Resilient Modulus (1000 psi)	
				Plane Stress	Plane Strain	Plane Stress	Plane Strain
4	26.2	1597	193	0.162	0.139	23.4	23.0
6	26.2	1458	170	0.148	0.129	25.7	25.2
8	26.2	1319	152	0.142	0.125	28.4	27.9
4	34.6	2153	281	0.196	0.164	22.9	22.3
6	34.6	1944	256	0.201	0.167	25.4	24.7
8	34.6	1806	217	0.161	0.139	27.4	26.8
4	69.2	4542	776	0.340	0.254	21.7	20.3
6	69.2	4028	668	0.322	0.244	24.5	23.0
8	69.2	3680	582	0.295	0.223	26.8	25.4
4	103.8	6666	1666	0.618	0.382	22.1	18.8
6	103.8	6111	1438	0.567	0.362	24.1	20.9
8	103.8	5555	1239	0.524	0.344	26.5	23.4
4	129.8	8333	2586	0.828	0.453	21.9	17.5
6	129.8	7222	2216	0.816	0.449	25.3	20.3
8	129.8	6666	1881	0.730	0.422	27.5	22.6

1lb=4.45N, 1psi=6.89kPa, 1inch=25.4mm

TABLE B.5 DIAMETRAL TEST RESULTS - MCKENZIE SUBGRADE SOIL, B-DRY

Confining Pressure (psi)	Diametral Load (lb)	Vertical Deformation (microinch)	Horizontal Deformation (microinch)	Poisson's Ratio		Resilient Modulus (1000 psi)	
				Plane Stress	Plane Strain	Plane Stress	Plane Strain
4	26.2	2708	335	0.173	0.147	13.8	13.5
6	26.2	2431	311	0.188	0.158	15.4	15.0
8	26.2	2222	294	0.204	0.169	16.8	16.3
4	34.6	3333	511	0.277	0.217	14.8	14.1
6	34.6	3056	467	0.276	0.216	16.1	15.4
8	34.6	2778	443	0.300	0.231	16.9	16.8
4	69.2	6389	1688	0.667	0.400	15.3	12.9
6	69.2	5972	1531	0.640	0.390	16.4	13.9
8	69.2	5556	1426	0.642	0.391	17.6	14.9
4	103.8	10069	4923	1.442	0.590	14.4	9.4
6	103.8	9375	4644	1.462	0.594	14.3	10.0
8	103.8	8681	4460	1.526	0.604	16.7	10.6
4	129.8	12500	6048	1.424	0.588	14.5	9.5
6	129.8	11806	5626	1.399	0.583	15.4	10.1
8	129.8	11111	5414	1.436	0.589	16.3	10.6

1lb=4.45N, 1psi=6.89kPa, 1inch=25.4mm

TABLE B.6 DIAMETRAL TEST RESULTS - MCKENZIE SUBGRADE SOIL, C-WET

Confining Pressure (psi)	Diametral Load (lb)	Vertical Deformation (microinch)	Horizontal Deformation (microinch)	Poisson's Ratio		Resilient Modulus (1000 psi)	
				Plane Stress	Plane Strain	Plane Stress	Plane Strain
4	26.2	3611	361	0.088	0.081	10.4	10.3
6	26.2	3472	341	0.082	0.076	10.8	10.7
8	26.2	3333	344	0.100	0.091	11.2	11.1
4	34.6	5333	613	0.142	0.124	10.2	9.1
6	34.6	4861	558	0.141	0.124	10.2	10.0
8	34.6	4583	571	0.176	0.149	10.8	10.5
4	69.2	8681	2480	0.743	0.426	11.3	9.2
6	69.2	8194	2133	0.654	0.395	12.0	10.1
8	69.2	7639	2239	0.769	0.435	12.8	10.4
4	103.8	10764	4563	1.220	0.550	13.5	9.4
6	103.8	10417	4496	1.246	0.555	14.0	9.7
8	103.8	10069	4149	1.180	0.541	14.5	10.2
4	129.8	12500	6147	1.451	0.592	14.5	9.4
6	129.8	11806	6012	1.510	0.602	15.3	9.8
8	129.8	11111	6075	1.637	0.621	16.3	10.0

1lb=4.45N, 1psi=6.89kPa, 1inch=25.4mm

TABLE B.7 DIAMETRAL TEST RESULTS - GRAY CINDER BASE, A-Dry

Confining Pressure (psi)	Diametral Load (lb)	Vertical Deformation (microinch)	Horizontal Deformation (microinch)	Poisson's Ratio		Resilient Modulus (1000 psi)	
				Plane Stress	Plane Strain	Plane Stress	Plane Strain
4	26.2	3167	303	0.074	0.069	11.8	11.7
6	26.2	2750	278	0.092	0.084	13.6	13.5
8	26.2	2528	266	0.107	0.096	14.8	14.7
4	34.6	4028	449	0.129	0.115	12.3	12.1
6	34.6	3611	408	0.135	0.119	13.7	13.5
8	34.6	3264	382	0.149	0.130	15.1	14.9
4	69.2	10833	1294	0.158	0.136	9.1	9.0
6	69.2	8889	1168	0.200	0.167	12.7	12.4
8	69.2	7779	1003	0.191	0.161	12.7	12.4
4	103.8	11111	2386	0.495	0.331	11,4	11.8
6	103.8	9583	2029	0.484	0.326	15.4	13.7
8	103.8	8611	1678	0.425	0.298	17.1	15.6
4	129.8	13749	3987	0.758	0.431	13.3	10.9
6	129.8	11943	3469	0.759	0.432	15.4	12.5
8	129.8	10833	2896	0.679	0.404	16.9	14.2

1lb=4.45N, 1psi=6.89kPa, 1inch=25.4mm

TABLE B.8 DIAMETRAL TEST RESULTS - GRAY CINDER BASE, B-DRY

Confining Pressure (psi)	Diametral Load (lb)	Vertical Deformation (microinch)	Horizontal Deformation (microinch)	Poisson's Ratio		Resilient Modulus (1000 psi)	
				Plane Stress	Plane Strain	Plane Stress	Plane Strain
4	26.2	2917	293	0.090	0.082	12.9	12.8
6	26.2	2583	251	0.078	0.072	14.5	14.4
8	26.2	2278	214	0.067	0.063	16.5	16.4
4	34.6	4305	436	0.090	0.082	11.4	11.3
6	34.6	3819	372	0.079	0.074	12.9	12.9
8	34.6	3361	325	0.077	0.071	14.7	14.7
4	69.2	6805	1072	0.293	0.227	14.5	13.8
6	69.2	6111	974	0.300	0.231	16.1	15.3
8	69.2	5694	842	0.258	0.205	17.3	16.6
4	103.8	9583	1965	0.461	0.315	15.4	13.9
6	103.8	8611	1739	0.449	0.310	17.1	15.5
8	103.8	7861	1529	0.423	0.298	18.8	17.1
4	129.8	10972	2689	0.601	0.375	16.8	14.4
6	129.8	10222	2441	0.579	0.367	18.0	15.6
8	129.8	9444	2127	0.531	0.347	19.5	17.2

1lb-4.45N, 1psi=6.89kPa, 1inch=25.4mm

TABLE B.9 DIAMETRAL TEST RESULTS - GRAY CINDER BASE, C-WET

Confining Pressure (psi)	Diametral Load (lb)	Vertical Deformation (microinch)	Horizontal Deformation (microinch)	Poisson's Ratio		Resilient Modulus (1000 psi)	
				Plane Stress	Plane Strain	Plane Stress	Plane Strain
4	26.2	3055	473	0.284	0.221	12.2	11.6
6	26.2	2639	387	0.255	0.203	14.2	13.6
8	26.2	2333	318	0.217	0.178	16.0	15.5
4	34.6	4166	707	0.335	0.251	12.4	11.1
6	34.6	3749	587	0.290	0.225	13.8	12.5
8	34.6	3263	478	0.254	0.202	15.9	14.5
4	69.2	9165	2331	0.633	0.387	10.7	9.1
6	69.2	8054	1959	0.594	0.373	12.2	10.5
8	69.2	7360	1549	0.479	0.324	13.4	12.0
4	103.8	13193	5328	1.151	0.535	11.0	7.9
6	103.8	11457	4518	1.118	0.528	12.7	9.2
8	103.8	10554	3645	0.949	0.487	13.8	10.6
4	129.8	15276	7848	1.525	0.604	11.8	7.5
6	129.8	13887	6471	1.363	0.577	13.1	8.7
8	129.8	12637	4959	1.112	0.526	14.4	10.4

1lb=4.45N, 1psi=6.89kPa,1inch=25.4mm

TABLE B.10 DIAMETRAL TEST RESULTS - RED CINDER BASE, A-DRY

Confining Pressure (psi)	Diametral Load (lb)	Vertical Deformation (microinch)	Horizontal Deformation (microinch)	Poisson's Ratio		Resilient Modulus (1000 psi)	
				Plane Stress	Plane Strain	Plane Stress	Plane Strain
4	26.2	2305	291	0.182	0.154	16.1	15.8
6	26.2	2069	265	0.187	0.158	17.9	17.6
8	26.2	1930	240	0.176	0.149	19.2	18.9
4	34.6	2750	434	0.294	0.227	17.7	17.0
6	34.6	2611	394	0.269	0.212	18.7	18.1
8	34.6	2361	368	0.287	0.223	20.6	19.9
4	69.2	6180	1474	0.578	0.366	15.6	13.7
6	69.2	5721	1246	0.505	0.336	16.9	15.2
8	69.2	5277	1140	0.499	0.333	18.3	16.6
4	103.8	8749	3302	1.060	0.515	16.4	12.3
6	103.8	8471	3256	1.084	0.520	16.9	12.4
8	103.8	7832	2750	0.970	0.492	18.3	14.1
4	129.8	10415	3780	1.010	0.503	17.2	13.1
6	129.8	9860	3572	1.008	0.502	18.2	13.9
8	129.8	9512	3444	1.007	0.502	18.9	14.4

1lb=4.45N, 1psi=6.89kPa, 1inch=25.4mm

TABLE B.11 DIAMETRAL TEST RESULTS - RED CINDER BASE, B-DRY

Confining Pressure (psi)	Diametral Load (lb)	Vertical Deformation (microinch)	Horizontal Deformation (microinch)	Poisson's Ratio		Resilient Modulus (1000 psi)	
				Plane Stress	Plane Strain	Plane Stress	Plane Strain
4	26.2	1652	183	0.126	0.112	22.7	22.4
6	26.2	1423	157	0.124	0.111	26.3	26.0
8	26.2	1264	140	0.127	0.113	29.6	29.3
4	34.6	2187	292	0.208	0.173	22.6	21.9
6	34.6	1909	245	0.190	0.160	25.8	25.2
8	34.6	1736	216	0.175	0.149	28.5	27.8
4	69.2	4166	903	0.502	0.334	23.6	21.0
6	69.2	3680	756	0.462	0.316	26.7	24.1
8	69.2	3263	651	0.441	0.306	30.1	27.3
4	103.8	6249	2038	0.883	0.469	23.4	18.3
6	103.8	5444	1669	0.815	0.449	26.9	21.5
8	103.8	4999	1391	0.717	0.418	29.4	24.3
4	129.8	7443	3181	1.232	0.552	24.4	17.0
6	129.8	6666	2771	1.192	0.544	27.3	19.2
8	129.8	6110	2260	1.034	0.508	29.9	22.2

1lb=4.45N, 1psi=6.89kPa, 1inch=25.4mm

TABLE B.12 DIAMETRAL TEST RESULTS - RED CINDER BASE, C-WET

Confining Pressure (psi)	Diametral Load (lb)	Vertical Deformation (microinch)	Horizontal Deformation (microinch)	Poisson's Ratio		Resilient Modulus (1000 psi)	
				Plane Stress	Plane Strain	Plane Stress	Plane Strain
4	26.2	2708	321	0.155	0.134	13.8	13.6
6	26.2	2222	254	0.140	0.123	16.9	16.6
8	26.2	1896	198	0.104	0.094	19.8	19.6
4	34.6	3333	490	0.256	0.204	14.8	14.2
6	34.6	2777	372	0.209	0.173	17.8	17.2
8	34.6	2389	298	0.176	0.150	20.7	20.2
4	69.2	6527	1810	0.713	0.416	15.0	12.4
6	69.2	5416	1259	0.557	0.358	18.1	15.8
8	69.2	4527	885	0.427	0.299	21.7	19.8
4	103.8	9304	4251	1.332	0.571	15.6	10.5
6	103.8	8055	3332	1.185	0.542	18.1	12.8
8	103.8	6944	2659	1.079	0.519	21.0	15.3
4	129.8	10554	5562	1.570	0.611	17.1	10.7
6	129.8	9443	4524	1.408	0.585	19.2	12.6
8	129.8	8277	3634	1.272	0.559	22.0	15.1

1lb=4.45N, 1psi=6.89kPa, 1inch=25.4mm

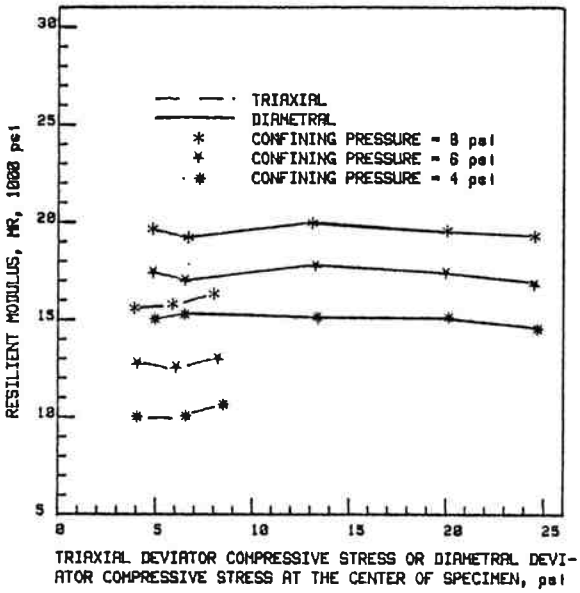

FIG.B.1 COMPARISON OF TRIAXIAL AND DIAMETRAL RESILIENT MODULUS - FREMONT SUBGRADE SOIL A-DRY, 1psi=6.9kPa

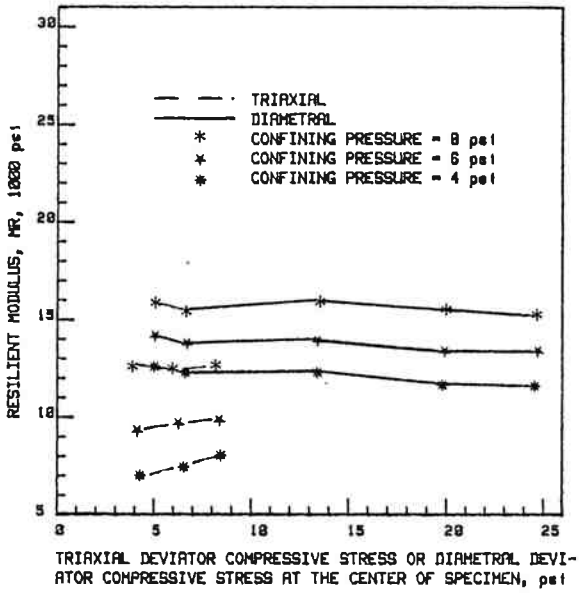

FIG.B.2 COMPARISON OF TRIAXIAL AND DIAMETRAL RESILIENT MODULUS - FREMONT SUBGRADE SOIL B-DRY, 1psi=6.9kPa

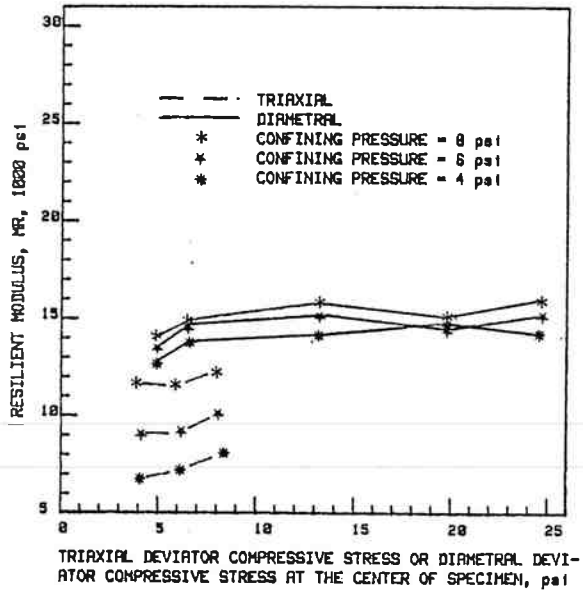

FIG.B.3 COMPARISON OF TRIAXIAL AND DIAMETRAL RESILIENT MODULUS - FREMONT SUBGRADE SOIL C-WET, 1psi=6.9kPa

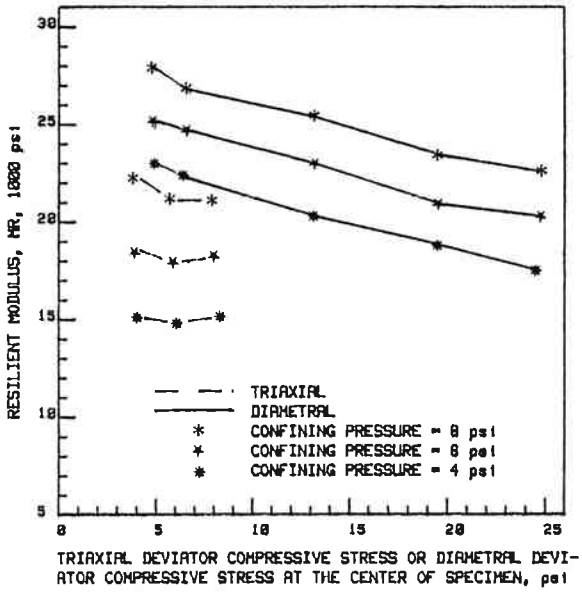

FIG.B.4 COMPARISON OF TRIAXIAL AND DIAMETRAL RESILIENT MODULUS - MCKENZIE SUBGRADE SOIL A-DRY, 1psi=6.9kPa

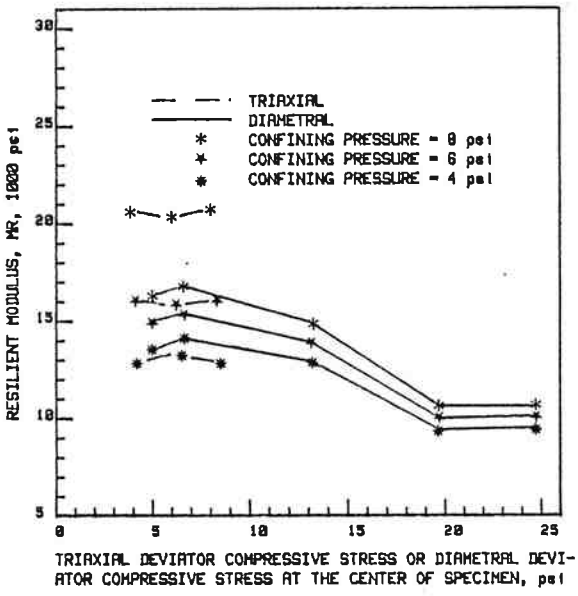

FIG.B.5 COMPARISON OF TRIAXIAL AND DIAMETRAL RESILIENT MODULUS - MCKENZIE SUBGRADE SOIL B-DRY, 1psi=6.9kPa

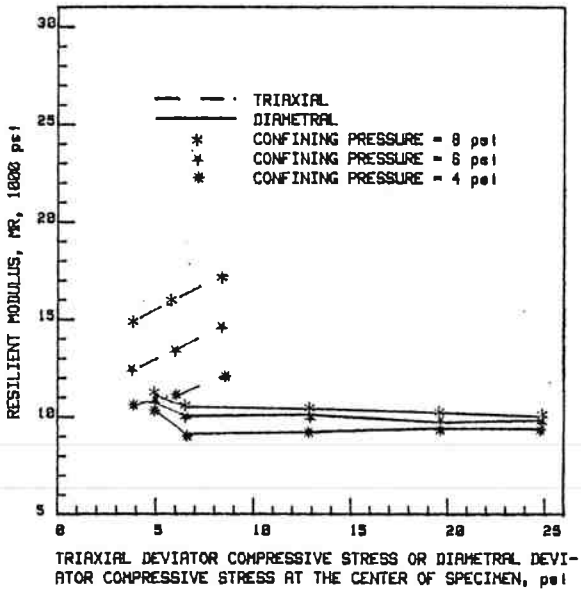

FIG.B.6 COMPARISON OF TRIAXIAL AND DIAMETRAL RESILIENT MODULUS - MCKENZIE SUBGRADE SOIL C-WET, 1psi=6.9kPa

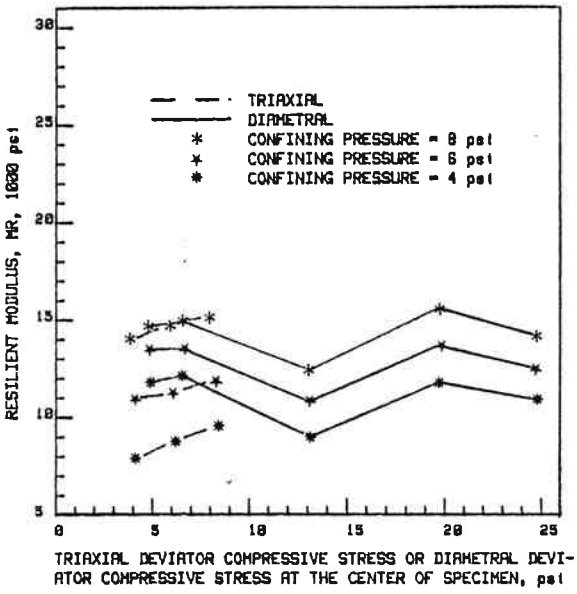

FIG.B.7 COMPARISON OF TRIAXIAL AND DIAMETRAL RESILIENT MODULUS - GRAY CINDER BASE A-DRY, 1psi=6.9kPa

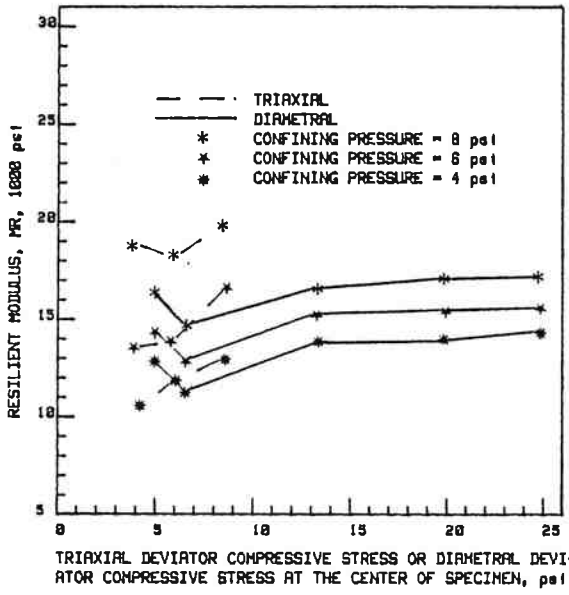

FIG.B.8 COMPARISON OF TRIAXIAL AND DIAMETRAL RESILIENT MODULUS - GRAY CINDER BASE B-DRY, 1psi=6.9kPa

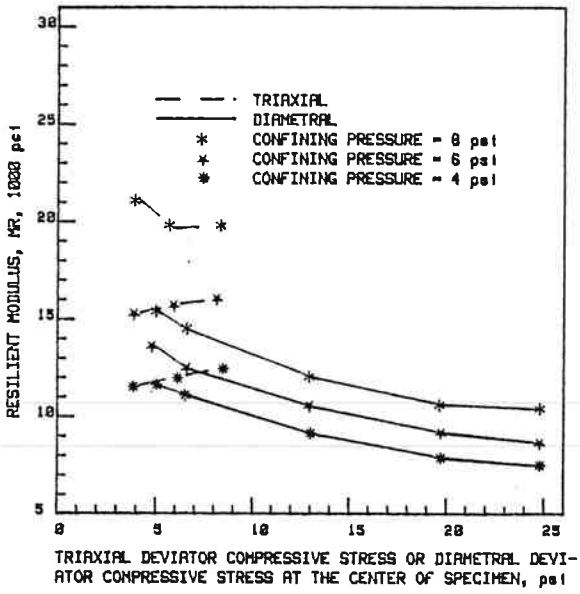

FIG.B.9 COMPARISON OF TRIAXIAL AND DIAMETRAL RESILIENT MODULUS - GRAY CINDER BASE C-WET, 1psi=6.9kPa

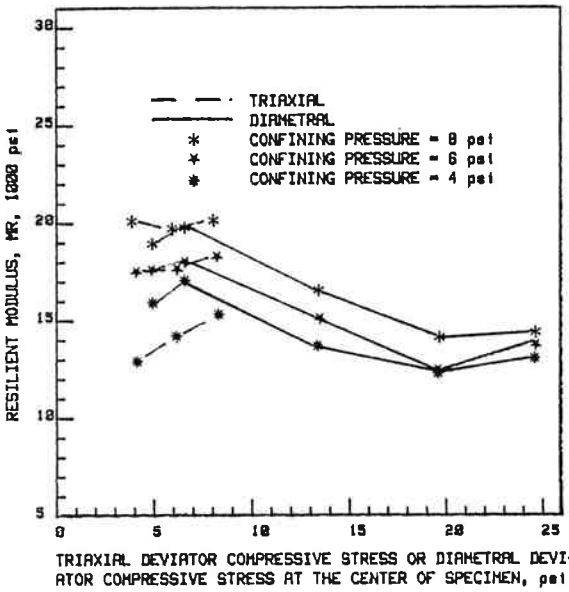

FIG.B.10 COMPARISON OF TRIAXIAL AND DIAMETRAL RESILIENT MODULUS - RED CINDER BASE A-DRY, 1psi=6.9kPa

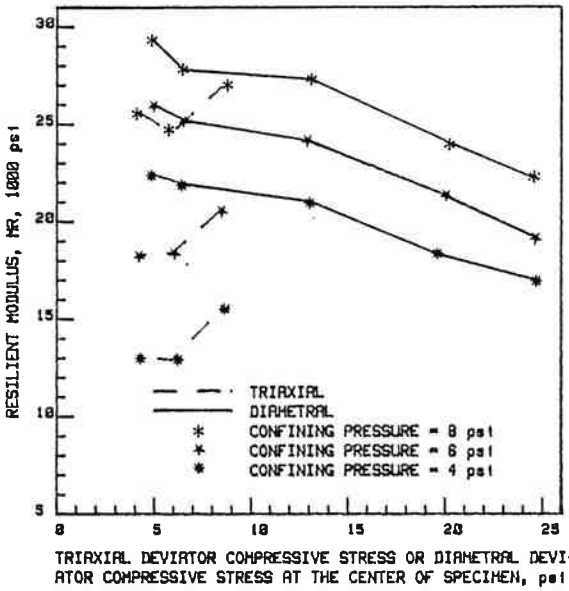

FIG.B.11 COMPARISON OF TRIAXIAL AND DIAMETRAL RESILIENT MODULUS - RED CINDER BASE B-DRY, 1psi=6.9kPa

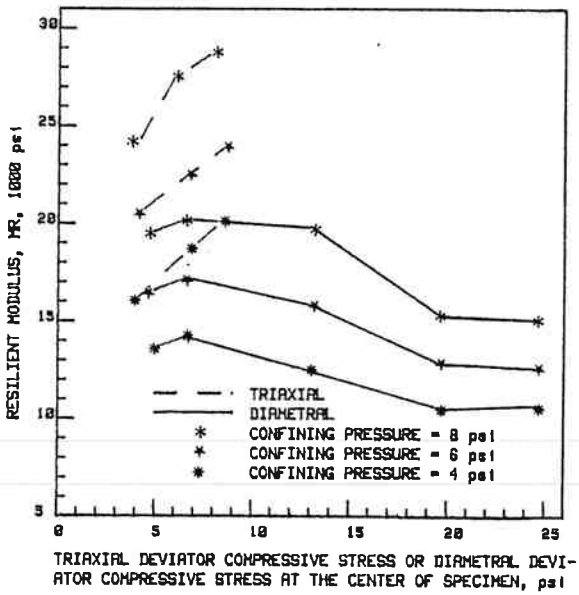

FIG.B.12 COMPARISON OF TRIAXIAL AND DIAMETRAL RESILIENT MODULUS - RED CINDER BASE C-WET, 1psi=6.9kPa

APPENDIX C

SUMMARY OF ODOT TEST RESULTS

This appendix summarizes the test data previously conducted at the ODOT test laboratories. These test results include: (1) gradation analysis, (2) specific gravity, (3) Standard Proctor Compaction test, and (4) "R" value test.

The gradation for each material are shown in Figures C.1 to C.4. The Fremont base course was classified as A-1-b (AASHTO). The McKenzie base course was classified as A-1-a (AASHTO). Two subgrade soils were classified as A-2-4 (AASHTO).

The specific gravity for the Fremont base course is 2.73. The specific gravity for the McKenzie base course is 2.75. The specific gravity for the Fremont subgrade soil is 2.60. The specific gravity for the McKenzie subgrade soil is 2.65.

The Standard Proctor Compaction test results are shown in Figures C.5 to C.8. The optimum water content and maximum dry density for the Fremont base course are 10% and 19 kN/m^3 (119 pcf). The optimum water content and maximum dry density for the McKenzie base course are 12% and 1360 kg/m^3 (85 pcf). The optimum water content and maximum dry density for the Fremont subgrade soil are 26.5% and 13.0 kN/m^3 (81.5 pcf). The optimum water content and maximum dry density for the McKenzie subgrade soil are 18% and 1570 kg/m^3 (98 pcf).

The "R" value test results are summarized in Table C.1. The design "R" values determined at an exudation pressure of 2067 kPa (300 psi) for the Fremont base course and subgrade soil are 70 and 77. The design "R" values determined at an exudation pressure of 2067 kPa (300 psi) for the McKenzie base course and subgrade soil are 86 and 70.

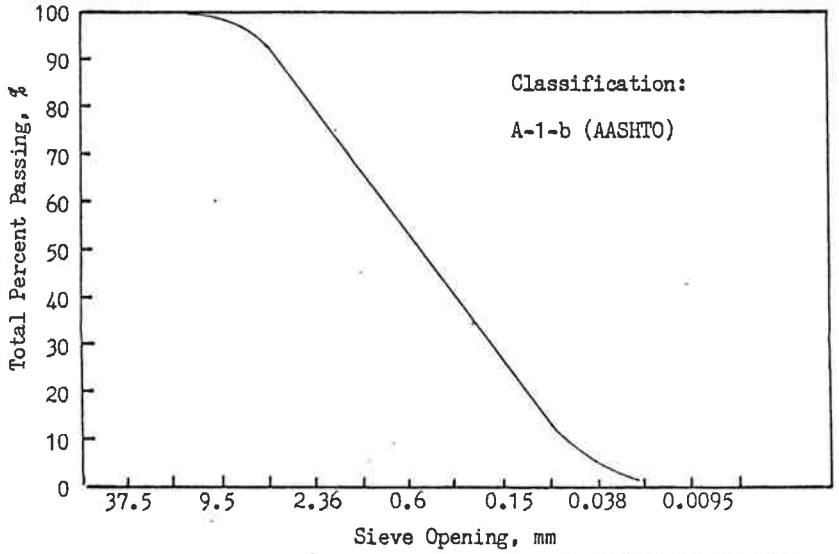

FIG. C.1 GRADATION ANALYSIS - FREMONT CINDER BASE

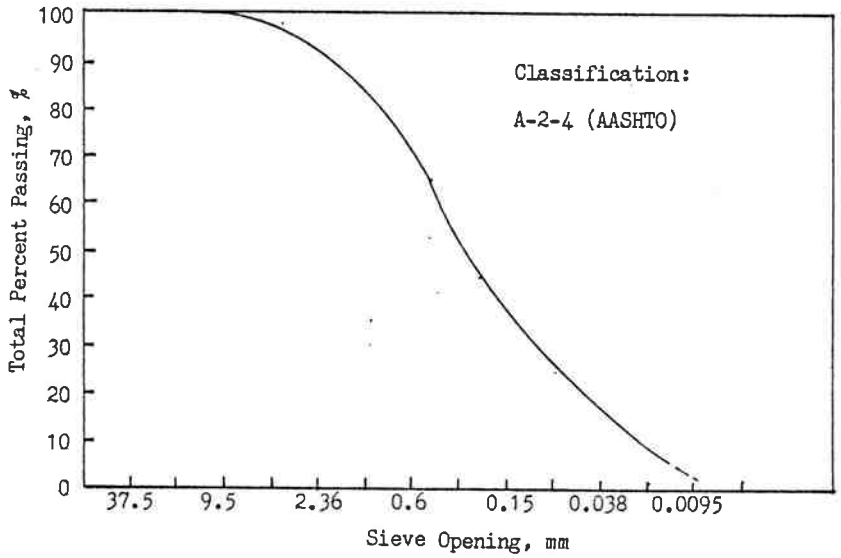

FIG. C.2 GRADATION ANALYSIS - FREMONT SUBGRADE SOIL

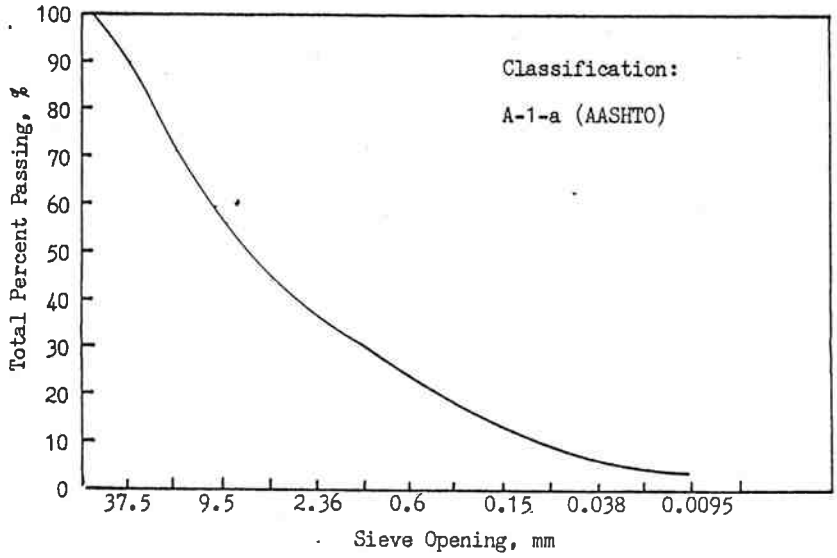

FIG. C.3 GRADATION ANALYSIS - MCKENZIE CINDER BASE

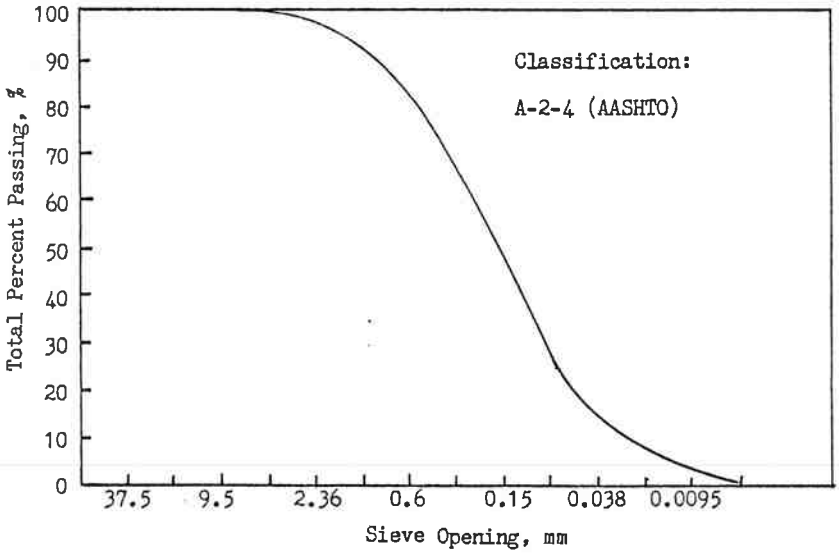

FIG. C.4 GRADATION ANALYSIS - MCKENZIE SUBGRADE SOIL

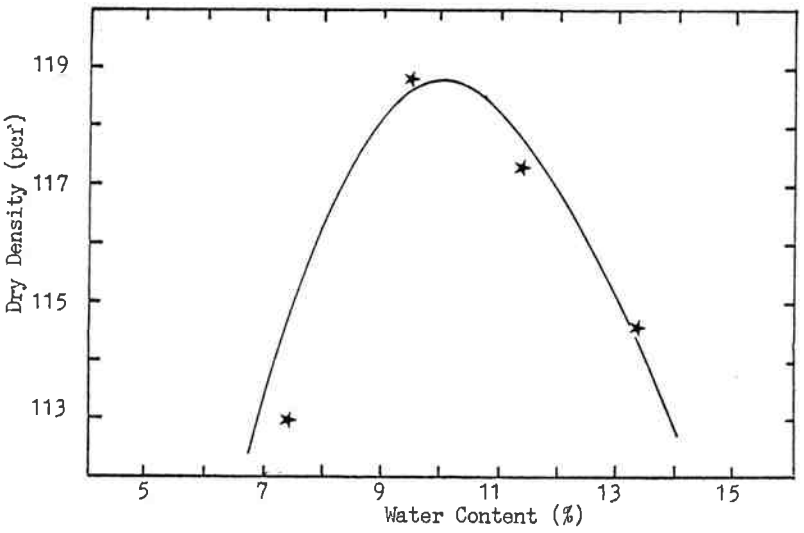

FIG. C.5 MOISTURE-DENSITY RELATIONSHIP - FREMONT BASE (T-99)

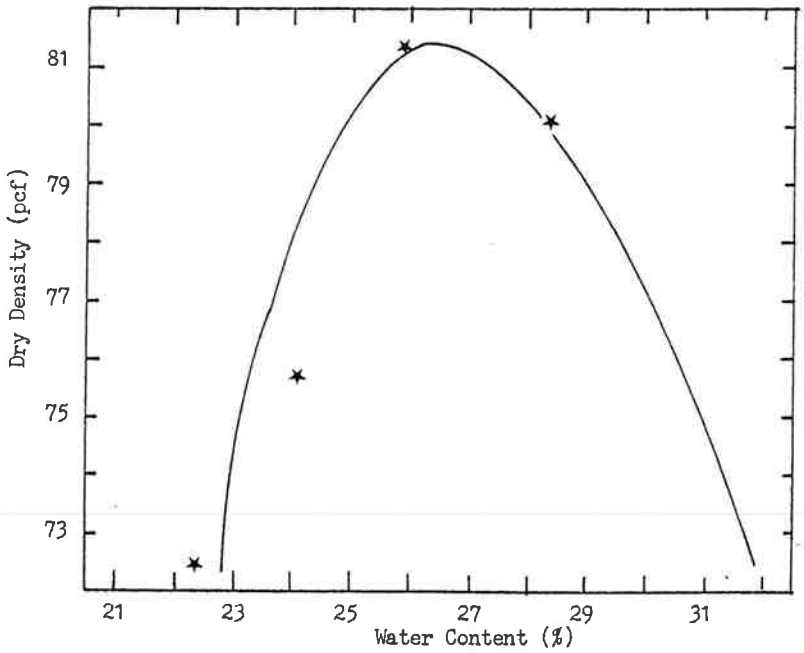

FIG. C.6 MOISTURE-DENSITY RELATIONSHIP - FREMONT SUBGRADE SOIL (T-99)

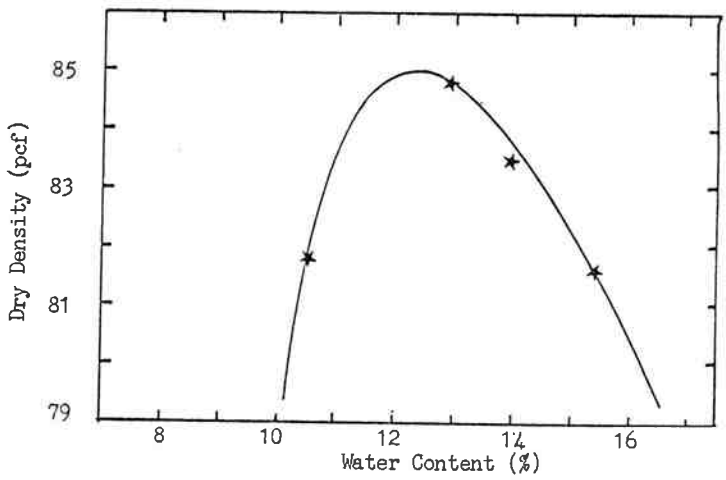

FIG. C.7 MOISTURE-DENSITY RELATIONSHIP - MCKENZIE BASE (T-99)

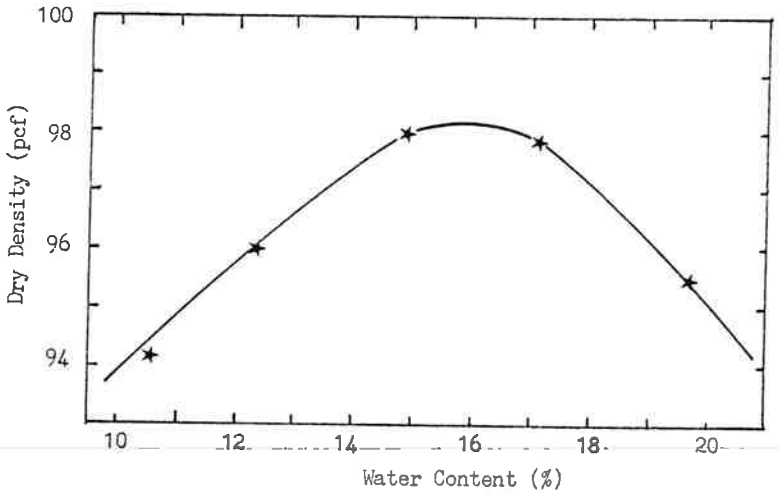

FIG. C.8 MOISTURE-DENSITY RELATIONSHIP - MCKENZIE SUBGRADE SOIL (T-99)

TABLE C.1 ODOT "R" VALUES TEST RESULTS

Location (1)	Water Content In Percent (2)	Dry Density in pcf (3)	Exudation Pressure in psi (4)	"R" Value (5)
Fremont Subgrade Soil	24.1	82.3		85
	25.6	81.1		80
	27.8	79.3		79
	32.1	76.1		72
Fremont Base Aggregate	10.7	119.4		80
	11.4	119.7		77
	12.8	116.1		72
McKenzie Subgrade Soil	19.2	97.0		80
	20.6	95.3		75
	22.1	92.5		73
McKenzie Base Aggregate	15.7	87.6		87
	17.0	84.5		85
	18.4	88.0		79
	19.8	86.0		77